

# **ENGINEERING NOVEL SUICIDE ENZYMES FOR IMPROVED CANCER GENE THERAPY**

By

ANDRESSA ARDIANI

A dissertation submitted in partial fulfillment of  
the requirements for the degree of

DOCTOR OF PHILOSOPHY

WASHINGTON STATE UNIVERSITY  
School of Molecular Biosciences

MAY 2009

© Copyright by ANDRESSA ARDIANI, 2009  
All Rights Reserved

© Copyright by ANDRESSA ARDIANI, 2009  
All Rights Reserved

To the Faculty of Washington State University:

The members of the Committee appointed to examine the dissertation of  
ANDRESSA ARDIANI find it satisfactory and recommend that it be accepted

---

Margaret Black, Ph.D., Chair

---

Chengtao Her, Ph.D.

---

Nancy S. Magnuson, Ph.D.

---

Susan Wang, Ph.D.

## **ACKNOWLEDGMENT**

My graduate school experience has been a journey of a lifetime, full of trials and tribulations and at the same time exceptionally rewarding. I am sincerely thankful to many people who have given tremendous support, advice, guidance and influenced my life in their own ways. However, first and foremost, I must thank the Lord Jesus Christ for giving me this amazing opportunity to pursue my doctorate degree and for His endless blessing and guidance throughout all these years.

Secondly, my sincerest and deepest thank you to my major advisor, Dr. Margaret E. Black. Since the day I joined her laboratory 5 years ago, I have received constant support from her and I consider myself to be very fortunate to have found a “home” laboratory under her guidance. She is an amazing mentor and she has always been so patient with me through the ups and downs of my graduate career. Most of all, however, I have to thank her for believing in me, for her enthusiasm, and for her endless encouragement especially during difficult times. I am and will always be thankful for everything that she has done for me and everything that I have learned from her.

I am earnestly and eternally grateful to my parents and my family for their love and the financial and emotional support that they have always given to me. My parents sacrificed so much for all their children and I can never thank them enough for showing me the greatest example of a parent’s unconditional love. They are fully committed and dedicated to their children so that all of us can have better education and lead a better life for ourselves. My brother and his family have provided nothing but love for me throughout all these years. I am forever grateful for Ashaunde Smith for his unyielding love for me and for his patience towards me especially at times when I am “difficult” to deal with. Thank you for always believing in me and

for always being there for me whenever I need a shoulder to cry on or a big hug or a big laugh or whenever I need someone to tell me that everything is going to be okay! I cannot thank him enough for being my rock and for all the emotional support that I have received and will continue to receive from him. I am also indebted to two special friends, Isabela Reinitati and Martha Susiarjo. A big thank you to Isabela, who has touched my life in so many different ways, I wouldn't know what to do without our lunch "dates" and all the lively phone conversations that always made my day better. Martha is a dear friend and I have to thank her for always having the right things to say at the right time. Both of them have been such amazing friends and will always be dear in my heart for years to come.

I would like to express my gratitude to my committee members, Dr. Nancy Magnuson, Dr. Chengtao Her, and Dr. Susan Wang. I appreciate the time and energy they have put into listening to me, reading my proposals, writing many recommendation letters, and I thank them for the helpful discussions, guidance and advice throughout my graduate career. I also would like to thank the School of Molecular Biosciences program, the Pharmacology and Toxicology program, all the professors who have taught me and the staff for their never-ending help and for answering all of my random questions. I would like to thank my fellow graduate students from both the SMB and P/T program, especially the present members of Black lab; Adam Johnson, Marilyn Sanchez-Bonilla, Kinta Serve and Dr. Hongmei Ruan. I cannot thank Adam enough for always amusing me with his jokes (and sarcasm!) and for the much needed coffee trips to Starbucks. I have to thank Marilyn for our entertaining chats during lunch breaks, for her caring nature, and for her willingness to help whenever needed. Hongmei has added much joy and happiness since she joined the laboratory and I have to thank her for her positive attitude and outlook in life. Thanks to Kinta for her work in HPLC and also for the entertaining random chats from time to time. I am indebted to each one of them for

putting up with me during my “crisis”, for constant support, and most of all for making my laboratory life fun. They all are amazing people, great friends and I am sure they will do great things in life. I am extremely thankful for the past members of the Black lab, especially Candice Willmon and Michi Fuchita. Candice has become one of my greatest friends and I have to thank her for her continuous support and help with my proposals, thesis and everything else throughout my graduate career. Deepest thanks for Michi, who did the bCD mutagenesis study, because it is through her hard work that I was fortunate enough to be able to characterize the amazing mutants that she created. Many thanks also go to our collaborators at the Fred Hutchinson Cancer Research Center, especially Dr. Barry Stoddard for his amazing science and helpfulness.

Finally, I wish to mention and thank those that have contributed monetarily or materially to my project. Without donors like the Motsenbocker, Bracken, Sue Harriet Monroe Mullen, or Otto Kennedy families, I would not be able to attend some of the conferences I have been very fortunate to attend. And, of course, I would like to acknowledge the NIH for the grant monies that provide funding and stipend for my research.

# **ENGINEERING NOVEL SUICIDE ENZYMES FOR IMPROVED CANCER GENE THERAPY**

## **Abstract**

By Andressa Ardiani, Ph.D.  
Washington State University  
May 2009

Chair: Margaret E. Black

Suicide gene therapy for cancer offers a selective approach to eliminating tumor cells while leaving normal cells unaffected. One major drawback is the low activity the enzyme displays towards the prodrug. In an effort to overcome this, we sought to optimize two suicide gene therapy systems for enhanced prodrug activity.

Herpes Simplex Virus thymidine kinase phosphorylates ganciclovir (GCV) to GCV-monophosphate (GCV-MP). Previously, we characterized two HSVTK-mutants with improved activity towards GCV and generated a fusion protein of HSVTK and mouse guanylate kinase (MGMK) that displayed a 175-fold decrease in  $IC_{50}$  for GCV. By combining these two approaches, we created mutant fusion constructs carrying HSVTK mutants and MGMK (MGMK/30 and MGMK/SR39). Both fusions displayed superior tumor killing *in vitro* and impressive tumor growth inhibition in an animal tumor model at very low doses of GCV. In addition, we were able to demonstrate that mutations at residue serine 37 in MGMK represent a previously undescribed

mechanism for 6-thioguanine resistance, a drug widely used as chemotherapeutic agent to treat leukemia.

Bacterial CD (bCD) deaminates 5-fluorocytosine to 5-fluorouracil. From a regio-specific mutagenesis library containing over one million mutants, three bCD variants with improved 5FC activity in *E. coli* were identified. Kinetic analyses revealed that all variants displayed 18- to 19-fold shifts in substrate preference toward 5FC, a significant reduction in IC<sub>50</sub> values and improved bystander effect compared to wild-type bCD in three different cancer cells. *In vivo*, the best mutant (1525), was shown to have significant tumor growth inhibition at doses that the wild-type enzyme was unresponsive to. When the same mutant is fused with uracil phosphoribosyltransferase, only a modest improvement in tumor killing and surprisingly weaker bystander activity were detected when compared to 1525 alone. We hypothesized that when UPRT was fused to bCD, another rate limiting step in this drug activation pathway developed. From a regio-specific mutagenesis study, three UPRT variants were identified to have enhanced activity towards 5FU in *E. coli* and kinetic analyses revealed slight shifts in substrate preference towards 5FU. Further studies will be done to generate UPRT mutants with further capability to enhance 5FU sensitization in cancer cells.



# TABLE OF CONTENTS

	Page
ACKNOWLEDGEMENT .....	iii
ABSTRACT.....	vi
LIST OF TABLES .....	xi
LIST OF FIGURES .....	xii
CHAPTER	
1. INTRODUCTION .....	1
HSVTK/GCV.....	8
CD/5FC.....	10
Suicide Gene Therapy Improvements	
Overview of Suicide Gene Therapy Delivery .....	15
Regio Specific Random Mutagenesis .....	21
Improving Thymidine Kinase .....	22
Improving Cytosine Deaminase.....	28
References .....	33
2. FUSION ENZYMES CONTAINING HSV-1 THYMIDINE KINASE MUTANTS	
AND GUANYLATE KINASE ENHANCE PRODRUG SENSITIVITY <i>IN VITRO</i>	
AND <i>IN VIVO</i>	
Abstract .....	38
Introduction .....	40
Results .....	43
Discussion.....	48
Acknowledgements.....	55
Materials and Methods .....	56

References .....	62
Figure Legends .....	65
Tables and Figures .....	68
3. MUTATIONS AT SERINE 37 IN MOUSE GUANYLATE KINASE CONFER	
RESISTANCE TO 6-THIOGUANINE	
Abstract .....	75
Introduction .....	76
Materials and Methods .....	79
Results .....	83
Discussion .....	87
Funding .....	91
Acknowledgement .....	91
References .....	92
Figure Legends .....	93
Tables and Figures .....	96
4. BACTERIAL CYTOSINE DEAMINASE MUTANTS CREATED BY MOLECULAR	
ENGINEERING DEMONSTRATE IMPROVED 5FC-MEDIATED CELL KILLING	
<i>IN VITRO AND IN VIVO</i>	
Abstract .....	101
Introduction .....	102
Materials and Methods .....	103
Results and Discussion.....	107
References .....	117
Figure Legends .....	120
Acknowledgements.....	122
Tables and Figures .....	123
Supplementary Information .....	128

5. ENGINEERING NOVEL FUSION ENZYME CYTOSINE DEAMINASE/URACIL PHOSPHORIBOSYLTRANSFERASE FOR IMPROVED CANCER GENE THERAPY	
Abstract .....	130
Introduction .....	132
Materials and Methods .....	135
Results .....	145
Discussion .....	151
Future Work .....	154
References .....	157
6. SUMMARY .....	159
References .....	166

## LIST OF TABLES

	Page
1.1 Key differences between the <i>E. coli</i> (bCD) and <i>S. cerevisiae</i> (yCD) ..... 14 cytosine deaminases	14
1.2 Kinetic properties of wild type HSV-TK and HSV-TK mutants..... 26	26
2.1 <i>In vitro</i> response of rat C6 glioma cells expressing wild type,..... 68 mutant HSVTKs, wild type fusion or mutant fusion constructs to GCV	68
2.2 <i>In vivo</i> response of rat C6 tumors expressing wild type HSVTK, ..... 68 mutant 30, MGMK/HSVTK or MGMK/30 to PBS or GCV treatment	68
2.3 <i>In vivo</i> response of rat C6 tumors expressing SR39 or MGMK/SR39 ..... 69 to PBS or GCV treatment	69
3.1 Growth pattern profile in <i>E. coli</i> ..... 96	96
3.2 Kinetic parameters of wild-type MGMK and S37 mutants..... 96	96
4.1 Enzyme Kinetics of wild-type bCD and bCD mutants ..... 123	123
S4.1 List of oligonucleotides..... 128	128
S4.2 DNA sequence analysis of bCD mutants ..... 129	129
S4.3 Crystallography statistics from data collection and refinement ..... 129	129
5.1 List of oligonucleotides..... 144	144
5.2 Kinetic parameters of wild-type bUPRT and bUPRT mutants ..... 150	150

## LIST of FIGURES

	Page
1.1 Schematic representation of suicide gene therapy .....	3
1.2 Structure of Thymidine, GCV and ACV .....	9
1.3 Activation of GCV by HSVTK .....	9
1.4 Cytosine Deaminase catalyzes the deamination of cytosine to uracil and 5FC to 5FU .....	10
1.5 5FC metabolites and their fates in the pyrimidine metabolism pathway .	12
1.6 Crystal structure of bCD and yCD .....	15
1.7 Regio-specific random mutagenesis methodology .....	23
2.1 GCV sensitivity assays of rat C6 transfectants.....	70
2.2 Bystander analysis of rat C6 transfectants in the presence of GCV.....	71
2.3 Tumor growth during and after GCV treatment in xenograft tumor model .....	72
2.4 Bystander xenograft tumor model of mutant 30 and MGMK/30 .....	73
2.5 Bystander xenograft tumor model of SR39 and MGMK/SR39.....	74
3.1 Schematic of active site with the location of S37 and T83 with respect to guanine in MGMK .....	97
3.2 Functional complementation of the conditional guanylate kinase strain <i>E. coli</i> TS202A(DE3) by wild type and mutant mouse guanylate kinases .....	98
3.3 Growth of conditional GMK-deficient strain TS202A(DE3) harboring vector, wild-type mgmk and mgmk mutants.....	99
3.4 Guanylate kinase enzyme assay of purified wild-type and mutant GMKs.....	100
4.1 Cartoon diagram of wild-type bCD monomer .....	123

4.2	5FC sensitivity assays of cells stably transfected with wild-type or mutant bCDs .....	124
4.3	Bystander analysis of stable transfectants to 5FC and HPLC analysis of mutant 1525.....	125
4.4	Tumor growth during and after 5FC treatment in a xenograft model ...	126
4.5	Electron density for bound substrate analogue 2-hydroxypyrimidine (or dihydroxypyrimidine, DHP) (left) and 5-fluoro-DHP (right) bound in the active site of bCD .....	127
5.1	5FC metabolites and their fates in the pyrimidine metabolism pathway	133
5.2	<i>In vitro</i> response of fusion CD/UPRT to 5FC in rat C6 cells.....	147
5.3	<i>In vitro</i> bystander response of fusion CD/UPRT to 5FC in rat C6 cells..	148
5.4	<i>In vitro</i> cytotoxic assays of UPRT mutants .....	150

# CHAPTER ONE

## Introduction

Cancer can be generally defined as the uncontrollable growth and spread of abnormal cells. It is the second leading cause of death in United States after heart disease. In the U.S alone, approximately 1.5 million new cases of cancer are expected to be diagnosed annually and approximately 565,650 Americans were expected to die of cancer in 2008. Even though cancer remains a major health concern in the US and around the world, advances in technology have produced reliable and effective treatments that allow patients to combat cancer. Of these treatments, chemotherapy, radiation, and surgery are standard treatments widely used to fight cancer. Depending on the tumor stage, surgical resection may or may not result in complete tumor regression and oftentimes, combinations of treatments are needed to achieve complete tumor regression. While the sole purpose of cancer treatment is to rapidly and effectively eradicate tumor cells without destroying normal cells, chemotherapy and radiation do not specifically kill tumor cells, but instead they destroy all dividing cells including normal cells. The effectiveness of these standard treatments is also frequently hindered by the emergence of drug-resistant and radiation-resistant tumor cells. For example, hypoxic regions, which have a very low oxygen level, have proven to be highly resistant to both of these treatments<sup>1</sup>. In addition, chemotherapy and radiation have short-term negative side effects, such as hair loss, drastic weight loss, extreme fatigue, and constant nausea. Long-term effects, such as infertility, organ damage, and cataracts have also been reported ([www.cancer.org](http://www.cancer.org)). Most importantly, exposure to these treatments may further induce genetic mutations, which in turn may cause the development of

another form of cancer. For example, according to the American Cancer Society, one may develop leukemia due to bone marrow cell damage from radiation. Several studies have also reported the appearance of secondary cancer following these treatments<sup>2,3</sup>.

The quest to discover safer and more potent cancer treatments is being pursued by scientists around the globe. Numerous cancer therapies are currently under investigation in preclinical studies and clinical trials, many of which will be introduced to the public in the foreseeable future. One of the relatively new and promising treatments for cancer is suicide gene therapy. This approach is based on the delivery to and expression of the suicide gene exclusively in tumor cells. Following non-toxic prodrug administration, the prodrug is converted to a toxic compound by the actions of the gene product (Figure 1.1). The general mode of action of most prodrugs is by interfering with DNA synthesis, which consequently results in tumor cell apoptosis<sup>4</sup>. The toxicity of these drugs can be maximized in cancer cells as they inherently proliferate at much faster rate than normal cells. Because of the ability to preferentially deliver the genes to tumor cells, this strategy offers selective tumor killing and thus spares normal healthy cells, a luxury that standard chemotherapeutic and radiotherapy approaches do not offer. Even though suicide gene therapy is a fairly new anti-cancer treatment, it was originally described more than two decades ago in 1986 by Moolten<sup>5</sup>. He also described the existence of bystander effect, a fundamental feature of suicide gene therapy<sup>5</sup>. By definition, the bystander effect can be described as the extension of killing effects from transfected cells to non-transfected neighboring tumor cells<sup>4,6,7</sup>. This phenomenon is crucial to the overall efficiency of suicide gene therapy due to the low transfection efficiencies achieved by current delivery systems, and is also the reason that complete tumor regression can be achieved when only a small subpopulation of tumor cells are successfully transfected<sup>8-10</sup>. The bystander effect occurs via two major mechanisms:



local and immune-mediated<sup>4</sup>. The local mechanism involves the killing of untransfected nearby cells due to the transfer of toxic materials through gap junctions, apoptotic vesicles, or through diffusion of soluble toxic metabolites<sup>4,11,12</sup>. Gap junctions are vital in cell-cell interactions and are responsible for the transfer of ions, nucleotides, and small molecules, to adjacent cells<sup>6,13</sup>. The transfer of toxic drugs through gap junctions, however, has some limitations because certain types of tumors, such as breast tumors, have been reported to down regulate intracellular gap junction communication, and in turn disorganized and non-functional gap junctions are created<sup>4,6,13</sup>.

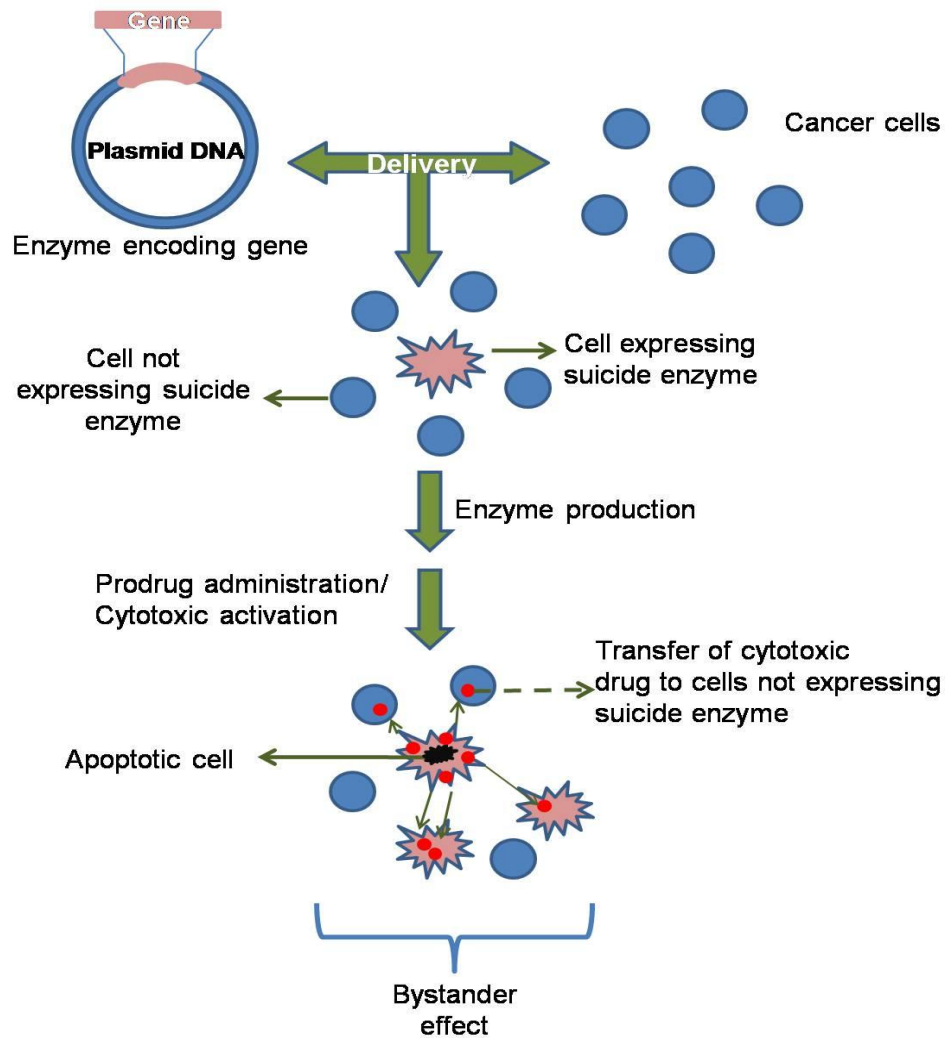


**Figure 1.1.** Schematic representation of suicide gene therapy.

Many studies have been initiated to take advantage of the bystander effect. For example, up-regulation of connexins (Cx), which are the building blocks of gap junctions, has been shown to enhance bystander and killing effects of suicide gene therapy<sup>4</sup>. From the immune-mediated perspective, it has been reported that following suicide gene administration, the immune system releases cytokines and chemokines<sup>8</sup>. These cytokines and chemokines further induce the production of immuno-regulatory molecules able to stimulate a more robust anti-cancer effect. Additionally, because death of transfected cells is through apoptosis, numerous inflammatory signals are released to evoke a potent immune response<sup>4,8,12</sup>.

In general, the success of suicide gene therapy relies upon several key factors. First, the suicide gene must be efficiently and selectively transfected to cancerous cells, limiting expression to tumor sites. The selectivity of suicide gene therapy towards cancer cells is primarily due to the vector or the delivery vehicle. This subject will be discussed in more detail in the "suicide gene therapy improvements" section. Another equally important aspect for the success of suicide gene therapy is achieving clinically relevant gene expression levels. Implied in this statement is that a high percentage of, if not all, cancer cells must be transfected in order to produce sufficient amounts of suicide enzyme. Even though significant improvements and advances in gene delivery have been seen especially within the past decade, current delivery methods are still limited and unable to effectively deliver the suicide gene to all target cells. Therefore, it is imperative that the most appropriate suicide enzyme and prodrug combination be utilized to achieve tumor killing. In theory, the best suicide enzyme/prodrug combinations must follow these criteria: 1) the suicide enzyme must be exclusively expressed in tumor cells or at least be expressed at significantly higher levels within tumor cells when compared to normal cells; 2) the suicide enzyme should have high catalytic activity towards the prodrug in order to rapidly and efficiently convert the prodrug even when present at

low concentrations; 3) the prodrug should be tolerable and does not cause any toxicity to normal cells; 4) the expression of the suicide enzyme itself should not cause any significant toxicity; and 5) a strong bystander effect should take place.

Since the first description of suicide gene therapy in 1986, hundreds of clinical trials have been conducted worldwide that contain various elements of GDEPT (gene-directed enzyme prodrug therapy) strategies. As of June 2007, three of these trials have advanced to phase III multicenter programs<sup>14,15</sup>. Currently, there are 22 suicide gene therapy/prodrug systems described in the literature<sup>16</sup>. Among these are several systems that will be briefly described in the next section. The two most studied and widely used system, Herpes Simplex Virus thymidine kinase/ganciclovir (HSVTK/GCV) and cytosine deaminase/5-fluorocytosine (CD/5FC), are the main focus of this dissertation and will be further described in greater details. It is important to note that the use of non-human suicide enzymes, such as HSVTK and CD can be more beneficial in suicide gene therapy compared to human-origin suicide enzymes because, for instance, normal tissue damage that may occur due to activation of the anti-metabolites in non-transfected tissues by human-origin suicide enzymes can be minimized.

### **Nitroreductase/CB1954 Dinitrobenzamide Mustards**

Nitroreductases (NTR) are enzymes that are able to reduce nitroaromatic groups to hydroxylamines and amines<sup>17</sup>. NTR has been evaluated for use in suicide gene therapy in conjunction with the mustard prodrug CB1954 (5-(aziridin-1-yl)-2,4-dinitrobenzamide). CB1954 is a weak monofunctional alkylator and in humans it can be activated by the enzyme DT diaphorase into a potent DNA cross-linking agent<sup>18</sup>. *E. coli* nitroreductase (NTR) catalyzes this reaction approximately 100-fold faster than the human DT diaphorase and is able to convert CB1954 to a cytotoxin when expressed in mammalian cells<sup>19,20</sup>. Activated CB1954 is a powerful cell killer, causing

p53-independent apoptosis initiated by the inhibition of DNA function resulted from the induction of highly toxic interstrand and difficult to repair crosslinks<sup>17</sup>. The NTR/CB1954 system appears to act more rapidly than most enzyme/prodrug combinations, which may be due to the fact that the activated drug is able to kill both proliferating and non-proliferating cells<sup>17</sup>. Its efficacy has been well documented *in vitro*, in animal xenograft tumor models, and in pre-clinical studies<sup>17,21,22</sup>. An efficient bystander effect was also demonstrated in a number of cell lines and in animal models, regardless of cell-to-cell contact and gap junction status<sup>23</sup>.

### **Cytochrome P450/Cyclophosphamide (CP)**

The oxazaphosphorine prodrug cyclophosphamide (CP) is activated by liver cytochrome P450 (CYP) into its 4-hydroxy-forms, which are instable metabolites and are prone to decay into phosphoramidate mustard. Phosphoramidate mustards mediate DNA alkylation, which leads to DNA cross-links, G2-M arrest and apoptosis in a cycle-independent fashion<sup>17</sup>. A strong bystander effect is usually associated with this system due to freely diffusible 4-hydroxy metabolites that, in contrast to phosphoramidate mustards, are able to efficiently enter tumor cells<sup>17</sup>. The isomeric analogue isophosphamide (IP) is activated in a similar way. Overexpression of CYP enzymes in genetically engineered tumor cells lead to selective sensitization to oxazaphosphorines<sup>24-26</sup>. In co-culture experiments, 75% decrease in proliferation was induced when only 10% of the CP-exposed population expressed CYP2B1, independently of cell-to-cell contact<sup>25,26</sup>.

### **Carboxypeptidase G2 (CPG2)/CMDA**

The suicide enzyme carboxypeptidase G2 (CPG2), derived from *Pseudomonas* strain RS-16, has no human analogue and is able to cleave the glutamic acid moiety

from the prodrug 4-((2-chloroethyl)(2-mesyloxyethyl)amino)benzoyl-L-glutamic acid (CMDA), releasing the DNA-cross-linking mustard drug 4-((2-chloroethyl)(2-mesyloxyethyl)amino)benzoic acid without further catalytic requirements. The application of the CPG2/CMDA combination in prodrug gene therapy applications leads to an increase in sensitivity among transfected cells as shown in reduction in  $IC_{50}$  values ranging from 11- to 95-fold<sup>27</sup>. The CPG2/CMDA system has been shown to induce a robust bystander effect that seems to be mediated independent of gap junctions<sup>17</sup>.

### **Deoxycytidine Kinase/Gemcitabine**

Human deoxycytidine kinase (dCK) is an important enzyme in the salvage pathway of deoxyribonucleotides. Like HSVTK, dCK has a broad substrate specificity and is able to phosphorylate deoxycytidine and related analogues, such as gemcitabine (dFdC or 2', 2'-difluorodeoxycytidine) and cytosine arabinoside (araC or 1- $\beta$ -D-arabinofuranosylcytidine)<sup>28,29</sup>. Gemcitabine, by itself, is currently used as an anticancer agent to treat solid tumors, such as pancreatic adenocarcinomas, and head and neck malignancies<sup>30</sup>. Endogenously, dCK is active in resting and proliferating leukocytes although dCK lacks activity in liver, brain and heart<sup>31,32</sup>. Recent attempts to utilize deoxycytidine kinase as a suicide gene have been only partially successful<sup>28,29</sup>. One caveat is that low level expression of dCK in normal cells precludes use of therapeutic doses of araC or gemcitabine without toxicity to normal cells. And in addition, a minimal bystander effect is observed with dCK in the presence of gemcitabine probably due to a low amount of the phosphorylated product<sup>28</sup>.

### **Herpes Simplex Virus Thymidine Kinase/Ganciclovir (HSVTK/GCV)**

Thymidine kinase is an enzyme in the pyrimidine salvage pathway that catalyzes the transfer of  $\gamma$ -phosphate from ATP to thymidine to form dTMP<sup>20</sup>. Unlike human thymidine kinase, HSVTK has a broad substrate specificity. HSVTK, a dimer of 45 kDa subunits, is able to phosphorylate pyrimidines, pyrimidine analogues (thymidine, deoxycytidine, and azidothymidine), and purine analogues (ganciclovir, acyclovir, buciclovir, and penciclovir) (Figure 1.2)<sup>33-35</sup>. One purine analogue, ganciclovir (GCV), is currently being used in combination with HSVTK in numerous clinical trials for cancer. GCV was initially designed as an antiviral agent to treat Human Cytomegalovirus, Herpes Simplex Virus type 1 and 2, Varicella Zoster Virus, and Epstein-Barr Virus infections<sup>36</sup>. Following initial phosphorylation by HSVTK, GCV is further phosphorylated by cellular kinases to its toxic triphosphate form (GCV-TP) (Figure 1.3)<sup>36,37</sup>. Even though GCV-TP is the predominant toxic form of the prodrug, the exact mechanism of GCV-mediated toxicity in cells is less well understood. Unlike acyclovir (ACV) that has only one hydroxyl group in its acyclic 'sugar' moiety, causing immediate chain termination following incorporation into DNA, GCV has two hydroxyl groups and can also be incorporated into the elongating DNA chain<sup>38</sup>. However, some may argue that although GCV has two hydroxyl groups, the lack of a complete sugar ring makes GCV-TP a poor substrate for DNA synthesis and chain termination occurs upon its incorporation<sup>36</sup>. GCV-TP is a highly charged molecule insoluble in lipid membranes and cannot passively diffuse across the membrane. Because of this, the HSVTK/GCV system relies heavily on the transfer of activated prodrug through direct cell-cell contact via gap junctions for the bystander effect to occur. ACV was originally considered as an alternative prodrug because of its low toxicity but the  $K_m$  value of wild type HSVTK for ACV is extremely high ( $K_m > 400 \mu\text{M}$ ) and thus preclude its use with HSVTK in suicide gene therapy applications<sup>39</sup>.

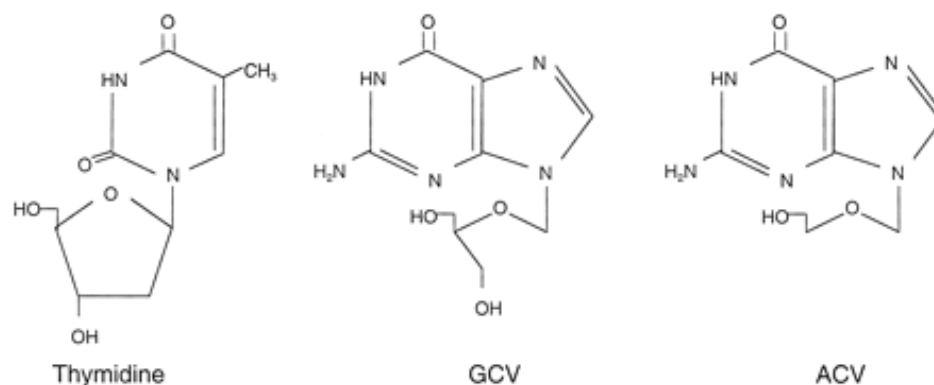
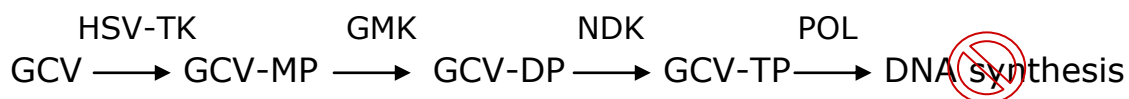


**Figure 1.2.** Structures of Thymidine, GCV and ACV.

While HSVTK is responsible for the first phosphorylation step of GCV or ACV, guanylate kinase (GMK) is responsible for its conversion to the diphosphate form. Guanylate kinase is an essential endogenous enzyme that catalyzes the phosphorylation of guanosine 5'-monophosphate (GMP) and dGMP to form guanosine 5'-diphosphate (GDP) and dGDP, respectively<sup>40</sup>. As such, this enzyme is important in the biosynthesis of guanosine 5'-triphosphate (GTP). In addition, GMK serves in the activation pathway of other anticancer drugs, such as 6-thioguanine (6TG) and 6-mercaptopurine<sup>41</sup>.



HSVTK:	Herpes Simplex Virus Thymidine Kinase
GMK:	Guanylate Kinase
NDK:	Nucleoside diphosphokinase
POL:	Polymerase
GCV-MP:	Ganciclovir-monophosphate
GCV-DP:	Ganciclovir-diphosphate
GCV-TP:	Ganciclovir-triphosphate

**Figure 1.3.** Activation of GCV by HSVTK. GCV and ACV are initially phosphorylated by HSVTK and subsequent phosphorylation to di- and tri-phosphate forms are performed by endogenous GMK and NDK. The GCV-TP is incorporated into nascent DNA synthesis by DNA polymerase (POL) during cell division, inhibiting DNA synthesis and ultimately resulting in cell death.

### Cytosine Deaminase/5-Fluorocytosine (CD/5FC)

Cytosine deaminase (CD) is an enzyme in the pyrimidine salvage pathway and catalyzes the deamination of cytosine to uracil and ammonia<sup>42</sup>. This enzyme is absent in mammals and uniquely present in fungi and bacteria. It is used in suicide gene therapy because of its ability to deaminate 5-fluorocytosine (5FC), an antifungal drug, to 5-fluorouracil (5FU), a potent anti-tumor drug (Figure 1.4). 5FC, one of the oldest antifungal agents, was originally synthesized in 1957 as a potential antitumor agent but was later found to not be sufficiently active against tumors<sup>43</sup>.

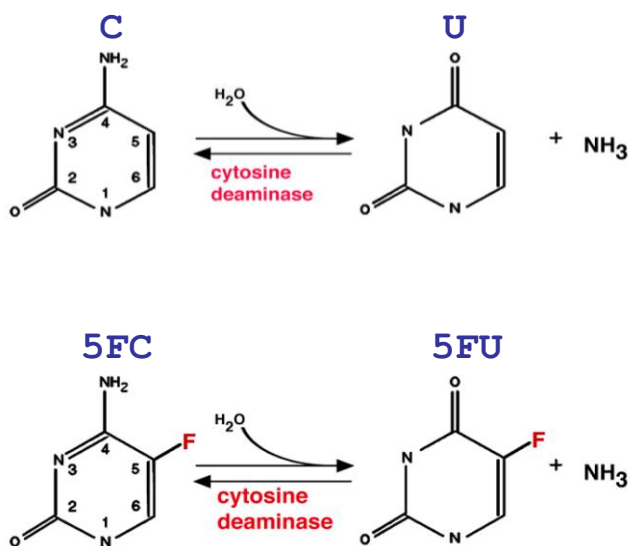


**Figure 1.4.** Cytosine deaminase catalyzes the deamination of cytosine to uracil and 5FC to 5FU.

Years later, however, 5FC was found to be effective in treating human candidosis, cryptococcosis and against fungi causing chromoblastomycosis<sup>43</sup>. In 1985, 5FC regained attention as an anti-cancer drug when one study demonstrated local antineoplastic activity at tumor sites which had been locally implanted with capsules containing CD enzyme followed by systemic administration of 5FC in an *in vivo* model<sup>44</sup>. However, it was not until 1993 when the bacterial CD (bCD) gene became available, that the use of bCD in combination with 5FC transformed into a



promising gene therapy approach for cancer<sup>45</sup>. The active antimetabolite of 5FC, 5FU, was developed in the 1950s as an anticancer agent. 5FU has a fluorine atom at the C-5 position in place of hydrogen and has been widely used as a first line chemotherapeutic regimen to treat colorectal, breast and prostate cancers<sup>46</sup>. In human cells, 5FU is converted into several active metabolites: 5-fluoro-2'-deoxyuridine 5'-monophosphate (5FdUMP), 5-fluorodeoxyuridine-triphosphate (5FdUTP) and 5-fluorouridine-triphosphate (5FUTP) (Figure 1.5), which can cause cell apoptosis via three different mechanisms. The first mechanism of action, which is considered the major cause of cellular death, is the inhibition of thymidylate synthase (TS) by 5FdUMP. Endogenously, TS catalyzes the reductive methylation of deoxyuridine monophosphate (dUMP) to deoxythymidine monophosphate (dTMP), with reduced folate 5,10-methylenetetrahydrofolate (CH<sub>2</sub>THF) as the methyl donor. This reaction is important in DNA synthesis as it provides the sole *de novo* source of thymidylate, necessary for dTTP production and subsequent DNA replication and repair. When 5FdUMP is present in the cell it can form an irreversible covalent bond with TS and together with CH<sub>2</sub>THF, 5FdUMP and TS can ultimately form a stable ternary complex blocking the binding of the normal substrate dUMP and as a result inhibits dTMP synthesis<sup>46</sup>.

Depletion of dTMP pools results in reduced dTTP levels, which can also disturb the normal levels of other deoxynucleotides (dATP, dGTP, and dCTP) through various feedback mechanisms<sup>46</sup>. Consequently, imbalanced deoxynucleotide pools are thought to severely disrupt DNA synthesis and repair, oftentimes resulting in lethal DNA damage. The second mechanism of action of 5FU is the misincorporation of 5FdUTP during DNA synthesis. This misincorporation is repaired by the nucleotide excision repair enzyme uracil-N-glycosylase (UNG). However, the repair is generally futile and results in further false-nucleotide incorporation, which ultimately causes DNA strand breaks and cell death<sup>46</sup>. The third mechanism of action of 5FU is the

incorporation of 5FUTP into RNA, which can interrupt normal RNA processing and function. For example, it is thought that 5FUTP misincorporation into RNA can not only inhibit the processing of pre-rRNA into mature rRNA and disrupt post-translational modification of tRNAs, but also prevent splicing of pre-mRNAs<sup>46</sup>.

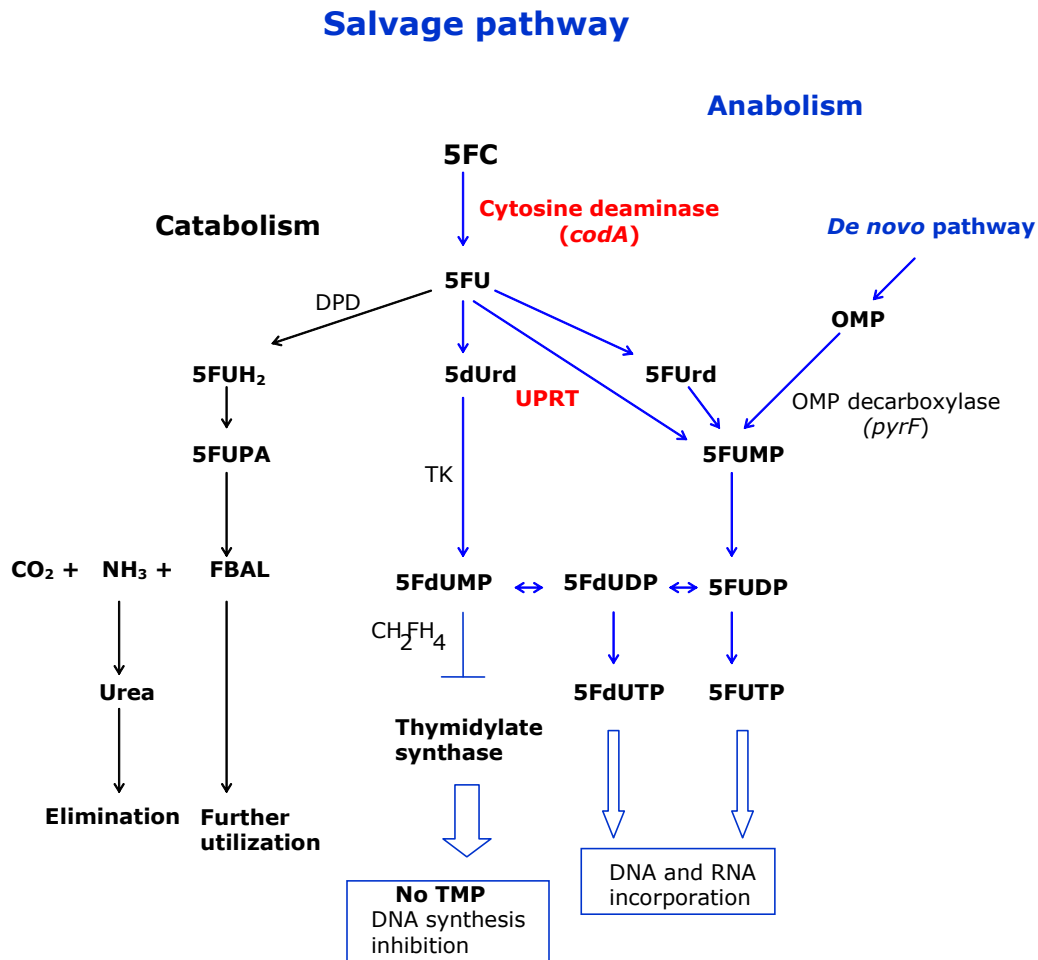


**Figure 1.5.** 5FC metabolites and their fates in the pyrimidine metabolism pathway. DPD: dihydropyrimidine dehydrogenase, TK: thymidine kinase, UPRT: uracil phosphoribosyltransferase, OMP: orotidine-5'-monophosphate,  $\text{CH}_2\text{FH}_4$ :  $N^5, N^{10}$ -methylenetetrahydrofolate, 5FUH<sub>2</sub>: 5,6-dihydro-5-fluorouracil, 5FUPA: 5- $\alpha$ -fluoro- $\beta$ -ureidopropionic acid, 5- $\alpha$ -fluoro- $\beta$ -alanine. Enzymes highlighted in red and bold (CD and UPRT) are absent in mammals.

Despite its high level of toxicity to normal cells, 5FU-based chemotherapy has improved overall survival and led to disease-free patients with resected stage III colorectal cancer. Nonetheless, with only a 10-15% response rates seen in 5FU-

based chemotherapy and the emergence of 5FU-resistant cancer cells, new therapeutic strategies are needed. 5FU-resistant cancer cells develop due to a number of factors, but the key factor of 5FU resistance is most likely the high levels of TS expression in cancer cells. Indeed, many studies have successfully demonstrated that overexpression of TS correlates with poor prognosis and low survival rates in colorectal, gastric, breast and lung cancers<sup>46</sup>. The overexpression and/or high levels of dihydropyrimidine dehydrogenase (DPD), which is an enzyme responsible in 5FU catabolism and converts 5FU its inactive form dihydrofluorouracil (DFHU), can also be responsible for generating 5FU-resistant cells<sup>46</sup>. Normally, DPD catabolizes more than 80% of administered 5FU in the liver where DPD is abundantly expressed. Because of the emergence of 5FU-resistant cells and low response rates to 5FU-based chemotherapy, combinational treatments using newer chemotherapies with improved response rates have been adapted in the clinic. For example, the chemotherapy drug leucovorin is often used to modulate 5FU regimens to obtain better response rates. Specifically, following cell entry, leucovorin is anabolized to form CH<sub>2</sub>THF and as a result can lead to high levels of CH<sub>2</sub>THF. These high levels of CH<sub>2</sub>THF subsequently lead to more optimal binding of 5FdUMP to TS. This stable ternary complex between CH<sub>2</sub>THF, TS and 5FdUMP in turn prevents TS from performing its normal function<sup>46</sup>. Unfortunately, while a combination treatment of leucovorin and 5FU shows significant improvements in the response rates of advanced colorectal cancer patients compared to the single treatment with 5FU, no improved overall survival rates were observed<sup>46</sup>.

Bacterial CD (bCD) and yeast CD (yCD) are two different CD enzymes are currently being pursued for their use in suicide gene therapy. While the two enzymes have similar functions, they have evolved independently. For example, both enzymes have different distinct characteristics at several levels: primary

sequence, quaternary structure, metal requirements, relative substrate specificities and affinities, and thermostability (Table 1.1 and Figure 1.6).

**Table 1.1.** Key differences between the *E. coli* (bCD) and *S. cerevisiae* (yCD) cytosine deaminases.

	<u><i>E. coli</i></u>	<u><i>S. cerevisiae</i></u>
Monomer size	48 kDa	17.5 kDa
Fold	TIM Barrel	Amidohydrolase
Active Enzyme	Hexamer	Homodimer
Catalytic metal	Iron	Zinc
Half life @ 37°C	>100 hrs	< 6 hrs
Kinetic Parameters		
cytosine		
$K_m$	0.2 mM	1.17 mM
$k_{cat}$	165 s <sup>-1</sup>	170 s <sup>-1</sup>
$k_{cat}/K_m$	825 s <sup>-1</sup> /mM	145 s <sup>-1</sup> /mM
5FC		
$K_m$	3.3 mM	0.083mM
$k_{cat}$	75.6 s <sup>-1</sup>	18.8 s <sup>-1</sup>
$k_{cat}/K_m$	23 s <sup>-1</sup> /mM	226 s <sup>-1</sup> /mM

One of the advantages of utilizing CD/5FC in suicide gene therapy compared to HSVTK/GCV is that the bystander effect mediated by this system is not dependent upon gap junctions. This is due to 5FU being a small, uncharged molecule giving it the ability to diffuse through cellular membranes. Another advantage of the CD/5FC system that can be clinically beneficial in patients is the ability of 5FC to cross the blood-brain barrier, a unique property that 5FU lacks<sup>43</sup>. An additional benefit of this approach is that 5FU has radiosensitizing properties, which is important since it is unlikely that suicide gene therapy would be the only course of action in cancer patients<sup>47</sup>. Despite this advantage, the presence of bacteria in the intestinal flora pose serious problems as they can utilize 5FC leading to normal cell killing and unwanted side effects<sup>43</sup>.

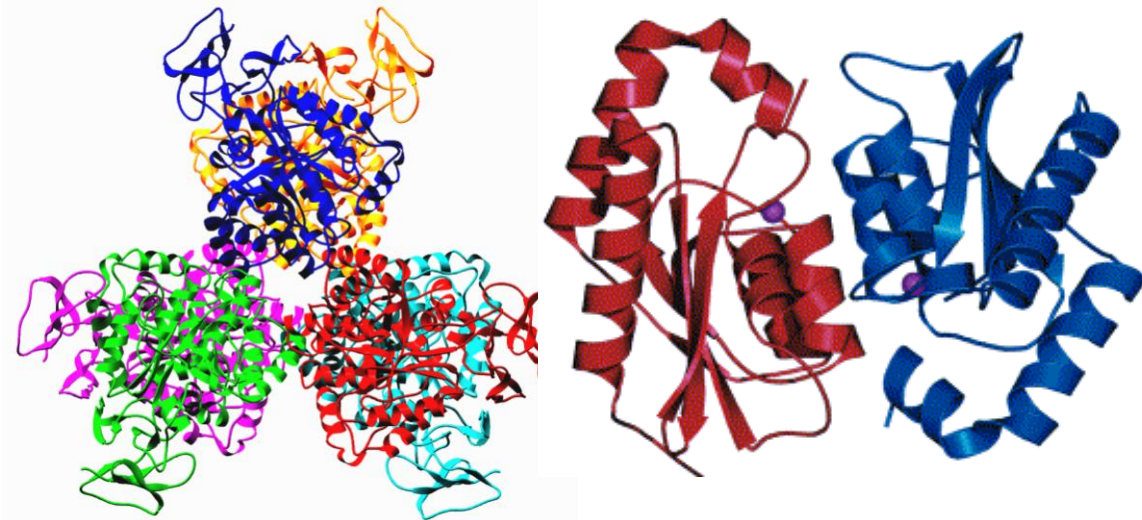


**Figure 1.6.** Crystal structures of bCD (left) and yCD (right)<sup>48,49</sup>.

### **Suicide Gene Therapy Improvements**

#### Overview of suicide gene therapy delivery

Even though suicide gene therapy for cancer has shown promising results *in vitro*, in animal models, and to some extent in clinical trials, it has yet proven to be completely fruitful. The major limitation in the suicide gene therapy field is having safe and tumor-specific delivery vehicles with exceptional efficacy and specificity to transfer genes to cancer cells. This problem is exacerbated by another major limiting factor: the poor prodrug converting activity of the suicide enzymes used in this therapy. Combined together, this creates a serious predicament since it can be difficult to achieve clinically relevant doses without inducing toxicities. In general, the suicide gene is delivered into tumor cells via viral, non-viral, bacterial vectors or via cell carriers. Viral vectors are the most studied delivery systems for suicide gene therapy. In most cases, viral vectors have better transfection efficiencies although they may have more safety issues than nonviral vectors as direct injection of viral vectors into patients' bloodstream can induce strong inflammatory responses. Another promising approach is to use stem cells or immune cells (dendritic cells, T

cells, and B cells) in carrier cells approach<sup>50,51</sup>. Nonviral vectors, such as liposomes, polymers, peptides, and proteins are safer than viral vectors but have much lower transfection efficiencies and therefore not as effective. Bacteria, similarly to viruses, have the ability to infect and lyse cells including tumor cells. Therefore, the idea of using bacteria, such as *Salmonella*, *Clostridium*, and *Bifidobacterium* as delivery vehicles has recently become popular and several studies have been performed<sup>4,52-54</sup>. Despite the fact that non-viral, bacterial, and T-cell based delivery vectors continue to attract interest, viral-based delivery systems are still the most efficient<sup>55</sup>. These next paragraphs are geared towards viral-, cell carriers- and bacterial-based therapy for cancer as advances in these fields are paramount compared to non-viral-based delivery.

To overcome the limitations of gene delivery, numerous studies aimed at enhancing transduction efficiency, improving specific tumor targeting, and increasing the bio-safety of viral vectors have been and are currently being pursued. For example, viral vectors can be engineered to target distinct antigens on the surface of tumor cells, such as the carcinoembryonic antigen or prostate-specific antigen<sup>55,56</sup>. Another example is improving tumor-specific targeting by pseudo-typing or a complete substitution of the envelope protein with that from a different virus<sup>57</sup>. Another way to achieve greater tumor selectivity is by attaching particular ligands, such as sequences from erythropoietin or EGF, onto the extracellular domain of the envelope glycoprotein<sup>55</sup>. In general, there are two kinds of viral vectors being pursued: oncolytic viruses (replication-competent) and non-oncolytic viruses (replication-defective). Herpes simplex virus, measles virus, and certain replication-competent adenoviruses are examples of oncolytic viruses. Because of their specificity to replicate in and lyse tumor cells, oncolytic viruses offer more powerful anti-cancer activity than non-oncolytic viruses. This is especially attractive and beneficial in treating distant metastatic tumor cells<sup>57</sup>. However, the inability to

control viral spread, replication and non-specific tissue destruction continues to raise bio-safety concerns with the use of oncolytic viruses in gene therapy. Furthermore, oncolytic adenoviruses are known to cause an acute inflammatory response within 6-24 hours upon first administration<sup>58</sup>. Because of their inherent toxicity and difficulty to control, scientists have been searching for safer alternatives to oncolytic viruses. One alternative is to utilize naturally non-oncolytic viruses and to engineer replication-deficient viruses.

Retrovirus, lentivirus, and AAV vectors are some examples of natural non-oncolytic viruses. Replication-defective adenoviruses have been constructed as well. Retroviruses have been predominantly investigated for gene therapy for inherited genetic diseases. The reason is that retroviral vectors actively integrate proviral DNA into the host cell genome and this offers the potential for long-term cure of inherited genetic diseases, such as cystic fibrosis, severe immune combined immunodeficiency (SCID), and  $\beta$ -thalassemia<sup>57,59</sup>. However, it has been reported in the first successful clinical trial in SCID patients that three out of eleven participants developed T-cell leukemia almost three years after the treatment, and subsequently resulted in the death of one patient<sup>59,60</sup>. The random integration of proviral DNA close to the promoter of the LMO2 proto-oncogene, which leads to abnormal expression of the LMO2 protein is believed to be the cause of the spontaneous development of leukemia in these patients<sup>59</sup>. Non-oncolytic adenovirus and AAV vectors have also been extensively studied<sup>57,59</sup>. However, because both viruses are human viruses, the presence of host neutralizing antibodies remains a major obstacle for the use of these vectors in gene therapy. Depending on the patients' age group and location, it has been shown that specific antibodies against adenovirus and AAV are detectable in 50-97% of individuals<sup>61</sup>. Such strong immunity can eliminate viral particles and reduce the chance of viral transduction of tumor cells. In addition, even though the use non-oncolytic adenoviruses is believed to have

lower toxicity than oncolytic adenoviruses, the idea of using replication-defective adenovirus was seriously questioned after the use of adenovirus expressing ornithine transcarbamylase (OTC) in enzyme replacement therapy caused the death of 18-year old Jesse Gelsinger in 1999 only 48 hours after virus injection<sup>58,59</sup>. Clearly, the use of both oncolytic and non-oncolytic viruses in humans may raise major safety concerns. Nevertheless, within the past few years, it appears that oncolytic viruses have garnered more attention for viral-based therapy and have also been more extensively evaluated in pre-clinical studies and in clinical trials compared to non-oncolytic viruses, mainly due to their ability to offer more robust tumor killing activity. However, because viral-based therapy is yet to provide complete cancer cures when used alone, the field has been slowly moving towards combining the oncolytic viruses with the standard radiation, chemotherapy and/or surgery treatments<sup>50</sup>. Additionally, work to improve tumor targeting and the bio-safety of oncolytic viruses, for example by inserting organ-specific promoters, and to help viruses evade immune clearance is underway.

One strategy to down-regulate the immune response is by benefiting the immunosuppressive side effects of certain chemotherapeutics such as cyclophosphamide (CPA)<sup>50</sup>. An alternative strategy to improve tumor targeting and shielding viruses from immune clearance, as well as reducing their ability to stimulate strong immune response, is by applying biological and chemical shields to the viral particles. Chemical shielding can be done by chemically cross-linking polymers, such as polyethylene glycol (PEG) or poly-(N-(2-hydroxypropyl)methacrylamide) (pHPMA) to viruses to protect them from neutralizing antibodies and reduce new antibody and T-cell responses<sup>50</sup>. More recently, a promising idea employing carrier cells has been evaluated *in vitro* and *in vivo*. In this approach, the use of carrier cells is exploited to conceal viruses from the host immune system, improve specific targeting to tumor site, and limit the



natural tendency of viruses to traffic to the liver, spleen, and lung<sup>50</sup>. Immune cells, such as T or B cells, and stem (progenitor) cells have been identified as potential carrier cells. Generally, carrier cells are collected from a cancer patient, infected *ex vivo* with engineered viruses and administered back to the patient systemically. These transfected carrier cells should home to tumor sites and release the virus ultimately causing tumor cell oncolysis. Although this approach is novel, it has shown promising results and is believed to have the potential to provide alternative strategies over direct injection of viruses into the bloodstream.

Another completely different strategy under consideration is to use bacteria as gene delivery vehicles to treat cancer. As early as 300 years ago, the original observation of tumor regression, or even recovery, of certain cancer patients from concurrent bacterial infections was made<sup>62</sup>. However, it was not until 1976 when Morales, Eiding and Bruce reported the success of Bacillus Calmette-Guerin (BCG) to treat superficial bladder cancer that gained this therapy significant attention in the cancer field<sup>1,62</sup>. When BCG is instilled into the bladder, it stimulates a very robust immune response and strong inflammation reactions result, a situation that is rather similar to urinary tract infections. These colossal immune responses are responsible to not only clear up the bacterial infection but to also eradicate cancerous cells in the bladder at the same time. Today, BCG has become the first line of treatment for high-risk, superficial bladder cancer in most countries for approximately 1 million patients per year<sup>62</sup>. There are two types of bacteria that have been extensively studied for this purpose: anaerobic and facultative anaerobic bacteria. The unique solid-tumor microenvironment, where hypoxic regions usually present, provides a haven for these bacteria. Currently, there are three classes of bacteria tested for cancer therapy: 1) the lactic acid, gram-positive anaerobic bacteria, such as the members of the *Bifidobacterium* genus, 2) the intracellular, gram-negative facultative anaerobes, such as certain strains of *Salmonella* and *Listeria*, and 3) the

strictly anaerobic, gram-positive saccharolytic/proteolytic bacteria, such as certain strains of *Clostridia*. Among these, work in cancer therapy using engineered clostridia has been the most promising in mouse models and in clinical trials ([www.clinicaltrials.gov/ct](http://www.clinicaltrials.gov/ct)). Nonetheless, the bacterial-based therapy for cancer is unable to provide complete cancer cures when used alone. Indeed, multimodal therapy must be used to achieve absolute tumor killing as it was shown that although destruction of a significant portion of the tumor may take place, partial tumor colonization by the bacteria could lead to re-growth of tumors from an outer rim of viable non-hypoxic tumor cells that manage to escape this treatment<sup>62</sup>. For instance, the use of genetically engineered *Clostridium* expressing the CD gene successfully enhanced the sensitivity of EMT6 carcinoma cells to 5-FC by 500-fold and ultimately resulted in increased tumor destruction<sup>62</sup>. In addition, co-administration of bacteria with several chemotherapeutics and/or radiation treatment has proven to provide synergistic and enhanced tumor killing effects<sup>1,62</sup>. However, in reality, this approach is less well-explored than viral-based cancer therapies. With the advances in technology and a deeper understanding in biology of these microorganisms, bacterial-based therapy for cancer could provide a promising and perhaps safer alternative to deliver suicide genes and cause oncolysis at tumor sites.

Despite these advances in gene delivery, however, the task to generate a perfect delivery vehicle that is safe, not immunogenic, and has the ability to target every cancerous cell is quite undertaking and is yet to be fully realized. It is imperative that the second key limitation in the gene therapy field, the poor prodrug converting activity of the suicide enzyme that severely limits successful tumor cell killing, is not ignored. Several approaches have been reported to overcome this limitation including the use of multiple gene copies to yield high expression<sup>63</sup>, synthesizing novel prodrugs for gene therapy<sup>64</sup>, the use of other chemotherapeutic drugs to modulate nucleoside metabolizing pathway<sup>65</sup>, multimodal therapies<sup>66,67</sup>, and

the use of mutant suicide genes with improved activity towards clinically relevant prodrugs<sup>33,42,68,69</sup>. For the purpose of this dissertation, the focus of the next section will be on the last approach discussed above, which is the use of mutants with improved activity towards prodrugs. Regio specific random mutagenesis has been the major approach that our laboratory employs to successfully generate superior mutants with improved activity towards their prodrugs. To begin the discussion of enzyme optimization, an overview of the regio-specific random mutagenesis scheme will be given and followed by improvements that have been taken to generate superior HSVTK, bCD and yCD variants.

#### Regio-specific random mutagenesis

Regio-specific random mutagenesis is a powerful method to introduce multiple random mutations within a target region and is designed to generate large random sequence libraries. Generally, one would target residues in the active site of an enzyme where substrate binds or target residues important in catalysis. By targeting important residues, meaningful and phenotypically desired mutants can be obtained. The first step of performing regio-specific random mutagenesis is to design one or two overlapping random oligonucleotides (Figure 1.7). The random oligonucleotides are designed not only to introduce mutations within the target region but also to exclude amino acids residues that are absolutely conserved in sequence alignments. One or both of these overlapping random nucleotides are randomized and contain sequences that code for restriction endonuclease sites at each end. The oligonucleotides are annealed and the hybrid DNA extended using DNA polymerase. The product will be double stranded DNA, which is then amplified using the Polymerase Chain Reaction (PCR). The PCR products are inserted into the corresponding region of the nonfunctional target gene. The use of positive and negative selections will enable us to identify desired mutants. Positive selection

employs the use of selection conditions/media that will only enable growth of the functional mutants. On the other hand, negative selection is a system that employs the use of restricted conditions/media that will restrict the growth of the desired mutants in the presence of prodrug. In this project, negative selection allows us to identify mutants with increased sensitivity toward the prodrug, as they will not be able to grow in the medium containing concentrations of prodrug that allow the growth of wild-type clones. This approach was used in our laboratory to successfully obtain HSVTK and CD mutants.

### Improving thymidine kinase

Unlike human TK, HSVTK has a broad substrate specificity and is able to phosphorylate purine analogues 1000-fold more efficiently than human TK<sup>7</sup>. From a medical perspective, however, wild type HSVTK still inefficiently phosphorylates GCV. The  $K_m$  value of wild type HSVTK for GCV is much higher than its  $K_m$  value for thymidine ( $K_m=47\mu\text{M}$  versus  $K_m=0.5\mu\text{M}$ )<sup>39</sup>. Because of this, although GCV is deemed to be a “non-toxic prodrug”, clinically relevant doses of GCV are high and result in undesirable side effects such as severe bone marrow toxicity and myelosuppression in patients<sup>4</sup>. There are two ways to circumvent this problem: 1) by engineering HSVTK to create mutants with increased activity to GCV and 2) by performing pathway engineering to create a fusion enzyme harboring functional TK and GMK activities as a means to shunt the prodrug to the cytotoxic agent more efficiently. Initial mutagenesis of HSVTK for gene therapy was done in 1993 when Munir *et al.* altered the substrate preference for 3'-azido-3'-deoxythymidine (AZT) and also enhanced this enzyme's thermostability<sup>70</sup>. The same technique was then used to create a larger library of variants, by targeting two conserved motifs that were previously identified to be involved in substrate binding<sup>71</sup>.

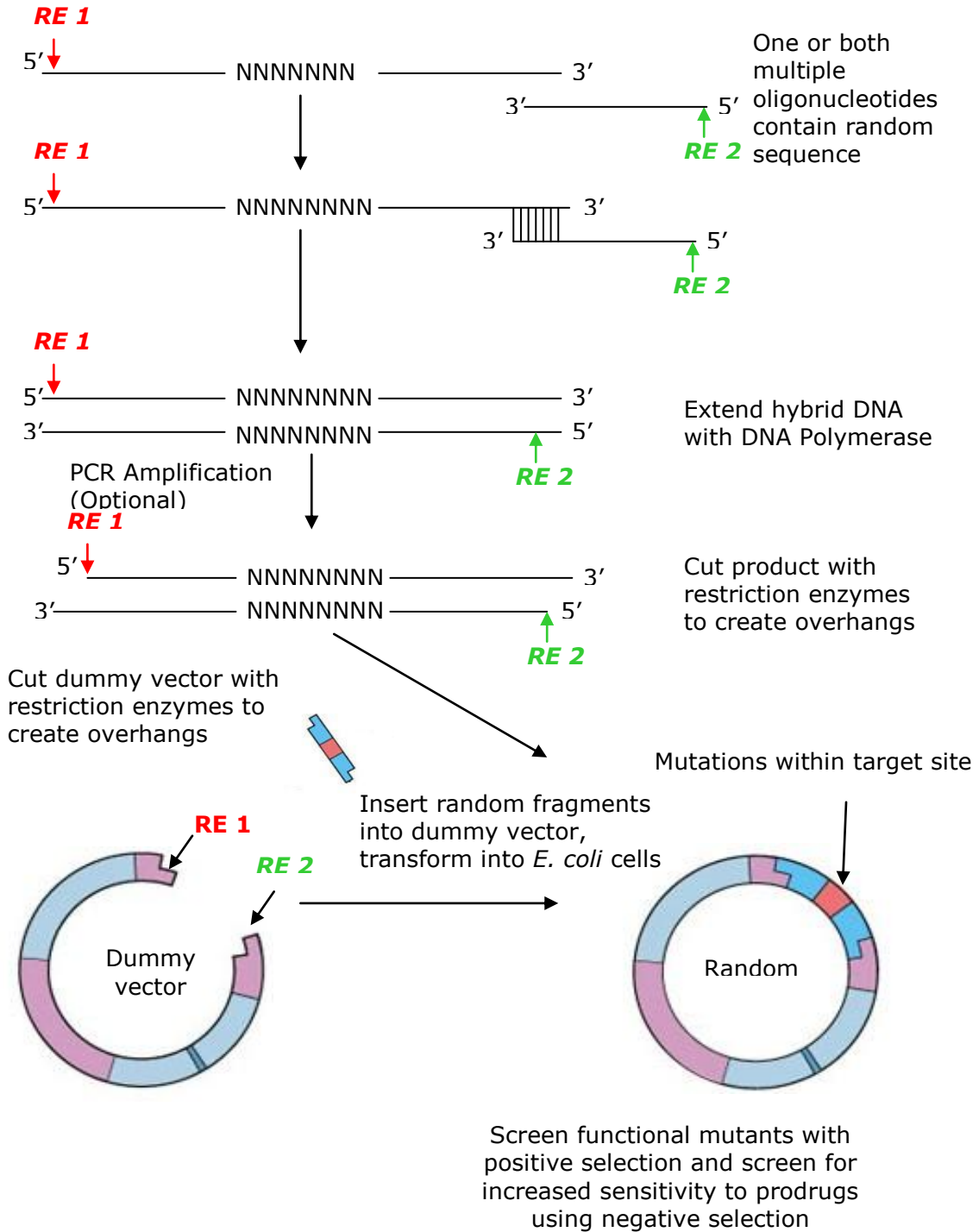


**Figure 1.7.** Regio-specific random mutagenesis methodology  
 N = Randomized residues  
 RE = Restriction enzyme

These variants were screened for increased sensitivity to either GCV or ACV, and from this large library of mutants, a total of 26 mutants displayed increased sensitivity to GCV and 54 to ACV<sup>71</sup>. Six amino acid residues were targeted in this study: Leucine(L)159, Isoleucine(I)160, Phenylalanine(F)161, Alanine(A)168, L169, and L170, therefore this library was named the "LIF-ALL" library. Another round of semi-random mutagenesis was then subsequently performed using sequence from the best mutants from the first library. From this second mutagenesis study, seven mutants were identified to have further enhanced activity to GCV or ACV. Two mutants were of particular interest due to their significant increase in activity towards to GCV. Both mutants were found to have amino acid substitutions at five of the six targeted codons (LIF-ALL) and were extensively evaluated and well characterized biochemically, *in vitro* and *in vivo*<sup>33,34,72,73</sup>. Kinetic analysis revealed that both mutants display seemingly different kinetic properties towards thymidine and GCV or ACV (Table 1.2). Relative catalytic activity, which expresses the catalytic efficiency of the mutant enzymes when both thymidine and the prodrug are present as substrates, revealed the substrate preference of these mutants for GCV or ACV is greater than that of the wild-type HSVTK. Mutant SR39 was shown to prefer GCV as its substrate 80-fold more than wild-type HSVTK (Table 1.2). Furthermore, the same mutant has been shown to successfully suppress tumor progression in mouse model tests and is currently being evaluated in clinical trials<sup>72</sup>. Kinetic analyses of mutant 30 revealed no change in overall enzyme catalytic efficacy toward GCV compared to HSVTK. When GCV is used as substrate,  $K_m$  value of mutant 30 is 7-fold higher compared to wild type HSVTK. Additionally, the turnover rate ( $k_{cat}$ ) of mutant 30 for GCV is approximately 6-fold lower than wild type, which subsequently translates to a 41-fold reduction in overall enzyme catalytic efficiency<sup>74</sup>. Therefore one might predict that mutant 30 would not elicit enhanced prodrug sensitivity to cells. However, because endogenous thymidine (natural substrate of HSVTK) within

the cell competes with the prodrug for the active site, it is important to consider how well the mutant 30 performs in catalyzing thymidine. Indeed, mutant 30 demonstrates much poorer activity towards thymidine when compared to wild type HSVTK. When thymidine is used as substrate, mutant 30 shows approximately a 3,000-fold reduction in overall enzyme catalytic efficiency compared to wild type HSVTK<sup>74</sup>. Therefore, despite its poor catalytic activity towards GCV and ACV, mutant 30 was shown to exhibit increased prodrug sensitivity *in vitro*<sup>73</sup>.

**Table 1.2.** Kinetic properties of wild type HSVTK and HSVTK mutants

Enzyme	Substrate						Relative Catalytic Activity <sup>a</sup>	
	Thymidine		Acyclovir		Ganciclovir			
	$k_{cat}$ (sec <sup>-1</sup> )	$K_m$ (μM)	$k_{cat}$ (sec <sup>-1</sup> )	$K_m$ (μM)	$k_{cat}$ (sec <sup>-1</sup> )	$K_m$ (μM)	ACV	GCV
HSVTK	0.455	0.5	0.015	417	0.102	47	1	1
SR39	0.017	2.6	0.00043	9.8	0.0035	3.3	239	80
Mut30	0.005	13	0.002	455	0.018	333	345	67

<sup>a</sup>This was calculated using the equation  $[k_{cat}/K_m(\text{prodrug})] / [k_{cat}/K_m(\text{dT}) + k_{cat}/K_m(\text{prodrug})]$

Another way to circumvent inefficient GCV activation by HSVTK is by creating a fusion enzyme of HSVTK and GMK. Previous reports have suggested that a bottleneck problem arises in the HSVTK/GCV system, leading to accumulation of ineffective intermediate products, i.e., GCV-monophosphate (GCV-MP) and GCV-diphosphate (GCV-DP)<sup>37,75</sup>. This bottleneck problem occurs presumably because endogenous GMK is limited in its ability to convert GCV-MP to GCV-DP. Indeed, the  $K_m$  value of GMK for GCV-MP is approximately 2-fold higher than its  $K_m$  value for its natural substrate, GMP<sup>40,76</sup>. This implies that higher expression of GMK is required to overcome the bottleneck problem in order to produce larger amounts of active antimetabolites. Earlier experiments co-expressing HSVTK and GMK as separate proteins failed to demonstrate notable improvements in GCV sensitivity (data not shown and Akrüyek *et al.*<sup>77</sup>). However, when a fusion enzyme encoding both

functional HSVTK and mouse GMK (MGMK/HSVTK) was created and analyzed *in vitro*, a promising story emerged. Indeed, *in vitro* cytotoxicity assays using this fusion protein demonstrated that rat C6 cells stably transfected with MGMK/HSVTK confer a ~175-fold decrease in IC<sub>50</sub> value compared to HSVTK alone in response to GCV treatment<sup>75</sup>. Mouse GMK is used in this study because the mouse enzyme was soluble in *E. coli* whereas the human enzyme was not<sup>40</sup>. To further augment its GCV-mediated tumor killing and bystander activity, another step was taken where fusion mutants were created by engineering the improved HSVTK mutants (mutant 30 and SR39) into a fusion protein construct. These novel fusion mutants demonstrated a superior GCV-mediated toxicity and bystander killing activity at very low doses of GCV *in vitro* and in an *in vivo* xenograft tumor model compared to wild type fusion MGMK/HSVTK and their respective single gene construct. This work is discussed in Chapter 2.

Besides playing an important role in GCV activation, another major therapeutic role of GMK is in the activation of the guanine analog, 6-thioguanine (6-TG) which has been primarily used as a treatment for childhood and adult leukemia since the 1950s<sup>41</sup>. 6-TG also has the ability to kill proliferating T cells, contributing to its immunosuppressive properties. This has led to its use as an immunosuppressant in transplant surgery and as an anti-inflammatory agent in autoimmune diseases such as inflammatory bowel disease. The emergence of resistance to chemotherapeutic agents, however, frequently hinders the success of 6-TG treatment and is a key cause of treatment failure. A better understanding of the molecular factors that result in the loss of drug potency may lead to the development of improved dosing regimens and treatment options for patients. A complete list of the potential mechanism(s) of 6-TG resistance remains elusive because not all cases of resistance can be explained by mutational events in known targets. Therefore, we propose that mutations in GMK could reveal a novel 6-TG



resistance mechanism. Our results demonstrate that GMK containing amino acid substitutions at S37 (S37A, S37T and S37Y) retain varying degrees of essential GMP activity but do not display detectable activity towards 6-TGMP. Mutations in guanylate kinase, therefore, represent a previously undescribed mechanism for 6-TG resistance. This work is discussed in detail in Chapter 3.

### Improving cytosine deaminase

Similar to HSVTK, CD has a less than optimal activity towards 5FC. As mentioned earlier, yCD is thermolabile at 37°C and still is not very active towards 5FC with a  $K_m$  in the millimolar range, making it less suitable for suicide gene therapy applications in humans. Although bCD is thermostable at 37°C, it has much poorer activity towards 5FC when compared to yCD. Because of these limitations, high doses of 5FC are needed to achieve significant tumor killing. Unfortunately, even though 5FC is considered to be fairly non-toxic, patients treated with 5FC often suffer from severe bone marrow depression and gastrointestinal complications that may be mainly due to the presence of microbial flora in the gastrointestinal tract<sup>43</sup>. Several mutagenesis studies to date have been completed by our laboratory in an attempt to resolve these problems<sup>42,68,78</sup>.

A computational design study was done to improve the thermostability of yCD<sup>68</sup>. This study yielded two important mutants, one with two amino acid substitutions (double-yCD) and the other one with three amino acid changes (triple-yCD). Both mutants have the same amino acid substitutions at A23L and V108L, and another substitution at I140L for the triple-yCD mutant. Double-yCD and triple-yCD mutants display approximately 5- and 30-fold increases in the enzymatic half-lives at physiological temperature, respectively, while retaining enzymatic properties towards both cytosine and 5FC<sup>68</sup>. In addition, both mutants display apparent melting temperatures 6°C to 10°C higher than wild type yCD. However, when both mutants

were analyzed for *in vitro* cytotoxicity in rat C6 glioma cell lines, only the triple-yCD mutant demonstrated a modest improvement shown by a reduction in IC<sub>50</sub> value of approximately 2- to 3- fold compared to wild type yCD transfectants<sup>68</sup>. In an animal tumor model, triple-yCD bearing nude mice were shown to have enhanced tumor growth inhibition compared to wild-type yCD bearing nude mice when treated with 5FC<sup>68</sup>. Another mutagenesis study aimed to improve the kinetic parameters was performed to improve enzymatic activity and substrate preferences of yCD towards 5FC. To generate a large library of yCD variants, regio-specific random mutagenesis was performed and three single mutants (D92E, M93L, and I98L) were found to have the highest degree of sensitivity to 5FC in negative complementation assay in *E. coli*. However, only one mutant (D92E) was found to confer enhanced 5FC sensitivity in rat C6 cell lines as indicated by approximately a 30% reduction in IC<sub>50</sub> value compared with wild type yCD-transfected cells<sup>68</sup>. When tested in an animal tumor model, mice harboring D92E-transfected tumors were found to demonstrate significant tumor growth inhibition compared to mice harboring wild type yCD-transfected tumors when dosed with 5FC<sup>68</sup>. Surprisingly, although the D92E mutant was originally selected based on its ability to confer increased sensitivity to 5FC in *E. coli*, this enzyme unexpectedly also displays an increase in its apparent denaturation temperature, corresponding to a T<sub>m</sub> 4°C higher than the T<sub>m</sub> for wild type yCD<sup>68</sup>. Subsequent kinetic analysis revealed that the D92E mutant exhibits comparable kinetic properties towards cytosine and 5FC when compared to wild-type yCD. Triple yCD was generated via a computational design analysis that aimed at improving the thermostability of yCD and mutant D92E was generated by regio-specific random mutagenesis that was designed to create yCD variants with improved activity to 5FC. It is indeed interesting that two thermostable yCD mutants were obtained from two different mutagenesis strategies that were designed to address different problems.

With regards to improving bCD activity towards 5FC, alanine scanning mutagenesis and site-specific mutagenesis were performed<sup>42,78</sup>. From this series of studies, three particular mutants were identified to confer increased 5FC sensitivity in *E. coli* in a negative complementation assay. These mutants, D314G, D314A, D314S, were analyzed for their kinetic properties towards cytosine and 5FC. The D314G and D314S substitutions displayed kinetic parameters that indicated a shift in substrate preference towards 5FC. However *in vitro* analysis revealed that these three variants provide modest benefit with only a 2- to 4-fold decrease in IC<sub>50</sub> for 5FC as compared to wild type bCD transfectants. Therefore, using structural information as well as previous mutagenesis results, two regions lining the active site of bCD (residues 149-159 and 310-320) were targeted for random mutagenesis in an effort to identify mutants with the capacity to confer enhanced sensitivity to 5FC *in vitro* and *in vivo*. From these double-targeted libraries, one bCD variant (1525), with three amino acid substitutions at V152A, F316C, and D317G, displayed substrate preference towards 5FC and confers the greatest sensitivity to 5FC in three different cancer cell lines. In an animal tumor model, significant tumor growth inhibition was observed in mice harboring 1525-transfected tumors compared to mice harboring wild type bCD-transfected tumors when 5FC was administered. To provide further insight, mutant D314A from earlier mutagenesis study and mutant 1525 from the double-targeted library were both analyzed structurally. Results from X-ray crystallography experiments indicated that mutations at D314 and D317 are mutually exclusive due to the cavity formed when a small side chain occupies 314. D317G allows aspartate 314 to swing away from the fluorinated substrate to recapitulate the cavity observed with D314A. This work is discussed in detail in Chapter 3.

Similar to the fusion of HSVTK/MGMK, a fusion enzyme of CD and uracil phosphoribosyltransferase (UPRT) confers increased sensitivity to its counterpart

prodrug 5FC. UPRT is an important enzyme involved in the pyrimidine salvage pathway, catalyzing the transfer of a ribosyl-phosphate group to uracil to form uridine-monophosphate. In the 5FC activation pathway, UPRT is also responsible for the conversion of 5FU to 5FU-monophosphate (5FUMP) (Figure 1.5). Similar to CD, UPRT is absent in mammalian cells and present in fungi and bacteria. Earlier reports demonstrate that the fusion of CD with UPRT (CD/UPRT) along with 5FC imparts greater tumor killing activity than CD alone *in vitro* and *in vivo*<sup>79</sup>. Therefore, to further enhance the production of cytotoxic compounds, we sought to incorporate mutant 1525 into the fusion construct bCD/UPRT. The fusion construct (1525/UPRT) was evaluated for its cell killing and bystander effects *in vitro*. Because 1525/UPRT offers only a modest increase in sensitivity toward 5FC and shows no improvement in bystander killing effect, we hypothesize that the conversion of 5FU to 5FUMP by UPRT is rate limiting in this drug activation pathway. To overcome this limitation, we performed regio-specific random mutagenesis to generate UPRT mutants and coupled with genetic complementation in *E. coli*, identified variants with increased activity toward 5FU. Three UPRT mutants were identified to confer 5FC sensitivity in *E. coli* and further analyzed biochemically and *in vitro* in rat C6 glioma cell lines. This work is discussed in detail in Chapter 5.

While HSVTK is widely used, there are two key reasons for optimizing additional suicide enzymes and novel fusion enzymes: 1) not all cancers are equally responsive to the same drug and 2) should treatment with one suicide gene fail, alternate suicide genes that the immune system has not been exposed to previously, could be used in a second round of therapy to ablate tumors. Ultimately, the goal of this study is to create improved suicide enzymes and novel fusion enzymes using mutagenesis techniques. These novel enzymes with superior activity towards their respective prodrugs will allow lower and less toxic doses of drugs to be administered, thereby minimizing side effects to normal cells, and still exhibit superior tumor killing

activity. Towards that end, the ability of suicide gene therapy to localize drug cytotoxicity within tumor sites, along with the potency of these novel enzymes is clinically beneficial and should make suicide gene therapy become a more promising and powerful alternative treatment for cancer.

## References

1. Bettegowda, C. *et al.* Overcoming the hypoxic barrier to radiation therapy with anaerobic bacteria. *Proc Natl Acad Sci USA* **100**, 15083-15088 (2003).
2. Kaldor, J. *et al.* Leukemia following chemotherapy for ovarian cancer. *N Engl J Med* **322**, 1-6 (1990).
3. Relling, M. V. *et al.* High incidence of secondary brain tumours after radiotherapy and antimetabolites. *The Lancet* **354**, 34-39 (1999).
4. Greco, O. & Dachs, G. Gene directed enzyme/prodrug therapy of cancer: historical appraisal and future prospective. *J Cell Physiol* **187**, 22-36 (2001).
5. Moolten, F. L. Tumor sensitivity conferred by inserted herpes thymidine kinase genes: paradigm for a prospective cancer control strategy. *Cancer Res* **46**, 5276-5281 (1986).
6. Carystinos, G. D. *et al.* Cyclic-AMP induction of gap junctional intercellular communication increases bystander effect in suicide gene therapy. *Clin Cancer Res* **5**, 61-68 (1999).
7. Springer, C. J. & Niculescu-Duvaz, I. *Cancer Gene Therapy: Contemporary Cancer Research*. Curiel, D. T. & Douglas, J. T. (eds.), pp. 81-118 (Humana Press, Totowa, New Jersey, 2005).
8. Freeman, S. M., Ramesh, R. & Marrogi, A. J. Immune system in suicide-gene therapy. *The Lancet* **349**, 2-3 (1997).
9. Freeman, S. M. *et al.* The "bystander effect": tumor regression when a fraction of the tumor mass is genetically modified. *Cancer Res* **53**, 5274-5283 (1993).
10. Huber, B. E., Austin, E. A., Richards, C. A., Davis, S. T. & Good, S. S. Metabolism of 5-fluorocytosine to 5-fluorouracil in human colorectal tumor cells transduced with the cytosine deaminase gene: significant antitumor effects when only a small percentage of tumor cells express cytosine deaminase. *Proc Natl Acad Sci USA* **91**, 8302-8306 (1994).
11. Dilber, M. S. *et al.* Gap junctions promote the bystander effect of herpes simplex virus thymidine kinase *in vivo*. *Cancer Res* **57**, 1523-1528 (1997).
12. Springer, C. J. & Niculescu-Duvaz, I. Gene-directed enzyme prodrug therapy (GDEPT): choice of prodrugs. *Adv Drug Deliv Rev* **22**, 351-364 (1996).
13. Vrionis, F. D. *et al.* The bystander effect exerted by tumor cells expressing the herpes simplex virus thymidine kinase (HSVtk) gene is dependent on connexin expression and cell communication via gap junctions. *Gene Ther* **4**, 577-585 (1997).
14. Dachs, G. U., Tupper, J. & Tozer, G. From bench to bedside for gene-directed enzyme prodrug therapy of cancer. *Anticancer Drugs* **16**, 349-359 (2005).

15. Norris, J. S. *et al.* The present and future for gene and viral therapy of directly accessible prostate and squamous cell cancers of the head and neck. *Future Oncol.* **1**, 115-123 (2005).
16. Niculescu-Duvaz, I. & Springer, C. J. Introduction to the background, principles, and state of the art in suicide gene therapy. *Mol Biotechnol* **30**, 71-87 (2005).
17. Portsmouth, D., Hlavaty, J. & Renner, M. Suicide genes for cancer therapy. *Molecular Aspects of Medicine* **28**, 4-41 (2007).
18. Knox, R. J., Friedlos, F., Jarman, M. & Roberts, J. J. A new cytotoxic, DNA interstrand crosslinking agent, 5-(aziridin-1-yl)-4-hydroxylamino-2-nitrobenzamide, is formed from 5-(aziridin-1-yl)-2,4-dinitrobenzamide (CB 1954) by a nitroreductase enzyme in walker carcinoma cells. *Biochemical Pharmacology* **37**, 4661-4669 (1988).
19. Anlezark, G. M. *et al.* The bioactivation of 5-(aziridin-1-yl)-2,4-dinitrobenzamide (CB1954)--I: Purification and properties of a nitroreductase enzyme from *Escherichia coli*--A potential enzyme for antibody-directed enzyme prodrug therapy (ADEPT). *Biochemical Pharmacology* **44**, 2289-2295 (1992).
20. Knox, R. J., Friedlos, F., Sherwood, R. F., Melton, R. G. & Anlezark, G. M. The bioactivation of 5-(aziridin-1-yl)-2,4-dinitrobenzamide (CB1954)--II: A comparison of an *Escherichia coli* nitroreductase and Walker DT diaphorase. *Biochemical Pharmacology* **44**, 2297-2301 (1992).
21. Bridgewater, J. *et al.* Expression of the bacterial nitroreductase enzyme in mammalian cells renders them selectively sensitive to killing by the prodrug CB1954. *Eur J Cancer* **31A**, 2362-2370 (1995).
22. Cui, W., Guesterson, B. & Clark, A. Nitroreductase-mediated cell ablation is very rapid and mediated by a p53-independent apoptotic pathway. *Gene Ther* **6**, 764-770 (1999).
23. Bridgewater, J., Knox, R., Pitts, J., Collins, M. & Springer, C. The bystander effect of the nitroreductase/CB 1954 enzyme/prodrug system is due to a cell-permeable metabolite. *Hum Gene Ther* **8**, 709-717 (1997).
24. Chang, T. K. H. & Waxman, D. J. Cyclophosphamide modulates rat hepatic cytochrome P450 2C11 and steroid 5 $\alpha$ -reductase activity and messenger RNA levels through the combined action of acrolein and phosphoramidate mustard. *Cancer Res* **53**, 2490-2497 (1993).
25. Chen, L. & Waxman, D. J. Intratumoral activation and enhanced chemotherapeutic effect of oxazaphosphorines following cytochrome P-450 gene transfer: development of a combined chemotherapy/cancer gene therapy strategy. *Cancer Res* **55**, 581-589 (1995).
26. Manome, Y. *et al.* Gene therapy for malignant gliomas using replication incompetent retroviral and adenoviral vectors encoding the cytochrome P450 2B1 gene together with cyclophosphamide. *Gene Ther* **3**, 513-520 (1996).

27. Marais, R., Spooner, R. A., Light, Y., Martin, J. & Springer, C. J. Gene-directed enzyme prodrug therapy with a mustard prodrug/carboxypeptidase G2 combination. *Cancer Res* **56**, 4735-4742 (1996).
28. Manome, Y. *et al.* Viral vector transduction of the human deoxycytidine kinase cDNA sensitizes glioma cells to the cytotoxic effects of cytosine arabinoside *in vitro* and *in vivo*. *Nat Med* **2**, 567-573 (1996).
29. Hapke, D. M., Stegmann, A. P. A. & Mitchell, B. S. Retroviral transfer of deoxycytidine kinase into tumor cell lines enhances nucleoside toxicity. *Cancer Res* **56**, 2343-2347 (1996).
30. Patterson, A. V., Saunders, M. P. & Greco, O. Prodrugs in genetic chemoradiotherapy. *Curr Pharm Design* **9**, 2131-2154 (2003).
31. Eriksson, S., Cederlund, E., Bergman, T., Jönvall, H. & Bohman, C. Characterization of human deoxycytidine kinase correlation with cDNA sequences. *FEBS Letters* **280**, 363-366 (1991).
32. Eriksson, S., Kierdaszuk, B., Much-Peterson, B., Oberg, B. & Johansson, N. Comparison of the substrate specificities of human thymidine kinase 1 and 2 and deoxycytidine kinase toward antiviral and cytostatic nucleoside analogs. *Biochem Biophys Res Commun* **176**, 586-592 (1991).
33. Kokoris, M. S. & Black, M. E. Characterization of herpes simplex virus type 1 thymidine kinase mutants engineered for improved ganciclovir or acyclovir activity. *Protein Sci* **11**, 2267-2272 (2002).
34. Kokoris, M. S., Sabo, P. & Black, M. *In vitro* evaluation of mutant HSV-1 thymidine kinase for suicide gene therapy. *Anticancer Res* **20**, 964 (2000).
35. Devantathan S, Willmon, C. L., Mahan, S. D. & Black, M. E. Engineering enzymes for improved cancer gene therapy. *Res. Adv. In Cancer* 315-326 (2002).
36. Fillat, C., Carrio, M., Cascade, A. & Sangro, B. Suicide gene therapy mediated by the herpes simplex virus thymidine kinase gene/ganciclovir system: fifteen years of application. *Curr Gene Ther* **3**, 13-26 (2003).
37. Miller, W. H. & Miller, R. L. Phosphorylation of acyclovir (acycloguanosine) monophosphate by GMP kinase. *J. Biol. Chem.* **255**, 7204-7207 (1980).
38. Thust, R., Tomicic, M., Klocking, R., Wutzler, P. & Kaina, B. Cytogenetic genotoxicity of anti-herpes purine nucleoside analogues in CHO cells expressing the thymidine kinase gene of herpes simplex virus type 1: comparison of ganciclovir, penciclovir and aciclovir. *Mutagenesis* **15**, 177-184 (2000).
39. Black, M. E. Enzyme and pathway engineering for suicide gene therapy. *Genetic Engineering* **23**, 113-127 (2001).



40. Brady, W. A., Kokoris, M. S., Fitzgibbon, M. & Black, M. Cloning, characterization, and modeling of mouse and human guanylate kinases. *J Biol Chem* **271**, 16734-16740 (1996).
41. Karran, P. & Attard, N. Thiopurines in current medical practice: molecular mechanisms and contributions to therapy-related cancer. *Nat Rev Cancer* **8**, 24-36 (2008).
42. Mahan, S. D., Ireton, G. C., Stoddard, B. L. & Black, M. E. Alanine-scanning mutagenesis reveals a cytosine deaminase mutant with altered substrate preference. *Biochemistry* **43**, 8957-8964 (2004).
43. Vermes, A., Guchelaar, H. J. & Dankert, J. Flucytosine: a review of its pharmacology, clinical indications, pharmacokinetics, toxicity and drug interactions. *J Antimicrob Chemother* **46**, 171-179 (2000).
44. Nishiyama, T. *et al.* Antineoplastic effects in rats of 5-Fluorocytosine in combination with cytosine deaminase capsules. *Cancer Res* **45**, 1753-1761 (1985).
45. Austin, E. A. & Huber, B. E. A first step in the development of gene therapy for colorectal carcinoma: cloning, sequencing, and expression of *Escherichia coli* cytosine deaminase. *Mol Pharmacol* **43**, 380-387 (1993).
46. Longley, D. B., Harkin, D. P. & Johnston, P. G. 5-Fluorouracil: mechanisms of action and clinical strategies. *Nat Rev Cancer* **3**, 330-338 (2003).
47. Kievit, E. *et al.* Yeast Cytosine Deaminase Improves Radiosensitization and Bystander Effect by 5-Fluorocytosine of Human Colorectal Cancer Xenografts. *Cancer Res* **60**, 6649-6655 (2000).
48. Ireton, G. C., McDermott, G., Black, M. E. & Stoddard, B. L. The structure of *Escherichia coli* cytosine deaminase. *J Mol Biol* **315**, 687-697 (2002).
49. Ireton, G. C., Black, M. E. & Stoddard, B. L. The 1.14 Å crystal structure of yeast cytosine deaminase: evolution of nucleotide salvage enzymes and implications for genetic chemotherapy. *Structure* **11**, 961-972 (2003).
50. Cattaneo, R., Miest, T., Shashkova, E. V. & Barry, M. A. Reprogrammed viruses as cancer therapeutics: targeted, armed and shielded. *Nat Rev Micro* **6**, 529-540 (2008).
51. Kershaw, M. H., Teng, M. W. L., Smyth, M. J. & Darcy, P. K. Supernatural T cells: Genetic Modification of T Cells for Cancer Therapy. *Nat Rev Immunol* **5**, 928-940 (2005).
52. King, I. *et al.* Tumor-targeted *Salmonella* expressing cytosine deaminase as an anticancer agent. *Hum. Gene Ther.* **13**, 1225-1233 (2002).
53. Lee, C. H., Wu, C. L. & Shiau, A. L. Systemic administration of attenuated *Salmonella choleraesuis* carrying thrombospondin-1 gene leads to tumor-specific transgene expression, delayed tumor growth and prolonged survival in the murine melanoma model. *Cancer Gene Ther* **12**, 175-184 (2004).

54. Yazawa, K., Fujimori, M., Amano, J., Kano, Y. & Taniguchi, S. *Bifidobacterium longum* as a delivery system for cancer gene therapy: selective localization and growth in Hypoxic Tumors. *Cancer Gene Ther* **7**, 269-274 (2000).
55. Waehler, R., Russell, S. J. & Curiel, D. T. Engineering targeted viral vectors for gene therapy. *Nat Rev Genet* **8**, 573-587 (2007).
56. Dachs, G., Dougherty, G. J., Stratford, I. J. & Chaplin, D. J. Targeting gene therapy to cancer: a review. *Oncol Res* **9**, 313-325 (1997).
57. Young, L. S., Searle, P. F., Onion, D. & Mautner, V. Viral gene therapy strategies: from basic science to clinical application. *Journal of Pathol* **208**, 299-318 (2006).
58. Bangari, D. & Mittal, S. K. Current strategies and future directions for eluding adenoviral vector immunity. *Current Gene Ther* **6**, 215-226 (2006).
59. Thomas, C. E., Ehrhardt, A. & Kay, M. A. Progress and problems with the use of viral vectors for gene therapy. *Nat Rev Genet* **4**, 346-358 (2003).
60. Glover, D. J., Lipps, H. J. & Jans, D. A. Towards safe, non-viral therapeutic gene expression in humans. *Nat Rev Genet* **6**, 299-310 (2005).
61. Wang, C.-Y., Li, F., Yang, Y., Guo, H.-Y. & Wang, S. Recombinant baculovirus containing the diphtheria toxin A gene for malignant glioma therapy. *Cancer Res* **66**, 5798-5806 (2006).
62. Wei, M. Q., Mengesha, A., Good, D. & Annø, J. Bacterial targeted tumour therapy-dawn of a new era. *Cancer Letters* **259**, 16-27 (2008).
63. Kim, Y. G., Bi, W., Feliciano, F. S., Drake, R. R. & Stambrook, P. J. Ganciclovir-mediated cell killing and bystander effect is enhanced in cells with two copies of the herpes simplex virus thymidine kinase gene. *Cancer Gene Ther* **7**, 240-246 (2000).
64. Davies, L. C. *et al.* Novel fluorinated prodrugs for activation by carboxypeptidase G2 showing good *in vivo* antitumor activity in gene-directed enzyme prodrug therapy. *J Med Chem* **48**, 5321-5328 (2005).
65. Boucher, P. D., Ostruszka, L. J. & Shewach, D. S. Synergistic enhancement of herpes simplex virus thymidine kinase/ganciclovir-mediated cytotoxicity by hydroxyurea. *Cancer Res* **60**, 1631-1636 (2000).
66. Boucher, P. D., Im, M. M., Freytag, S. O. & Shewach, D. S. A novel mechanism of synergistic cytotoxicity with 5-fluorocytosine and ganciclovir in double suicide gene therapy. *Cancer Res* **66**, 3230-3237 (2006).
67. Kaliberov, S. A. *et al.* Combination of cytosine deaminase suicide gene expression with DR5 antibody treatment increases cancer cell cytotoxicity. *Cancer Gene Ther* **13**, 203-214 (2006).

68. Stolworthy, T. S. *et al.* Yeast cytosine deaminase mutants with increased thermostability impart sensitivity to 5-fluorocytosine. *J Mol Biol* **377**, 845-869 (2008).
69. Black, M. E., Newcomb, T. G., Wilson, H. M. & Loeb, L. A. Creation of drug-specific herpes simplex virus type 1 thymidine kinase mutants for gene therapy. *Proc Natl Acad Sci USA* **93**, 3525-3529 (1996).
70. Munir, K. M., French, D. C. & Loeb, L. A. Thymidine kinase mutants obtained by random sequence selection. *Proc Natl Acad Sci USA* **90**, 4012-4016 (1993).
71. Black, M. E. & Loeb, L. A. Identification of important residues within the putative nucleoside binding site of HSV-1 thymidine kinase by random sequence selection: analysis of selected mutants *in vitro*. *Biochemistry* **32**, 11618-11626 (1993).
72. Black, M. E., Kokoris, M. S. & Sabo, P. Herpes simplex virus-1 thymidine kinase mutants created by semi-random sequence mutagenesis improve prodrug-mediated tumor cell killing. *Cancer Res* **61**, 3022-3026 (2001).
73. Kokoris, M. S., Sabo P, Adman, E. T. & Black, M. E. Enhancement of tumor ablation by a selected HSV-1 thymidine kinase mutant. *Gene Therapy* **6**, 1415-1426 (1996).
74. Kokoris, M. S., Sabo P & Black, M. E. Enhancement of tumor ablation by a selected HSV-thymidine kinase mutant. *Gene Ther* **6**, 1415-1426 (1999).
75. Willmon, C. L., Krabbenhoft, E. & Black, M. E. A guanylate kinase//HSV-1 thymidine kinase fusion protein enhances prodrug-mediated cell killing. *Gene Ther* **13**, 1309-1312 (2006).
76. Boehme, R. Phosphorylation of 9- $\beta$ -D-arabinofuranosylguanine monophosphate by *Drosophila melanogaster* guanylate kinase. *J Biol Chem* **258**, 12346-12349 (1984).
77. Akyürek, L. *et al.* Coexpression of guanylate kinase with thymidine kinase enhances prodrug cell killing *in vitro* and suppresses vascular smooth muscle cell proliferation *in vivo*. *Mol Ther* **3**, 779-786 (2001).
78. Mahan, S. D., Ireton, G. C., Knoeber, C., Stoddard, B. L. & Black, M. E. Random mutagenesis and selection of *Escherichia coli* cytosine deaminase for cancer gene therapy. *Prot Eng Des Sel* **17**, 625-633 (2004).
79. Erbs, P. *et al.* *In vivo* cancer gene therapy by adenovirus-mediated transfer of a bifunctional yeast cytosine deaminase/uracil phosphoribosyltransferase fusion gene. *Cancer Res* **60**, 3813-3822 (2000).

## CHAPTER TWO

### **Fusion Enzymes Containing HSV-1 Thymidine Kinase Mutants and Guanylate Kinase Enhance Prodrug Sensitivity *In Vitro* and *In Vivo***

#### **ABSTRACT**

Herpes Simplex Virus thymidine kinase (HSVTK) with the guanosine analog ganciclovir (GCV) is currently the most widely used suicide gene/prodrug system for gene therapy for cancer. Despite the broad application, inefficient activation of GCV by HSVTK to its active antimetabolites remains to be a major limitation such that high and myelosuppressive doses of GCV are needed to observe an anti-tumor effect. One strategy to overcome this limitation is to create and utilize novel forms of HSVTK with altered substrate preferences towards GCV. HSVTK mutants (mutant 30 and SR39) were previously shown to have increased tumor killing *in vitro* and in an *in vivo* tumor model. Evidence suggests that conversion to the diphosphate form of GCV by endogenous *gmk* then becomes rate limiting. To overcome the bottleneck problem, a chimeric fusion protein encoding both HSVTK and MGMK (mouse GMK) was generated. Results from these studies shows that MGMK/HSVTK confers increased GCV sensitivity in glioma cells compared to HSVTK alone. As a mean to further enhance GCV activation, two MGMK/HSVTK constructs containing the HSVTK mutants (mutant 30 and SR39) were generated and evaluated for their tumor cytotoxicity and bystander killing effects in *in vitro* and in an *in vivo* xenograft tumor model. One fusion mutant in particular, MGMK/30, demonstrates a significant improvement in conferring *in vitro* cytotoxicity to GCV as shown by a reduction in  $IC_{50}$  values of approximately 12,500-fold, 100-fold, and 125-fold compared to HSVTK, mutant 30 or fusion MGMK/HSVTK, respectively. The constructed mutant chimeric proteins exhibit a potent tumor killing effect at a low GCV concentration

(1mg/kg) that has no effect on wild type HSVTK-, wild type fusion MGMK/HSVTK-, and previously characterized HSVTK mutants-transfected cells. In a xenograft tumor model, MGMK/30 displays the greatest inhibition of tumor growth. Both mutant chimeric proteins display substantial improvements in bystander killing in the presence of 1mg/kg GCV, even when only 5% of the tumor cells are transduced. Fusion mutants with exceptional prodrug converting properties will allow administration of lower and non-myelosuppressive doses of GCV concomitant with improvement in tumor killing. The use of such novel mutant fusion constructs will likely improve the clinical outcome of suicide gene therapy in cancer patients and compensate the inefficient and ineffective problems of the current delivery methods.

---

This manuscript was submitted to *Cancer Gene Therapy* in the following manuscript: **Ardiani, A.**, Sanchez-Bonilla, M., and Black, M.E. Fusion Enzymes Containing HSV-1 Thymidine Kinase Mutants and Guanylate Kinase Enhance Prodrug Sensitivity *In Vitro* and *In Vivo*.

## INTRODUCTION

Thymidine kinase (TK) (EC 2.7.1.21) is an essential enzyme in the pyrimidine salvage pathway, catalyzing the transfer of the  $\gamma$ -phosphate from ATP to thymidine to produce dTMP<sup>1</sup>. Unlike human TK, Herpes Simplex Virus type 1 (HSV-1) thymidine kinase (HSVTK) has a broad substrate specificity and is able to phosphorylate pyrimidines, pyrimidine analogues (thymidine, deoxycytidine, and azidothymidine), and guanosine analogues (ganciclovir, acyclovir, bucciclovir, and penciclovir). Originally suggested by Moolten, HSVTK has been widely used as a suicide gene in combination with the guanosine analogue ganciclovir (GCV) for the treatment of a variety of cancers<sup>2</sup>. To date, over 70 clinical trials using HSVTK and GCV have been approved<sup>3</sup>. Upon successful delivery of HSVTK into cancer cells followed by systemic administration of GCV, transduced cancer cells become sensitized to the prodrug. Inside the cell, GCV is initially phosphorylated by HSVTK to form GCV-monophosphate (GCV-MP), which is then further phosphorylated to GCV-diphosphate (GCV-DP) by cellular guanylate kinase (GMK) and to the active antimetabolite GCV-triphosphate (GCV-TP) by cellular nucleoside diphosphokinase<sup>4, 5</sup>. Cytotoxicity is mainly due to the action of GCV-TP after its incorporation into nascent DNA, which results in chain termination and ultimately leads to cell death<sup>5, 6</sup>. Since human TK has a narrow substrate specificity and is not active towards GCV, prodrug-associated toxicity is limited to the site of transfection. Because low gene transfer is a key problem in gene therapy, the success of suicide gene therapy relies heavily on a phenomenon called the bystander effect, in which untransfected neighboring cancer cells are eradicated by the transfer of antimetabolites via gap junctions or apoptotic vesicles<sup>2, 7</sup>. Previous studies reported that *in vivo* complete tumor ablation could be achieved in the presence of GCV even when only a small percentage of the tumor was transduced with retroviral vectors carrying HSVTK gene<sup>8</sup>. Implicit in the

bystander effect is that sufficient phosphorylated GCV is transferred to neighboring cells to elicit cell killing.

Although the bystander effect promotes tumor cell killing in HSVTK/GCV gene therapy, inefficient activation of GCV by HSVTK is a major limitation. The  $K_m$  value of HSVTK toward GCV ( $K_m = 47\mu\text{M}$ ) is approximately 10-fold higher than its  $K_m$  value for thymidine ( $K_m = 0.4\mu\text{M}$ ), its natural substrate<sup>9</sup>. This lower GCV binding ability is exacerbated by a 5-fold lower  $k_{\text{cat}}$  (turnover rate) and results in more than a 500-fold lower in overall enzyme catalytic efficiency ( $k_{\text{cat}}/K_m$ ). Due to the combination of low gene transfer and inadequate GCV activation by HSVTK, myelosuppressive doses of GCV are required to achieve significant or complete tumor ablation<sup>9</sup>. Moreover, there is evidence that once the GCV-MP is formed, a bottleneck occurs, leading to accumulation of the ineffective intermediate products<sup>10, 11</sup>. Guanylate kinase (GMK, ATP:GMP phosphotransferase, EC 2.7.4.8) is an essential enzyme involved in purine biosynthesis and is responsible for the phosphorylation of GMP and dGMP<sup>12</sup>. Previous reports have shown the  $K_m$  value of GMK for GCV-MP is 2-fold higher ( $K_m = 42\text{-}54\ \mu\text{M}$ ) than its  $K_m$  toward its natural substrate GMP ( $\sim 25\ \mu\text{M}$ )<sup>12, 13</sup>. This suggests that endogenous GMK may be a second rate limiting step during the production of sufficient antimetabolites to accomplish complete tumor ablation in the HSVTK/GCV system.

One approach to improve prodrug activation, which may consequently reduce the dose of GCV required to kill tumor cells and thereby limiting the prodrug-associated negative side effects, is to create HSVTK mutants with increased activity and/or substrate specificity toward GCV<sup>9, 14</sup>. We have previously reported the construction and characterization of HSVTK mutants with significant improvement toward GCV. Random sequence mutagenesis and semi random mutagenesis were used to identify two HSVTK mutants, mutant 30 and SR39<sup>9, 15</sup>. Both of these HSVTK mutants showed not only an improvement in kinetic properties towards GCV, but

also *in vitro* tumor killing and *in vivo* tumor growth inhibition compared to HSVTK alone. As a means to overcome the bottleneck of prodrug activation from the monophosphate to the diphosphate, a fusion or chimeric protein expressing both GMK and HSVTK (GMK/HSVTK) functions was generated. Mouse GMK (MGMK) was used because in our hands, the mouse enzyme was soluble in *E. coli* whereas the human enzyme was not<sup>12</sup>. *In vitro* cytotoxic assay using this fusion protein demonstrated that cells expressing MGMK/HSVTK confer a ~175-fold decrease in IC<sub>50</sub> value compared to HSVTK alone in response to GCV treatment in stably transfected rat C6 glioma cells<sup>16</sup>.

In this study, we further evaluated tumor toxicity and bystander killing activity of the previously created fusion MGMK/HSVTK *in vitro* and in an *in vivo* tumor model. Results from *in vivo* studies suggest that the fusion protein inhibits tumor growth at a GCV concentration (1mg/kg) that has no effect on wild type HSVTK-bearing tumors. Moreover, it also elicits a stronger bystander effect *in vitro* and *in vivo*. To further augment its GCV-mediated tumor killing activity, we have taken a further step by engineering the improved HSVTK mutants, mutant 30 and SR39, into the chimeric protein construct. Here, we report that the mutant chimeric proteins created in this study exhibit a superior GCV-mediated toxicity and bystander killing activity at very low doses of prodrug *in vitro* and in an *in vivo* xenograft tumor model compared to MGMK/HSVTK and their respective single gene constructs. The results reported here demonstrate that the mutant chimeric proteins offer a significant advantage to the suicide gene therapy approach to that of the widely used wild type HSVTK gene, previously characterized HSVTK mutants, or the previously created MGMK/HSVTK fusion construct.



## RESULTS

### *Genetic complementation*

Two new constructs were generated, MGMK/30 (containing HSVTK mutant 30) and MGMK/SR39 (containing HSVTK mutant SR39). To ascertain whether the constructed mutant fusions displayed functional TK and GMK activity, genetic complementation for both activities was independently evaluated using the previously established thymidine kinase (*tdk*<sup>-</sup>) and conditionally *gmk* deficient *E. coli* strain TS202A(DE3)<sup>17</sup>. *E. coli* strain TS202A(DE3) was created by integration of the mouse *gmk* gene downstream of the bacterial chromosomal arabinose promoter and disruption of the endogenous bacterial *gmk* gene by insertion of a kanamycin resistance gene into the bacterial *gmk* locus. Because GMK is an essential enzyme, the growth of *E. coli* TS202A(DE3) requires the presence of arabinose to induce expression of the integrated *mgmk* gene. In the absence of arabinose, the cells are not viable on selective medium unless a functional GMK is expressed from an introduced *gmk*-encoded plasmid. To assess TK activity, *E. coli* TS202A(DE3) is plated onto TK selection plates, and only cells harboring functional TK are able to grow on this selection medium<sup>14</sup>. Upon DNA sequencing verification, pET23d, pET23d:mgmk, pET23d:HSVTK, pET23d:30, pET23d:SR39, pET23d:mgmk/HSVTK, pET23d:mgmk/30 and pET23d:mgmk/SR39 were used to transform *E. coli* strain, TS202A(DE3) and plated onto TK and GMK selection media in the presence or absence of arabinose supplemented with kanamycin. As anticipated, cells harboring pET23d and pET23d:mgmk were not able to complement the TK deficiency of TS202A(DE3), whereas cells harboring pET23d:HSVTK, pET23d:30, pET23d:SR39 and their respective fusion constructs were viable (data not shown). Similarly, only pET23d:mgmk, pET23d:mgmk/HSVTK, pET23d:mgmk/30, and pET23d:mgmk/SR39 were viable on GMK selection medium in the absence of arabinose (data not shown). These results indicated that the fusion proteins were expressed and maintained both

TK and GMK activities. All cultures grew on the control non-selective minimal medium.

#### *In vitro prodrug sensitivity assays*

In order to analyze the efficacy of the constructed mutant chimeric proteins, we utilized rat C6 glioma cells. Rat C6 glioma cells have previously served as a model system to evaluate efficacy of the TK/GCV paradigm<sup>18, 19</sup>. Mammalian expression vectors (pUB) expressing suicide genes were constructed and used to stably transfect rat C6 glioma cells. Once stable transfection was achieved, expression levels of the suicide proteins were determined by immunoblots using polyclonal serum raised against HSVTK or MGMK. Immunoblots revealed the presence of HSVTK at around 45kDa when the anti-HSVTK serum was used, and MGMK at around 23kDa when anti-MGMK serum was used, these results are in accord with the predicted molecular masses for each protein. The fusion proteins cross-reacted with both anti-sera at the predicted molecular mass of approximately 68kDa and relatively equivalent protein levels were observed (data not shown). *In vitro* prodrug sensitivity assays were performed by subjecting stable transfectants to various concentrations of GCV (0 – 100  $\mu$ M). Cell survival was determined using Alamar Blue according to the manufacturer's instructions. Results of one representative experiment are shown as percent survival in Figure 2.1. This experiment was performed at least three times using different pools of transfectants with similar results. In the presence of GCV, wild type HSVTK expressing cells displayed an  $IC_{50}$  of  $\sim 50\mu$ M whereas wild type MGMK/HSVTK-, mutant 30- and fusion MGMK/30-expressing cells displayed an  $IC_{50}$  of 0.5  $\mu$ M, 0.4  $\mu$ M, and 0.004  $\mu$ M, respectively (Figure 2.1A and Table 2.1). Similar  $IC_{50}$  values were observed between cells expressing MGMK/HSVTK and cells expressing mutant 30. We noted a decrease in  $IC_{50}$  approximately 100-fold in cells expressing fusion MGMK/HSVTK compared to

those cells expressing HSVTK alone. Reduction in the IC<sub>50</sub> value of approximately 100-fold was also observed in cells expressing the fusion MGMK/30 as compared to cells expressing mutant 30 or the MGMK/HSVTK fusion. Surprisingly, when the other mutant construct, MGMK/SR39, was analyzed *in vitro*, no significant difference in tumor ablation was observed when compared to SR39. Similar IC<sub>50</sub> values of approximately 0.02 μM were observed in cells expressing either SR39 or fusion MGMK/SR39 (Figure 2.1B and Table 2.1). Microscopically, no cells were visible in the highest concentration of prodrugs with mutant 30, SR39, fusion MGMK/HSVTK, MGMK/30, and MGMK/SR39 despite the artifactual reading of 5% survival. This is likely due to dye being activated by remaining cell membrane debris.

#### *In vitro bystander activity analysis*

As described in the Materials and Methods section, cells stably transfected with empty vector (pUB) were mixed at different ratios with cells stably transfected with HSVTK, HSVTK mutants, or fusion constructs. Mixed cells were then subjected to 80 μM of GCV and cell survival was ascertained using Alamar Blue according to the manufacturer's instructions. Results of one representative experiment are shown as percent survival in Figure 2.2. This experiment was performed at least three times using different pools of transfectants with similar results. In the presence of GCV, all fusion constructs elicited stronger bystander effect compared to their respective single gene constructs. The results indicate that MGMK/SR39 demonstrates the strongest bystander activity. When only ~1% of tumor cells express MGMK/SR39, 60% tumor killing is achieved. This is a significant improvement over SR39 alone, where approximately 40% of tumor cell transduction was necessary to achieve the same killing effect. MGMK/30 demonstrates the second strongest bystander activity where only ~5% cells expressing fusion proteins were sufficient to induce about 75% of tumor cell killing. Mutant 30, SR39 and wild type fusion MGMK/HSVTK appeared

to have similar bystander activities, where approximately 50% of cell transduction resulted in 65% tumor ablation.

#### *Xenograft tumor model*

As described in the Materials and Methods section, pools of rat C6 glioma cells stably expressing suicide genes were injected subcutaneously into nude mice (n=5). When the tumor size reached ~3-4 mm, GCV (1mg/kg) or PBS was intraperitoneally administered twice a day for 8 days. During this time and for 8 days thereafter, tumor size was monitored by caliper measurements every other day. Figure 2.3 displays the time course of tumor growth. Tumor cells transfected with vector only (pUB) showed no statistical difference in tumor size between mice treated with PBS and those treated with GCV (Figures 2.3A and 2.3D) ( $P \geq 0.05$ ). Similarly, no statistical difference was observed in tumor volume in mice seeded with cells transfected with pUB:HSVTK that were injected with PBS or GCV (Figures 2.3A and 2.3D) or in mice seeded with cells transfected with empty vector (pUB) or pUB:HSVTK receiving GCV treatment (Figure 2.3A) ( $P$  values  $\geq 0.05$ ). The lack of difference is likely a reflection of the low GCV dose administered. The prodrug-treated mice bearing mutant 30- or fusion MGMK/HSVTK-expressing tumors elicited a similar anti-tumor response (Figure 2.3A). However, once GCV injection was stopped, rapid tumor growth was observed in these groups of mice. In contrast, mice bearing MGMK/30-expressing tumors treated with GCV displayed the greatest restriction in tumor growth (day 16 mean tumor volume:  $50.8\text{mm}^3$ ) (Table 2.2). This is an improvement of approximately 33-fold over fusion MGMK/HSVTK or mutant 30 ( $P$  values  $\leq 0.05$ ). In line with *in vitro* data, on the other hand, similar anti-tumor responses were observed between SR39 and MGMK/SR39. Though both are efficient in inhibiting tumor growth, no statistical difference was observed in

tumor volume in mice seeded with cells transfected with SR39 or MGMK/SR39 in the presence of 1mg/kg GCV (Figure 2.3B and Table 2.3) ( $P \geq 0.05$ ).

Since no difference in tumor growth inhibition was observable between SR39 and MGMK/SR39, we performed another round of *in vivo* xenograft tumor study using one tenth dose of GCV or 0.1 mg/kg (Figure 2.3C). When 0.1 mg/kg GCV was used to treat nude mice bearing SR39- or MGMK/SR39-expressing tumor cells, a difference in tumor growth was observed starting on day 4 up to day 14 (GCV treatment was stopped on day 8) (Figure 2.3C). At the lower dose of GCV, the efficacy to inhibit tumor growth was discerned and the results show that MGMK/SR39 generated a more potent GCV-mediated tumor growth impairment compared to SR39 alone (Figure 2.3C). On day 14, the mean tumor size for the MGMK/SR39-transfected tumor cells was 120.46 mm<sup>3</sup>, compared to mean tumor size for the SR39-transfected tumor cells at 214.04 mm<sup>3</sup> ( $P \leq 0.05$ ) (Table 2.3). Figure 2.3D displays the results obtained from nude mice receiving PBS from each group and the data suggest that all tumors grew at approximately the same rate with no statistical difference. Mice receiving PBS from all groups were sacrificed on day 10 due to heavy tumor burden.

#### *Bystander xenograft tumor model*

Pools of rat C6 glioma cells transfected with empty vector were co-cultured with pools of rat C6 glioma cells expressing HSVTK, MGMK/HSVTK, 30, or MGMK/30 at a ratio of 95:5 respectively as described in the Materials and Methods section. Mixed cells were injected subcutaneously into nude mice (n=5). When the tumor size reached ~3-4 mm, GCV (1mg/kg) or PBS was intraperitoneally administered twice a day for 8 days. During this time and for 8 days thereafter, tumor size was monitored by caliper measurements every other day. Figure 2.4 displays the time course of tumor growth. In the presence of GCV, MGMK/30 exhibited a substantial

bystander killing activity as indicated by the greatest inhibition in tumor growth. On the other hand, HSVTK, MGMK/HSVTK, and 30 did not exhibit sufficient bystander activity to suppress tumor growth (Figure 2.4A). Tumors from mice receiving PBS treatment all grew at approximately the same rate (Figure 2.4B).

In a separate series of experiments, the bystander activity of SR39 and MGMK/SR39 was evaluated. Following protocols described in the Materials and Methods section, the bystander activity of these constructs was analyzed in an *in vivo* xenograft tumor model and results are shown in Figure 2.5. In the presence of 1mg/kg GCV, MGMK/SR39 generated a slightly stronger bystander effect compared to SR39 alone as indicated by a more restricted tumor growth in mice bearing MGMK/SR39-expressing cells (Figure 2.5A). Taken together, MGMK/SR39 appeared to display the strongest bystander killing effect, followed by SR39, MGMK/30 and mutant 30. When PBS was used, tumors from all mice group grew at approximately the same rate (Figure 2.5B).

## **DISCUSSION**

Despite apparent progress, conventional treatments against cancer such as chemotherapy and radiotherapy still face limitations and place heavy tolls on patients. Systemic administration of chemotherapy not only affects and kills normal tissues, consequently causing unpleasant side effects, but can also lead to the appearance of secondary cancers<sup>20, 21</sup>. Suicide gene therapy is an attractive alternative treatment for cancer because it offers the prospect of selectively introducing genes into cancer cells, rendering them susceptible to specific antimetabolites, and therefore limits the anti-tumor effect to tumor sites<sup>7</sup>. The HSVTK/GCV is the most extensively studied and described system in suicide gene therapy. In contrast to human TK, HSVTK is able to phosphorylate select antiviral and anticancer drugs, such as the antiviral drug GCV. The efficacy and anti-tumor

effect of HSVTK/GCV has been well documented *in vitro* and *in vivo* with more than 70 clinical trials conducted. As of June 2007, three of these trials have advanced to phase III multicenter programs<sup>22, 23</sup>.

The selectivity of suicide gene therapy to target cancer cells is primarily due to the vector or the delivery vehicle. Unfortunately, successful, selective and effective delivery of suicide genes remains to be one of the most challenging factors in gene therapy area. This problem is exacerbated by another major limiting factor, the low efficiency and efficacy of the suicide enzymes towards the prodrugs. Because of these limitations, a potent bystander effect is crucial to achieve significant or complete tumor ablation<sup>24</sup>. The bystander effect associated with suicide gene therapy is achieved via two different mechanisms: local or immune-mediated<sup>7</sup>. In the local-mediated bystander effect, gap junctions play an important role because phosphorylated-GCV is transferred to neighboring cells via gap junctions<sup>18</sup>. The transfer of toxic drugs through gap junctions has some limitations because certain type of tumors, such as breast tumors have been reported to down-regulate intracellular gap junctions communications and thus may have disorganized and non-functional gap junctions<sup>7, 25</sup>. These tumors demonstrate extremely poor bystander effects. Throughout this study, we choose to perform both *in vitro* and *in vivo* GCV-sensitivity studies in rat C6 glioma cells due to their low level of intracellular communication by gap junctions<sup>18</sup>. By utilizing rat C6 cells, we hope to successfully demonstrate that despite the nature of these cells to have poor gap junctions; the fusion constructs are still able to generate a broader and stronger bystander killing effect by generating higher levels of antimetabolites compared to their single gene constructs. Local-mediated bystander effect can also be achieved through the transfer of apoptotic vesicles containing toxic metabolites to neighboring non-transduced cells<sup>7</sup>.

One strategy to enhance therapeutic response of HSVTK towards GCV is by improving enzyme activity and efficiency towards the prodrug. Enzymes with high catalytic activity can impact cell killing efficacy directly by generating more active prodrug or indirectly through a broader bystander effect. Ultimately, the use of enzymes with high catalytic activity allows lower prodrug doses to be administered and, therefore, reduces side effects. Previously, several HSVTK mutants with significant improvement towards GCV were generated and characterized. Two mutants in particular, mutant 30 and SR39, were analyzed in depth both *in vitro* and in an *in vivo* tumor model<sup>9, 15</sup>. Mutant SR39 contains five amino acid changes, while mutant 30 contains six amino acid substitutions; most of these changes are located at or near the active site. *In vitro* analyses revealed that both mutants enhanced C6 rat glioma cells sensitivity to GCV by more than 200-fold. When both mutants were evaluated *in vivo*, significant tumor growth inhibition was observed at a dose that does not affect wild type HSVTK. Clearly, both of these HSVTK mutants have significant advantage over wild type HSVTK.

Previous reports suggest that a bottleneck problem arises in the HSVTK/GCV system, leading to accumulation of the ineffective intermediate products, i.e., GCV-MP<sup>4, 16</sup>. We hypothesize that this bottleneck problem occurs because endogenous GMK has limited ability to convert GCV-MP to GCV-DP. Indeed, the  $K_m$  value of GMK for GCV-MP is approximately 2-fold higher than its  $K_m$  value for its natural substrate GMP<sup>12, 13</sup>. This implies that higher expression of GMK is required to overcome the bottleneck problem in order to produce higher amounts of active antimetabolites. Earlier experiments co-expressing HSVTK and GMK as separate proteins failed to demonstrate notable improvements in GCV sensitivity (data not shown and Akrüyek et al.<sup>26</sup>). We hypothesize that the creation of a fusion enzyme may alleviate this problem by creating more efficient and more rapid drug conversion to the active antimetabolites form. We created a fusion chimeric gene, encoding both HSVTK and



MGMK (mouse GMK) activities and showed a significant reduction in IC<sub>50</sub> value in rat C6 glioma cells compared to HSVTK alone in the presence of GCV<sup>16</sup>. The current study is aimed to evaluate anti-tumor and bystander killing activity of the previously described fusion protein MGMK/HSVTK *in vitro* and *in vivo*, and to further augment its anti-tumor activity by replacing the wild type HSVTK portion of the chimeric construct with the sequences of the well established HSVTK mutants, mutant 30 and SR39. Current *in vitro* cytotoxic assays data validate the earlier finding that wild type fusion MGMK/HSVTK sensitized rat C6 glioma cells to GCV. However, in our current findings, we observed approximately 100-fold reduction in IC<sub>50</sub> values. This slight discrepancy in IC<sub>50</sub> values (less than 2-fold) may be due to different mammalian promoters used in the earlier study (pREP8Δ7) and in the current study (pUB), and consequently protein levels may differ accordingly. Bystander activity of the wild type fusion enzyme was analyzed *in vitro* and it exhibited a stronger bystander effect than to HSVTK alone. This suggests that the presence of additional GMK intracellularly, in close proximity to HSVTK, may be important to produce sufficient antimetabolites to eradicate transfected cancer cells and neighboring untransfected tumor cells.

When mutant 30 was used to replace wild type HSVTK in the fusion construct, an improvement in tumor ablation and bystander activity was evident. In the presence of GCV, we observed a decrease in IC<sub>50</sub> values of approximately 100-fold in MGMK/30-expressing tumor cells compared to mutant 30-expressing cells, totaling in a 12,500-fold reduction in IC<sub>50</sub> compared to HSVTK-expressing cells. When MGMK/30-expressing cells were seeded into nude mice and treated with 1mg/kg GCV, no tumor growth was observed during GCV treatment (day 0 – day 8) and up to day 16, eight days after GCV treatment ended. Mice harboring mutant 30- and MGMK/HSVTK-expressing tumor cells demonstrated a delay in tumor growth during GCV treatment. Perhaps the most revealing finding was the exceptional

improvement in bystander activity of MGMK/30. The MGMK/30 fusion demonstrated a substantial bystander killing effect *in vitro* and was able to achieve a complete tumor cell killing when only ~25% of cells expressed the enzyme. This was approximately a 3-fold improvement over mutant 30 and MGMK/HSVTK, where approximately 75% of cell transduction was necessary to completely eradicate the cells. In a xenograft tumor model, a ratio of 95:5 (vector:suicide gene) was used and MGMK/30-expressing tumor cells demonstrated a highly potent bystander anti-tumor activity compared to mutant 30- or MGMK/HSVTK-expressing tumor cells, where bystander activities were almost non-existent. This absence of bystander activities could be attributed to the low dose of GCV (1mg/kg), short duration of prodrug treatment, and/or to the low level (5%) of MGMK/30-expressing cells used to evaluate the bystander activity. Slow tumor growth was observed in mice harboring 5% MGMK/30-expressing tumor cells during GCV treatment. Such a bystander killing effect in rat C6 glioma cells is in fact impressive given that these cells are notorious for their low levels of gap junctions. This further implies that in rat C6 cells, a high amount of active antimetabolites is required to achieve significant bystander activity. Furthermore, the use of immunocompromised (nude) mice in this study is likely to preclude the full extent of the bystander effect due to the deficiency of the immune-mediated component.

In contrast to MGMK/30 and its improvement over mutant 30, the fusion enzyme MGMK/SR39 only shows a marginal improvement compared to SR39. *In vitro* prodrug sensitivity assays revealed no statistical difference in IC<sub>50</sub> values between MGMK/SR39 and SR39-expressing cells. A similar pattern emerged *in vivo* where both groups of mice harboring either MGMK/SR39- or SR39-expressing tumor cells demonstrated relatively equal restriction in tumor growth when dosed with 1mg/kg GCV. When the dose of GCV is reduced to 0.1 mg/kg, a statistically significant difference in GCV-mediated tumor killing was observed; mice seeded with

MGMK/SR39-expressing tumor cells experienced a delay in tumor growth compared to those that received SR39-expressing cells. The impediment in tumor growth seen in *in vivo* bystander analysis between mice harboring MGMK/SR39-expressing cells and those received SR39-expressing cells with 1mg/kg GCV was marginal but statistically significant.

MGMK/30 demonstrates significant improvement in tumor killing and bystander activity compared to mutant 30, whereas only a minor improvement was observed in MGMK/SR39 compared to SR39. One possible explanation for this trend is the difference in kinetic properties toward GCV and thymidine exhibited by mutant 30 and mutant SR39. Kinetic analyses of mutant 30 revealed no change in overall enzyme catalytic efficacy toward GCV compared to HSVTK. When GCV is used as substrate,  $K_m$  value of mutant 30 is 7-fold higher compared to wild type HSVTK. Additionally, the turnover rate ( $k_{cat}$ ) of mutant 30 for GCV is approximately 6-fold lower than wild type, which subsequently translates to a 41-fold reduction in overall enzyme catalytic efficiency<sup>9</sup>. Therefore one might predict that mutant 30 would not elicit a greatly enhanced prodrug sensitivity to cells. However, because endogenous thymidine (natural substrate of HSVTK) within the cell competes with the prodrug for the active site, it is important to consider how well the mutant 30 performs in catalyzing thymidine. Indeed, mutant 30 demonstrates much poorer activity towards thymidine when compared to wild type HSVTK. When thymidine is used as substrate, mutant 30 shows approximately a 3,000-fold reduction in overall enzyme catalytic efficiency compared to wild type HSVTK<sup>9</sup>.

Mutant SR39, on the other hand, has an advantage over mutant 30 in regards to enzyme activity towards GCV as indicated by an improvement in  $K_m$  value for GCV by 14-fold compared to HSVTK<sup>1</sup>. Though mutant SR39's activity toward thymidine is slightly impaired, clearly its impairment (reduction in overall enzyme catalytic efficiency by 173-fold) is not nearly as dramatic as that of mutant 30. This latter

point provides an explanation for the observed difference in MGMK/30 and MGMK/SR39 tumor killing efficacy. Based on kinetic data, mutant 30-expressing cells are likely to generate lower amounts of GCV-MP than SR39-expressing cells. The current findings with MGMK/30 reveal that the combination of MGMK and mutant 30 demonstrates a much more striking improvement in tumor killing compared to that of SR39. Therefore, taken together we propose that the combination of MGMK and mutant 30 gave a “balancing” effect in the system, where mutant 30 generates sufficient amounts of GCV-MP to be shunted directly to MGMK and therefore phosphorylation of GCV-MP to GCV-DP can be performed effectively. And this can further results in higher production of active antimetabolites. On the other hand, with MGMK/SR39, escalated levels of GCV-MP generated by SR39 may overwhelm MGMK and consequently result in inefficient conversion of GCV-MP to GCV-DP (bottleneck). As such this ineffective production of GCV-DP is due to the limiting ability of MGMK and therefore even though more GCV-MP is generated, improvement in tumor killing by MGMK/SR39 was only marginal and not nearly as dramatic as seen in MGMK/30. The limited ability of GMK to phosphorylate GCV-MP to GCV DP may open up additional opportunities of improvement. Creation of MGMK mutants with improved activity towards GCV-MP should complement the increased production of GCV-MP by HSVTK mutants (mutant SR39 in particular) via subsequently generating higher amounts of GCV-DP, and ultimately higher levels of active antimetabolites (i.e., GCV-TP). The lack of complete tumor eradication in these studies may be due the short duration of GCV treatment (compared with that in other reports 14-21 days) and to the low dose of GCV that were used in this study. It is particularly important to state that the dose used in this study (total of 2mg/kg/day) is between 25- and 150-fold lower than the doses used in most animal experiments (up to 300mg/kg/day)<sup>7</sup>. A higher dose of GCV and longer GCV treatment may readily result in complete tumor eradication in concert with the use of

MGMK/30 and MGMK/SR39 fusion enzymes. Ultimately, the use of superior fusion enzymes offer significant advantage over wild type HSVTK, HSVTK mutants, or MGMK/HSVTK in at least two important ways: (a) by enhancing GCV-mediated cell killing and bystander killing effect and (b) by further reducing the amount of myelosuppressive GCV required for effective cell killing.

## **ACKNOWLEDGEMENTS**

This work was supported by the National Institutes of Health through grants R01CA85939 (to M.E.B) and T32-GM008336 (to M.S.B).

## **MATERIALS and METHODS**

### **Materials**

Oligonucleotides used to mutate and sequence HSVTK were obtained from Integrated DNA Technologies (Coralville, IA). Restriction endonucleases and T4 DNA ligase were purchased from New England Biolabs (Beverly, MA). DNA purification was done using several kits: Wizard PCR prep kits from Promega (Madison, WI), HiSpeed Plasmid Mini Kit from Qiagen (Valencia, CA), and StrataPrep EF Plasmid Midikit from Stratagene (La Jolla, CA). Alamar Blue was purchased from Serotec Limited (Oxford, UK). All cell culture reagents were purchased from Gibco (Carlsbad, CA). All other reagents were purchased from Sigma (St. Louis, MO) unless otherwise noted.

### **Bacterial strains**

*Escherichia coli* strain NM522 [ $F^+$   $lacI^q\Delta(lacZ)$ -M15 $proA^+B^+$ / $supE thi\Delta(lac-proAB)\Delta(hsdMS-mcrB)5(r_k^-m_k^-McrBC^-)$ ] and *E. coli* strain XL1-Blue [ $F'::Tn10 proA^+B^+ lacI^q D(lacZ) M15/recA1 endA1 gyrA96 (Nal^r) thi hsdR17 (r_k^-m_k^+) supE44 relA1 lac$ ] were used as a recipient for certain cloning procedures. *E. coli* strain TS202A(DE3) (LAM<sup>-</sup>, *tdk-1*, IN(*rrnD-rrnE*)1, *ilv*<sup>-</sup>276 kan<sup>R</sup> ara<sup>-</sup>), a thymidine kinase deficient and a conditional guanylate kinase deficient strain, was used in genetic complementation assays to assess thymidine kinase and guanylate kinase activity.

### **Construction of mgmk/TK fusion mutant constructs**

Construction of pET23d:mgmk/TK fusion mutant constructs was done as previously described by Willmon *et al.*, (2006)<sup>16</sup>. Briefly, the mouse gmK (mgmk) gene was isolated from pET23d:mgmk as an *Bgl*II/*Msc*I fragment and ligated to *Bgl*II/*Mlu*I (blunt ended)-digested pET23d:30 or pET23d:SR39. The resulting

plasmids, designated pET23d:mgmk/30 and pET23d:mgmk/SR39, were confirmed by DNA sequencing.

### **Genetic complementation**

For complementation studies, *E. coli* strain TS202A(DE3) harboring pET23d, pET23d:mgmk, pET23d:HSVTK, pET23d:mgmk/TK pET23d:mgmk/30 and pET23d:mgmk/SR39 were grown at 37°C on either GMK complementation media or TK complementation media as previously described<sup>14, 17</sup>. Briefly, all transformants were grown overnight at 37°C under non-selective conditions on minimal medium [For 1L - 15g Bacto Agar, 100µL 1M CaCl<sub>2</sub>, 1mM MgSO<sub>4</sub>, 11mM glucose, 22mM KH<sub>2</sub>PO<sub>4</sub>, 9mM NaCl, 19mM NH<sub>4</sub>Cl, 47mM Na<sub>2</sub>HPO<sub>4</sub>, 3mM L-isoleucine, 3mM L-valine] containing carbenicillin (carb) and kanamycin (kan) each at 50µg/mL and supplemented with 0.2% L-arabinose to provide expression of an endogenous guanylate kinase from an arabinose promoter. For *gmk* complementation, minimal medium plates containing kanamycin without arabinose was used. For complementation of the *tdk* deficiency, TK selection medium supplemented with arabinose and kanamycin was used.

### **Construction of mammalian expression vectors**

Fusion mutants constructed in this study (pET23d:mgmk/30 and pET23d:mgmk/SR39), previously constructed wild type fusion construct (pET23d:mgmk/HSVTK), and HSVTK mutant genes (pET23d:SR39, pET23d:30), HSVTK wild type gene (pET23d:HSVTK), mgmk gene (pET23d:mgmk) were all subcloned into the mammalian expression vector pUB6/V5-His B (Invitrogen, Carlsband, CA). The pET23d:mgmk, pET23d:SR39, pET23d:mgmk/HSVTK, pET23d:mgmk/30, and pET23d:mgmk/SR39 were subcloned into pUB6/V5-His B digested with *EcoRV* as *NcoI* (blunt-ended) fragments. After restriction enzyme

verification, DNA sequencing analysis confirmed the presence of the mgmk, SR39, mgmk/HSVTK, mgmk/30, and mgmk/SR39 genes. The resulting plasmids were designated pUB: mgmk, pUB: SR39, pUB:mgmk/HSVTK, pUB:mgmk/30, and pUB:mgmk/SR39, respectively. In order to expedite the construction of mammalian vectors, site-directed mutagenesis was performed on plasmid pUB:SR39 to introduce mutations derived from mutant 30 or to revert the sequence back to wild type HSVTK using the QuikChange site-directed mutagenesis kit from Stratagene according to the manufacturer's protocol. Two pairs of oligonucleotides containing wild type sequence at 159-161 amino acid residues (MB428 5'-GCCCTCACCTCATCTTCGACCGCCATCCC-3'/MB429 5'-GGGATGGCGGTCTGAAGATGAGGGTGAGGGC-3') and wild type sequence at 168-169 amino acid residues (MB432 5'-CCATCCCATCGCCGCCCTCCTGTGCTACCCG-3'/MB433 5'-CGGGTAGCACAGGAGGGCGGCGATGGGATGG-3') were used to generate wild type sequence of HSVTK. Two pairs of oligonucleotides containing mutant 30's amino acid substitutions at 159-161 amino acid residues (MB432 5'-GCCCTCACCATTTTTGGCTGACCGCCATCCC-3'/MB433 5'-GGGATGGCGGTCTAGCCAAAATGGTGAGGGC-3') and amino acid substitutions at 168-169 amino acid residues (MB434 5'-CCATCCCATCGCATATTTCTTATGCTACCCG-3'/MB435 5'-CGGGTAGCATAAGAAATATGCGATGGGATGG-3') were used to generate mutant 30 sequence. DNA sequencing analysis was performed to confirm the presence of the correct mutation in mutant 30 sequence (pUB:30) or the presence of HSVTK wild type sequence (pUB:HSVTK).

### **Cell lines**

Cell lines were maintained in a humidified incubator at 37°C in 5% CO<sub>2</sub>. Rat C6 glioma cells (C6) were purchased from ATCC (Manassass. VA) and were grown in Dulbecco's Modified Essential Medium containing 5% fetal bovine serum, 1mM



sodium pyruvate, 10mM HEPES, 100 $\mu$ M nonessential amino acids, 100U/mL penicillin G, 10 $\mu$ g/mL streptomycin sulfate, 292 $\mu$ g/mL L-glutamine, 100 $\mu$ M sodium citrate and 0.0014% NaCl. Transfected cells were cultured in media supplemented with blasticidin at concentration 4 $\mu$ g/mL for selection of stably transfectants.

### ***In vitro* cytotoxicity assay**

One  $\mu$ g of each DNA: pUB (vector alone), pUB:mgmk, pUB:HSVTK, pUB:30, pUB:SR39, pUB:mgmk/HSVTK, pUB:mgmk/30, and pUB:mgmk/SR39 was used to transfect  $1 \times 10^5$  rat C6 glioma cells by lipofection using FuGENE 6 transfection reagent (Roche Diagnostic, Penzberg, Germany) at a 3:1 ratio as described by the manufacturer. Protein expression levels were determined by immunoblot analyses. Briefly, pools of stable transfectants at passage 3 were harvested and resuspended at 100,000 cells/ $\mu$ L in lysis buffer (for 2mL: 2 $\mu$ L 1 M DTT, 20 $\mu$ L 1M HEPES, 40 $\mu$ L Nonidet P40 (Roche Diagnostic, Penzberg, Germany), 2 $\mu$ L MgAc<sub>2</sub>, H<sub>2</sub>O to final volume). The harvested cells were incubated on ice for 20 min and subjected to centrifugation at 4°C for 20 min to pellet debris. The collected samples (10 $\mu$ L per well) were subjected to 12% SDS PAGE, the proteins were then transferred to a nitrocellulose membrane and blocked with 3% gelatin in Tris-buffered saline. The membrane was probed with rabbit polyclonal HSVTK or mgmk antibody and followed by goat anti-rabbit-AP-conjugated antibody. Color reaction was developed using the AP Conjugate Substrate Kit (Bio-Rad, Hercules, CA). *In vitro* cytotoxicity assay was performed using stable transfectants confirmed by immunoblot. Pools of transfectants were transferred to 96-well microtiter plates at an initial density of 500 cells per well. Upon cell adherence overnight, GCV (0-100  $\mu$ M) was added in sets of eight wells for each concentration tested. The cells were subjected to GCV for 7 days, at which time the redox indicator dye Alamar Blue was added. Cell survival was determined by fluorescence recorded at a 530/590 nm, using a multi detector

microplate reader Biotek Synergy HT, several hours later as described by manufacturer and data were plotted with the standard deviation. At least three replicates were performed.

### ***In vitro* bystander experiment**

Rat glioma C6 cells stably transfected with pUB (vector only) were mixed at different ratios with stably transfectants harboring either pUB:HSVTK, pUB:30, pUB:SR39, pUB:mgmk/HSVTK, pUB:mgmk/30 or pUB:mgmk/SR39. The mixed cells were then transferred to 96-well microtiter plates at final density of 500 cells per well and upon cell adherence overnight, a GCV concentration of 80 $\mu$ M was added into the cells. Cell survival was determined as described above.

### **Xenograft tumor model**

Pools of C6 glioma cells stably transfected with pUB, pUB:HSVTK, pUB:30, pUB:SR39, pUB:mgmk/HSVTK, pUB:mgmk/30 or pUB:mgmk/SR39 ( $0.5 \times 10^6$  cells in 200 $\mu$ L of phosphate buffer saline (PBS) at pH 7.2) were injected subcutaneously into 5- to 6-week-old female nude mice ( $n = 5$  for each group) (Athymic NCr-*nu/nu*; National Cancer Institute, Frederick, MD, USA). Bystander xenograft tumor model experiments were done in similar fashion except nude mice ( $n=5$ ) were injected with pools of C6 glioma cells stably transfected with pUB (empty vector) that were mixed with pools of C6 glioma cells stably transfected with either pUB:HSVTK, pUB:30, pUB:SR39, pUB:mgmk/HSVTK, pUB:mgmk/30 or pUB:mgmk/SR39 at a ratio of 95:5 (vector:suicide gene). When the tumors reached 3-4 mm in diameter (day 0), PBS or GCV at 1mg/kg or 0.1mg/kg was administered by intraperitoneal injection twice a day for 8 consecutive days. Starting at day 0, the tumor volume was monitored using caliper measurement (length, width, and height) every other day until day 16 at which time the mice were euthanized. Tumor volume was calculated using the

formula:  $\frac{4}{3}\pi ((\text{Width} \times \text{Length} \times \text{Height})/2)$ . Tumor volume was plotted and analyzed for statistical significance using Student's T-test.

## References

1. Kokoris MS, Black ME. Characterization of herpes simplex virus type 1 thymidine kinase mutants engineered for improved ganciclovir or acyclovir activity. *Protein Sci* 2002;11:2267-2272.
2. Moolten FL. Tumor sensitivity conferred by inserted herpes thymidine kinase genes: paradigm for a prospective cancer control strategy. *Cancer Res* 1986;46:5276-5281.
3. Edelstein ML, Abedi MR, Wixon J, Edelstein RM. Gene Therapy Clinical Trials Worldwide 1989-2004 - An Overview. *The Journal of Gene Medicine* 2004;6:597-602.
4. Miller WH, Miller RL. Phosphorylation of acyclovir (acycloguanosine) monophosphate by GMP kinase. *J Biol Chem* 1980;255:7204-7207.
5. Reardon JE. Herpes simplex virus type 1 and human DNA polymerase interactions with 2'-deoxyguanosine 5'-triphosphate analogues. Kinetics of incorporation into DNA and induction of inhibition. *J Biol Chem* 1989;264:19039-19044.
6. Field AK, Davies ME, DeWitt C, Perry HC, Liou R, Germershausen J, Karkas JD, Ashton WT, Johnston DB, Tolman RL. 9-([2-hydroxy-1-(hydroxymethyl)ethoxy]methyl)guanine: a selective inhibitor of herpes group virus replication. *Proceedings of the National Academy of Sciences of the United States of America* 1983;80:4139-4143.
7. Greco O, Dachs G. Gene directed enzyme/prodrug therapy of cancer: historical appraisal and future prospective. *Journal of Cellular Physiology* 2001;187:22-36.
8. Freeman SM, Ramesh R, Marrogi AJ. Immune system in suicide-gene therapy. *The Lancet* 1997;349:2-3.
9. Kokoris MS, Sabo P, Black ME. Enhancement of tumor ablation by a selected HSV-thymidine kinase mutant. *Gene Ther* 1999;6:1415-1426.
10. Ostermann N, Lavie A, Padiyar S, Brundiers R, Veit T, Reinstein J, Goody RS, Konrad M, Schlichting I. Potentiating AZT activation: structures of wild-type and mutant human thymidylate kinase suggest reasons for the mutants' improved kinetics with the HIV prodrug metabolite AZTMP. *Journal of Molecular Biology* 2000;304:43-53.
11. Fridland A, Connelly MC, Ashmun R. Relationship of deoxynucleotide changes to inhibition of DNA synthesis induced by the antiretroviral agent 3'-azido-3'-deoxythymidine and release of its monophosphate by human lymphoid cells (CCRF-CEM). *Mol Pharmacol* 1990;37:665-670.

12. Brady WA, Kokoris MS, Fitzgibbon M, Black M. Cloning, characterization, and modeling of mouse and human guanylate kinases. *The Journal of Biological Chemistry* 1996;271:16734-16740.
13. Boehme R. Phosphorylation of 9-b-D-arabinofuranosylguanine monophosphate by *Drosophila melanogaster* guanylate kinase. *J Biol Chem* 1984;258:12346-12349.
14. Black ME, Newcomb TG, Wilson HM, Loeb LA. Creation of drug-specific herpes simplex virus type 1 thymidine kinase mutants for gene therapy. *PNAS* 1996;93:3525-3529.
15. Black ME, Kokoris MS, Sabo P. Herpes simplex virus-1 thymidine kinase mutants created by semi-random sequence mutagenesis improve prodrug-mediated tumor cell killing. *Cancer Res* 2001;61:3022-3026.
16. Willmon CL, Krabbenhoft E, Black ME. A guanylate kinase//HSV-1 thymidine kinase fusion protein enhances prodrug-mediated cell killing. *Gene Ther* 2006;13:1309-1312.
17. Stolworthy TS, Krabbenhoft E, Black ME. A novel *Escherichia coli* strain allows functional analysis of guanylate kinase drug resistance and sensitivity. *Analytical Biochemistry* 2003;322:40-47.
18. Dilber MS, Abedi MR, Christensson B, Bjorkstrand B, Kidder GM, Naus CCG, Gahrton G, Smith CIE. Gap junctions promote the bystander effect of herpes simplex virus thymidine kinase *in vivo*. *Cancer Res* 1997;57:1523-1528.
19. Culver KW, Ram Z, Wallbridge S, Ishii H, Oldfield EH, Blaese RM. In vivo gene transfer with retroviral vector-producer cells for treatment of experimental brain tumors. *Science* 1992;256:1550-1552.
20. Kaldor J, Day N, Pettersson F, Clarke E, Pederson D, Mehnert W, Bell J, Host H, Prior P, Kargalainen S, Neal F, Koch M, Band P, Choi W, Kirn V, Arslan A, Zaren B, Belch A, Storm H, Kittelmann B, Fraser P, Stovall M. Leukemia following chemotherapy for ovarian cancer. *New England Journal Medicine* 1990;322:1-6.
21. Relling MV, Rubnitz JE, Rivera GK, Boyett JM, Hancock ML, Felix CA, Kun LE, Walter AW, Evans WE, Pui CH. High incidence of secondary brain tumours after radiotherapy and antimetabolites. *The Lancet* 1999;354:34-39.
22. Dachs GU, Tupper J, Tozer G. From bench to bedside for gene-directed enzyme prodrug therapy of cancer. *Anticancer Drugs* 2005;16:349-359.
23. Norris JS, Norris KL, Holman DH, El-Zawahry A, Keane TE, Dong Jy, Tavassoli M. The present and future for gene and viral therapy of directly accessible prostate and squamous cell cancers of the head and neck. *Future Oncology* 2005;1:115-123.
24. Pope IM, Poston GJ, Kinsella AR. The role of the bystander effect in suicide gene therapy. *European Journal of Cancer* 1997;33:1005-1016.

25. Vrionis FD, Wu JK, Qi P, Waltzman M, Cherington V, Spray DC. The bystander effect exerted by tumor cells expressing the herpes simplex virus thymidine kinase (HSVtk) gene is dependent on connexin expression and cell communication via gap junctions. *Gene Therapy* 1997;4:577-585.
26. Akyürek L, Nallamshetty S, Aoki K, San H, Yang Z, Nabel G, Nabel G. Coexpression of guanylate kinase with thymidine kinase enhances prodrug cell killing *in vitro* and suppresses vascular smooth muscle cell proliferation *in vivo*. *Molecular Therapy* 2001;3:779-786.

## FIGURE LEGENDS

**Figure 2.1.** GCV sensitivity assays of rat C6 transfectants.

Pools of stably transfectants containing **(A)** vector only pUB (○), pUB:mgmk (●), pUB:HSVTK (□), pUB:mgmk/HSVTK (■), pUB:30 (Δ) and pUB:mgmk.30 (▲), or **(B)** pUB:SR39 (◇) and pUB:mgmk/SR39 (◆) were evaluated for GCV sensitivity as described in the Materials and Methods section. After 7 days of GCV treatment, cell survival was determined using Alamar Blue according to the manufacturer's instructions. Each data point (mean ± SEM; n=3; performed with 24 replicates) is expressed as a percentage of the value for control wells with no GCV treatment.

**Figure 2.2.** Bystander analysis of rat C6 transfectants in the presence of GCV.

Pools of rat C6 glioma cells containing vector only were mixed with cells harboring either pUB:HSVTK (□), pUB:mgmk/HSVTK (■), pUB:30 (Δ) and pUB:mgmk.30 (▲), pUB:SR39 (◇) or pUB:mgmk/SR39 (◆) at different ratios and were subjected to 80 μM GCV for a period of 7 days as described in Materials and Methods. Cell survival was determined using Alamar Blue according to the manufacturer's instructions. Each data point (mean ± SEM; n=3; performed with 24 replicates) is expressed as a percentage of the value for control wells with 0% of HSVTK expressing cells (pUB only).

**Figure 2.3.** Tumor growth during and after GCV treatment in xenograft tumor model.

Pools of rat C6 glioma cells transfected with **(A)** pUB (○), pUB:HSVTK (□), pUB:mgmk/HSVTK (■), pUB:30 (Δ) and pUB:mgmk/30 (▲); or **(B)** pUB (○), pUB:HSVTK (□), pUB:mgmk/HSVTK (■), pUB:SR39 (◇) and pUB:mgmk/SR39 (◆); or **(C)** pUB:SR39 (◇) and pUB:mgmk/SR39 (◆); or **(D)** pUB (○), pUB:HSVTK (□),

pUB:mgmK/HSVTK (■), pUB:30 (Δ), pUB:mgmK.30 (▲), pUB:SR39 (◇) and pUB:mgmK/SR39 (◆) were used to seed tumors in nude mice (n=5 for each group). When tumor size reached 3-4mm (day 0), **(A & B)** GCV (1mg/kg), **(C)** GCV (0.1mg/kg) or **(D)** PBS was intraperitoneally administered twice a day for 8 days. During this period, tumor growth was measured every other day. Tumor volume was calculated using the formula  $4/3\pi ((\text{Width} \times \text{Length} \times \text{Height})/2)$ , plotted and analyzed for statistical significance using Student's t-test. Asterisks denote statistical significance ( $P \leq 0.05$ ) in tumor sizes between: **(A)** mice harboring MGMK/30-expressing tumor cells and those that received either vector- or HSVTK-, or mutant 30- or MGMK/HSVTK-expressing tumor cells in the presence of 1mg/kg GCV; **(B)** mice harboring SR39- or MGMK/SR39-expressing cells (no statistical difference between the two) and those that received either vector- or HSVTK- or MGMK/HSVTK-expressing cell in the presence of 1mg/kg GCV; **(C)** mice harboring SR39 and those that received MGMK/SR39-expressing cells in the presence of 0.1mg/kg GCV.

**Figure 2.4.** Bystander xenograft tumor model of mutant 30 and MGMK/30

Pools of rat C6 glioma cells transfected with pUB were mixed with cells stably transfected with pUB:HSVTK (□), pUB:mgmK/HSVTK (■), pUB:30 (Δ) and pUB:mgmK/30 (▲) a ratio of 95:5 (vector:suicide genes, respectively). Mixed cells were used to seed tumors in nude mice (n=5 for each group). When tumor size reached 3-4mm (day 0), **(A)** GCV (1mg/kg) or **(B)** PBS was administered twice a day for 8 days. During this period, tumor growth was measured every other day. Tumor volume was calculated using the formula  $4/3\pi ((\text{Width} \times \text{Length} \times \text{Height})/2)$ , plotted and analyzed for statistical significance using Student's t-test. Asterisks denote statistical significance ( $P \leq 0.05$ ) in tumor sizes between mice harboring 5%



of MGMK/30-expressing tumor cells and those that received either 5% of HSVTK- or mutant 30- or MGMK/HSVTK-expressing tumor cells in the presence of 1mg/kg GCV.

**Figure 2.5.** Bystander xenograft tumor model of SR39 and MGMK/SR39

Pools of rat C6 glioma cells transfected with pUB were mixed with cells stably transfected with pUB:HSVTK (□), pUB:mgmk/HSVTK (■), pUB:SR39 (◇) and pUB:mgmk/SR39 (◆) were used to seed tumors in nude mice (n=5 for each group). When tumor size reached 3-4mm (day 0), **(A)** GCV (1mg/kg) or **(B)** PBS was administered twice a day for 8 days. During this period, tumor growth was measured every other day. Tumor volume was calculated using the formula  $4/3\pi ((\text{Width} \times \text{Length} \times \text{Height})/2)$ , plotted and analyzed for statistical significance using Student's t-test. Asterisks denote statistical significance ( $P \leq 0.05$ ) in tumor sizes between mice harboring 5% of MGMK/SR39-expressing tumor cells and those that received 5% of either HSVTK-, MGMK/HSVTK-, or SR39-expressing tumor cells in the presence of 1mg/kg GCV.

**Table 2.1.** *In vitro* response of rat C6 glioma cells expressing wild type, mutant HSVTKs, wild type fusion or mutant fusion constructs to GCV.

	GCV IC <sub>50</sub> ( $\mu$ M)	Relative to HSVTK
pUB	50	1
pUB:MGMK	65	0.77
pUB:HSVTK	50	1
pUB:30	0.4	125
pUB:SR39	0.02	2,500
pUB:MGMK/HSVTK	0.5	100
pUB:MGMK/30	0.004	12,500
pUB:MGMK/SR39	0.02	2,500

**Table 2.2.** *In vivo* response of rat C6 tumors expressing wild type HSVTK, mutant 30, MGMK/HSVTK or MGMK/30 to PBS or GCV treatment.

	Mean Tumor Volume (mm <sup>3</sup> )		
	Day 8		Day 16
	PBS	GCV (1mg/kg)	GCV (1mg/kg)
HSVTK	428.29 (39.27) <sup>a</sup>	453.42 (43.17)**	3622.50 (242.60)**
Mutant 30	399.30 (23.58)	126.19 (20.03)**	1681.80 (248.88)**
MGMK/HSVTK	438.51 (47.73)	109.85 (14.94)**	1679.10 (284.62)**
MGMK/30	473.76 (39.49)	16.60 (3.06)	33.39 (5.55)

<sup>a</sup> Standard error mean

\*\* P values  $\leq$  0.0001; this P values reflect a comparison between MGMK/30 and HSVTK, or between MGMK/30 and mutant 30, or between MGMK/30 and MGMK/HSVTK tumor sizes treated with GCV (1mg/kg) at two different time points (day 8 and day 16) (n=5).

**Table 2.3.** *In vivo* response of rat C6 tumors expressing SR39 or MGMK/SR39 to PBS or GCV treatment.

	Mean Tumor Volume (mm <sup>3</sup> )				
	Day 8	Day 8	Day 14	Day 8	Day 14
	PBS	GCV (1mg/kg)	GCV (1mg/kg)	GCV (0.1mg/kg)	GCV (0.1mg/kg)
SR39	582.88 (73.84) <sup>a</sup>	44.03 (8.23)	52.62 (7.87)	77.17 (13.39)*	214.04 (37.54)*
MGMK/SR39	562.96 (56.87)	50.10 (4.86)	46.16 (15.48)	18.15 (3.16)	120.46 (21.16)

<sup>a</sup> Standard error mean

\* P values ≤ 0.05, this P values reflect a comparison between SR39 and MGMK/SR39 tumor size treated with 0.1mg/kg GCV at two different time points (day 8 and day 14) (n=5).

**Figure 2.1**

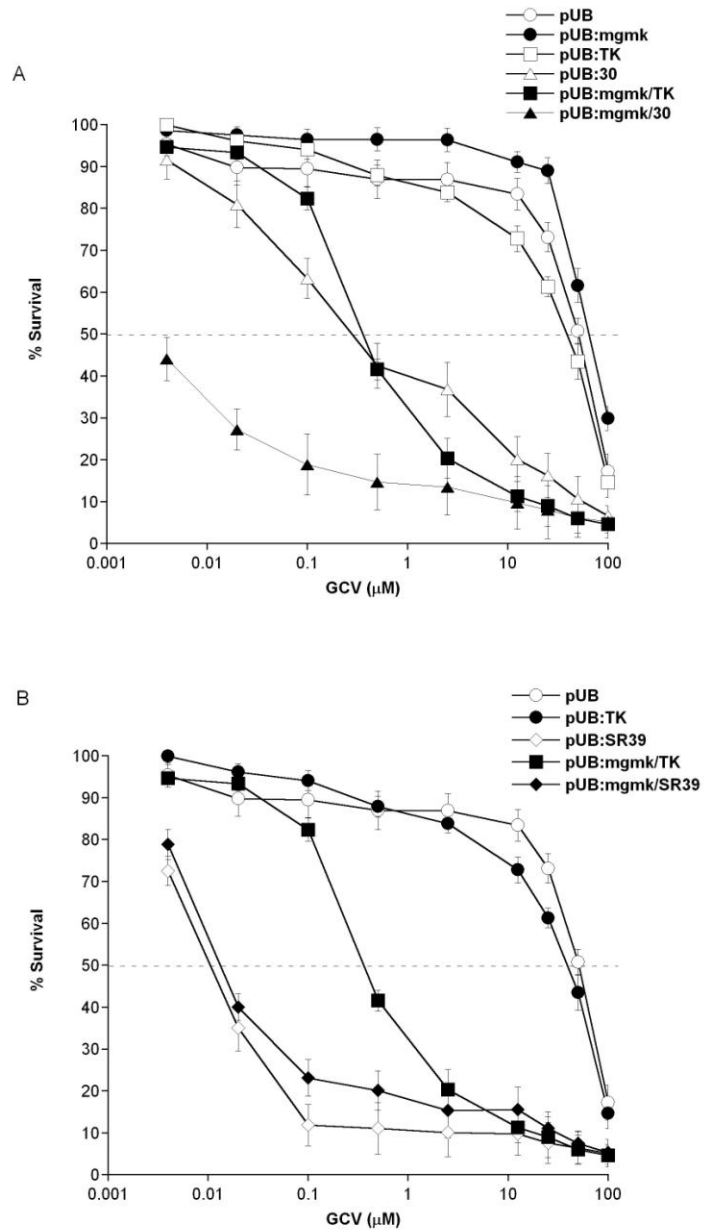
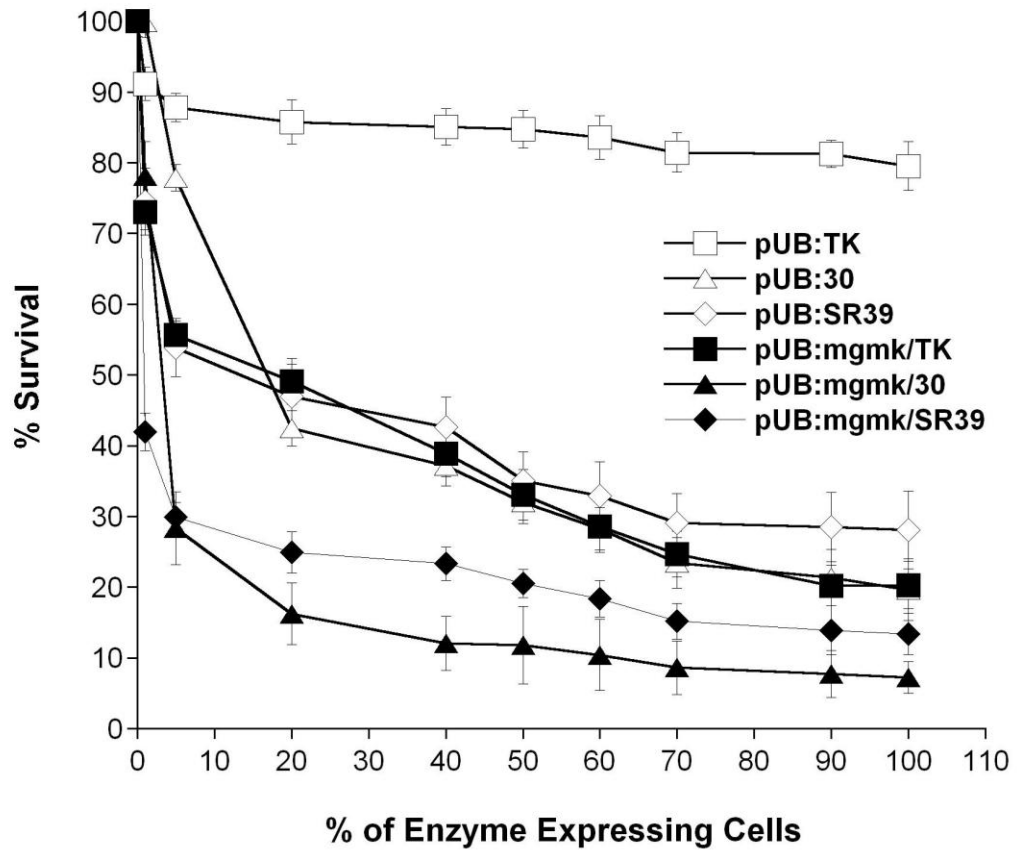


Figure 2.2



**Figure 2.3**

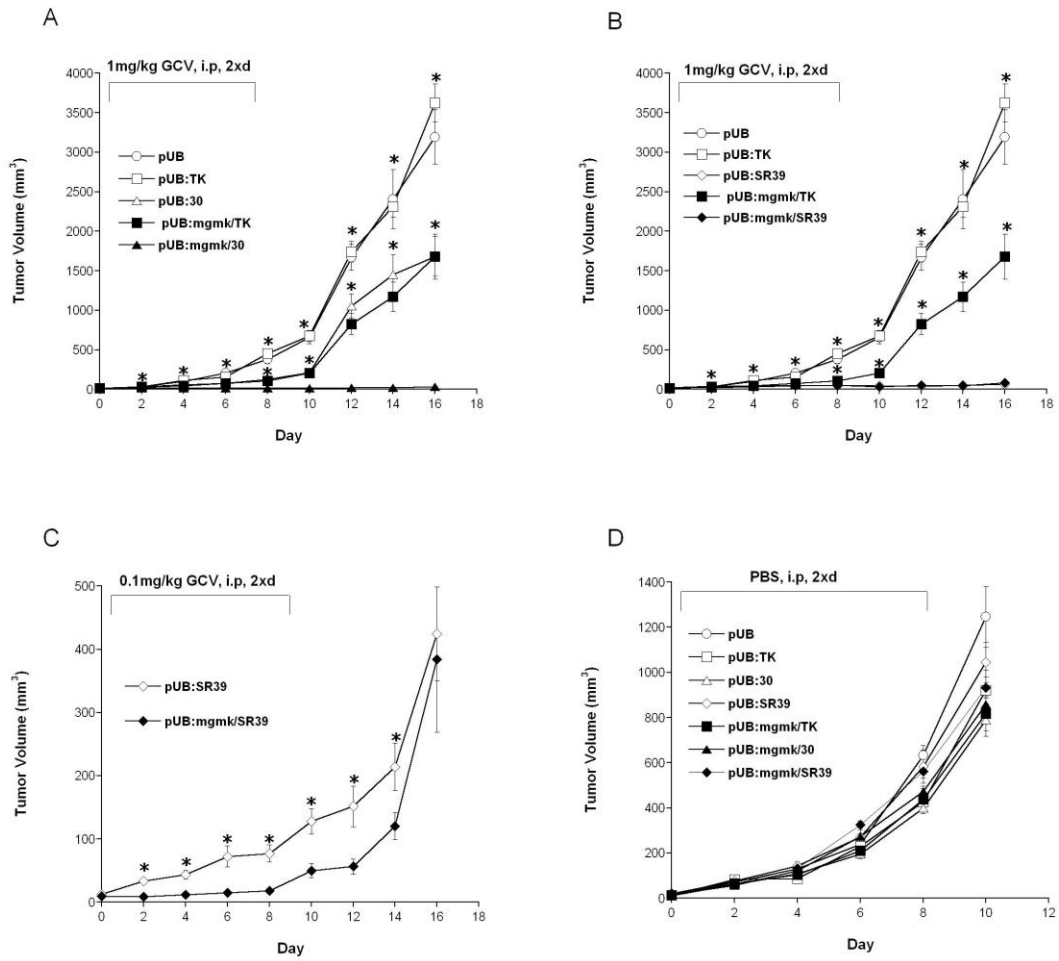


Figure 2.4

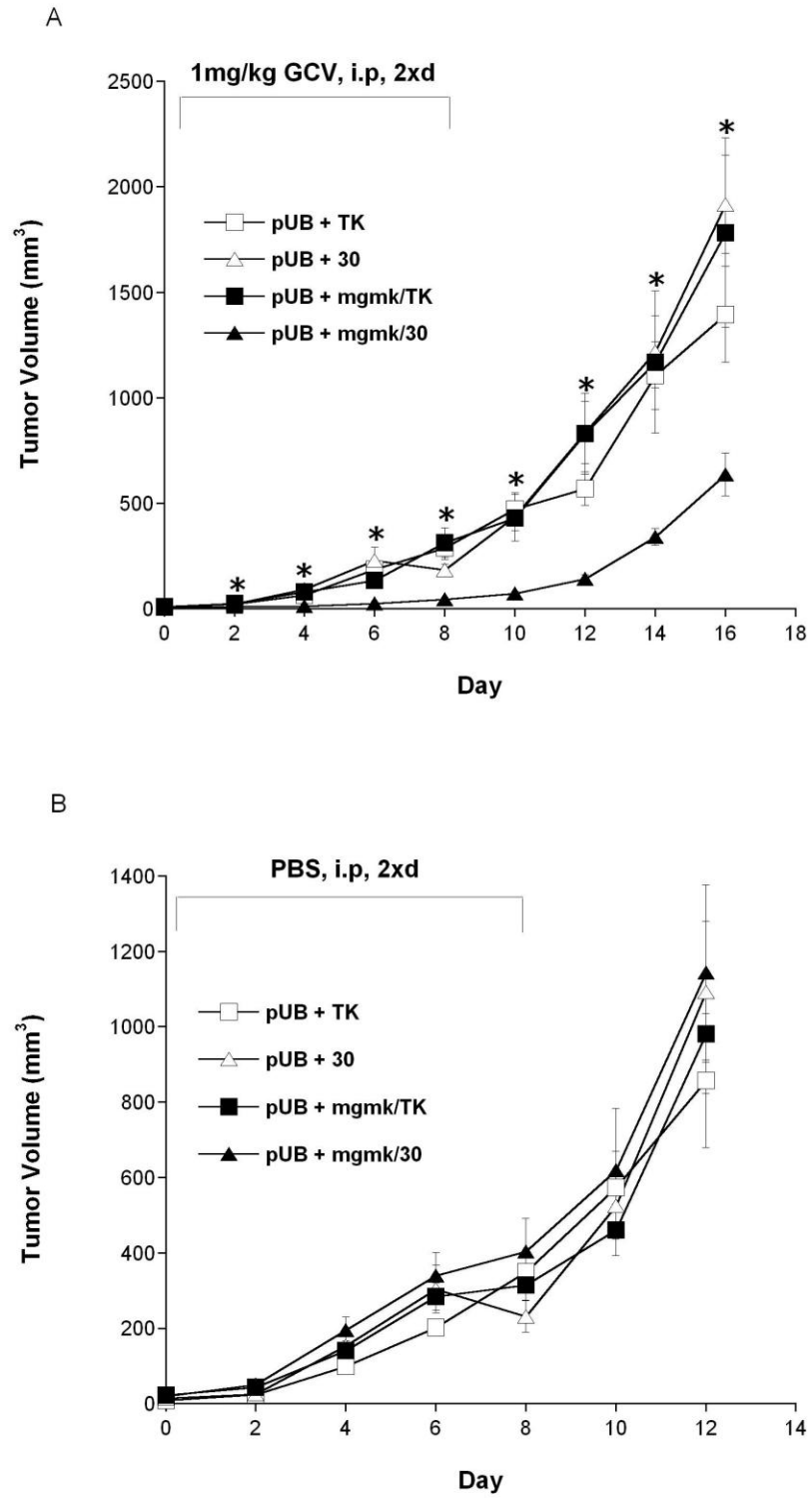
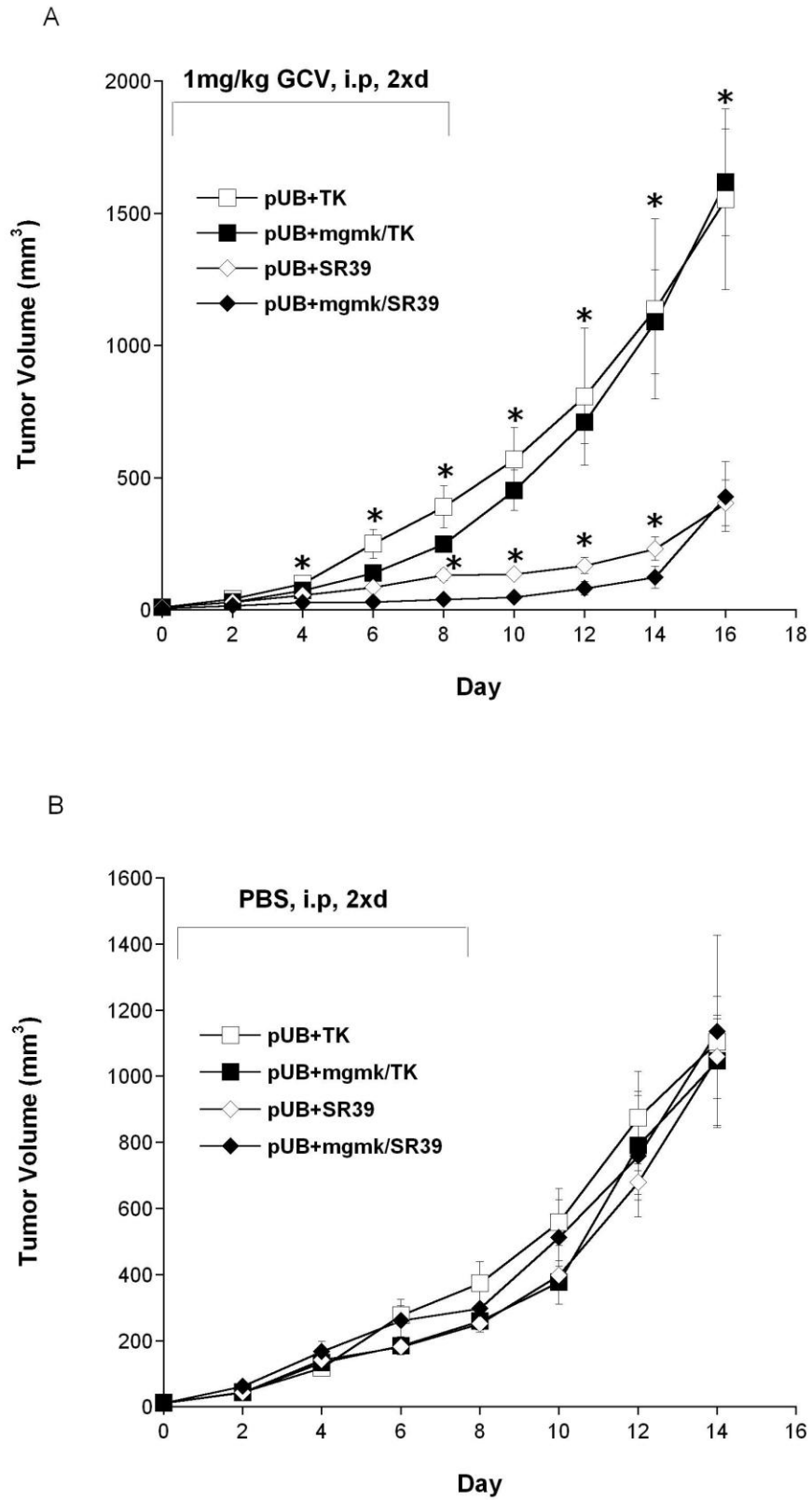


Figure 2.5





## CHAPTER THREE

### **Mutations at Serine 37 in Mouse Guanylate Kinase Confer Resistance to 6-Thioguanine**

#### **ABSTRACT**

Guanylate kinase (GMK) is an essential nucleoside monophosphate kinase that catalyzes the phosphorylation of GMP and dGMP to yield GDP and dGDP, respectively, important precursors for nucleotide synthesis. GMK is also responsible for the activation of 6-thioguanine (6-TG), a drug widely used as chemotherapeutic agent to treat leukemia. Several mechanisms of resistance to 6-TG have been reported but a subset of drug resistant cells cannot be explained by these mechanisms. We propose that mutations in GMK could result in drug resistance. Because cells require the presence of a functional GMK for viability, mutations that arise that lead to 6-TG resistance must retain activity toward GMP. We report three amino acid substitutions at serine 37 (S37) in mouse guanylate kinase that display activity towards GMP by conferring genetic complementation to a conditional guanylate kinase deficient *E. coli* and in enzyme assays. When 6-TG is included in complementation studies, cells expressing wild type GMK are sensitive whereas all S37 mutants examined are able to effectively discriminate against 6-TG and display a drug resistance phenotype. Activity of the three S37 mutant enzymes towards clinically relevant concentrations of 6-TGMP is undetectable. Mutations in guanylate kinase, therefore, represent a previously undescribed mechanism for 6-TG resistance.

---

This manuscript was accepted by Protein Engineering Design and Selection in the following manuscript: **Ardiani, A.**, Goyke, A., and Black, M.E. Mutations at Serine 37 in Mouse Guanylate Kinase Confer Resistance to 6-thioguanine. *Protein Engineering Design and Selection* **22/4**: 225-232.

## INTRODUCTION

Guanylate kinase (GMK, ATP:GMP phosphotransferase, EC 2.7.4.8) is an essential enzyme involved in purine biosynthesis and is responsible for the phosphorylation of GMP and dGMP. In addition, GMK functions in the recovery of cGMP and is therefore thought to regulate the supply of guanine nucleotides to signal transduction pathway components (Woods and Bryant, 1991; Gaidarov *et al.*, 1993). From a medical perspective guanylate kinase performs a key step in the activation of several important antiviral and anti-neoplastic agents. Following initial activation by the viral encoded thymidine kinase in herpes infected cells, the prodrugs acyclovir and gancyclovir require further activation by guanylate kinase (Miller and Miller, 1980; Boehme, 1984). Another major therapeutic role of GMK is in the activation of the guanine analog, 6-thioguanine (6-TG) which has been primarily used as a treatment for childhood and adult leukemia since the 1950s (Elion, 1989). 6-TG also has the ability to kill proliferating T cells, contributing to its immunosuppressive properties. This has led to its use as an immunosuppressant in transplant surgery and as an anti-inflammatory agent in autoimmune diseases such as inflammatory bowel disease (Karran, 2006). Despite the widespread use of 6-TG to treat a variety of diseases, the mechanism of 6-TG toxicity and drug resistance is not fully understood (Karran, 2006).

Structurally similar to guanine, 6-TG differs only at the carbon 6 position where the oxygen in guanine is replaced by a thiol. Upon entering the cell, hypoxanthine-guanine phosphoribosyltransferase (HGPRT) initiates the activation of 6-TG by transferring a phosphoribosyl group to 6-TG forming 6-thioguanine-monophosphate (6-TGMP) (Karran, 2006). 6-TGMP is then further phosphorylated to 6-thioguanine diphosphate (6-TGDP) and 6-thioguanine triphosphate (6-TGTP) by guanylate kinase and nucleoside diphosphokinase, respectively (Sekulic *et al.*, 2002). Once 6-TG enters the cell, the process of 6-TG degradation can be initiated by

thiopurine S-methyltransferase (TPMT) to form inactive methylated products (Karran, 2006). The presence of TPMT serves to protect patients from negative effects of 6-TG, such as myelosuppression and low whole blood cell counts (Karran, 2006). Indeed, in patients who inherit two low activity variant alleles of the TPMT gene are more prone to 6-TG induced hematopoietic toxicity from the accumulation of the inactive form and usually suffer intense myelosuppression (Karran, 2006).

Incorporation of 6-TGMP into DNA during synthesis has been reported to cause a plethora of DNA damaging events including single- and double-strand breaks, errors during sister-chromatid exchange events, protein cross-links and large-scale chromosomal damage (Bohon and de los Santos, 2003; Yan *et al.*, 2003; Karran and Attard, 2008). 6-TGMP-containing DNA has also been shown to be a poor template for replication by DNA polymerase and a poor substrate for DNA ligases, thereby interfering with both leading and lagging strand DNA replication (Ling *et al.*, 1992). Furthermore, once 6-TGMP is incorporated DNA, methylation by S-adenosylmethionine (SAM) results in the formation of S6-methylguanine (Me-6-TG). During DNA replication, Me-6-TG acts as a mutagenic lesion due to its preference to base pair with thymine, rather than cytosine. The abnormal base pairing subsequently activates the mismatch repair system (MMR), which results in lethal processing and leads to cell death. The general outcome is that while incorporation of 6-TGMP into DNA is not directly toxic to cells, it prevents subsequent replication by halting the cell cycle in G2 phase after one round of replication probably as a result of one or more of the many effects of 6-TG described above (Bohon and de los Santos, 2003). Needless to say, no single event has been associated with 6-TG toxicity.

Despite the wide application of 6-TG as an anti-leukemic agent, one major drawback with its use as a chemotherapeutic drug is the development of drug resistance. The majority of 6-TG resistance can be attributed to the increase

activity/production of TPMT or to a lack of, or reduced HGPRT activity (Lennard, 1992; Karran, 2006). To a lesser extent, an inactive MMR system or 6-TG transport impairment have also been reported to contribute to drug resistance (Swann *et al.*, 1996; Fotoohi *et al.*, 2006). However, not all 6-TG drug resistance can be accounted for by these mechanisms. Evidence indicates the presence of unknown and random inter-individual variations in 6-TG resistance cells of phenotypically normal individuals (Yamanaka *et al.*, 1985; Aubrecht *et al.*, 1997). There is also considerable inter-individual variability in mutation frequency that gives rise to 6-TG resistance in normal, nontransformed cells from patients with cancer prone disease such as Werner's syndrome (Fukuchi *et al.*, 1990; Davies *et al.*, 1992; Aubrecht *et al.*, 1997). Because there appears to be a subset of 6-TG resistance that cannot be attributed to mutations that affect HGPRT, MMR or transporter activities, we hypothesize that mutations could arise in the enzyme responsible for the second and rate limiting step in the 6-TG activation pathway, i. e., the phosphorylation of 6-TGMP to 6-TGDP by GMK. Such mutants would need to retain essential GMP phosphorylation activity but lack the ability to phosphorylate 6-TGMP. Our initial studies presented here focus on evaluating the potential that such mutation(s) in GMK exist. Towards that end, mouse guanylate kinase (MGMK) serine 37 (S37) was targeted for mutagenesis based on structural information that suggests that activation occurs when a bond is formed between S37 and the oxygen on carbon six (C6) of guanine or at the sulfur at C6 in 6-TG (Figure 3.1). Site-directed mutagenesis was used to introduce the larger polar residue, tyrosine, medium-size polar residue, threonine, or a small non-polar residue, alanine. These residues were selected to evaluate the influence of steric strain or a hydroxyl group on substrate binding and catalysis especially with regard to the 6-thioguanine substrate. This study explores the role of MGМК residue S37 in enzyme/substrate recognition with respect to the natural substrate GMP and the important anti-metabolite, 6-TGMP.

## **MATERIALS and METHODS**

### *Materials*

Restriction endonucleases and T4 DNA ligase were purchased from Gibco BRL (Rockville, MD) or New England Biolabs (Beverly, MA). Oligonucleotides used for site-directed mutagenesis and DNA sequencing were obtained from Operon (San Pablo, CA). Nickel columns (Ni-NTA Spin Kit) used to purify wild type and mutant guanylate kinases were purchased from Qiagen (Valencia, CA). 6-TGMP used in enzyme assays was custom synthesized by Moravek Biochemical (Brea, CA). Enzyme assay reagents and other chemicals were purchased from Sigma (St. Louis, MO) unless otherwise specified.

### *Bacterial strains*

*Escherichia coli* strain NM522 [ $F' lacI_q\Delta(lacZ)$ -M15 $proA_+B_+/supE thi\Delta(lac-proAB)\Delta(hsdMS-mcrB)5(r_k^-m_k^-McrBC^-)$ ] was used as a recipient for certain cloning procedures. *Escherichia coli* strain CJ236 ( $F^+$  LAM $^-$ ,  $ung-1$ ,  $relA1$ ,  $dut-1$ ,  $spoT1$ ,  $thi-1$ ) was used to produce single-stranded DNA for site directed mutagenesis (Kunkel, 1985). *Escherichia coli* strain TS202A(DE3) (LAM $^-$ ,  $tdk-1$ , IN( $rrnD-rrnE$ )1,  $ilv^-276$  kan $^R$  ara $^-$ ), a conditional guanylate kinase deficient strain, was used in genetic complementation experiments to assess guanylate kinase activity and sensitivity to 6-TG. Growth conditions were as previously described (Stolworthy *et al.*, 2003).

### *Construction of guanylate kinase mutants*

The bacterial expression vector, pETHT:mgmk, described previously, was used as a template for the introduction of amino acid substitutions at serine 37 by site-directed mutagenesis using the Kunkel method (Brady *et al.*, 1996; Stolworthy and Black, 2001; Kunkel, 1985). The mutagenic oligonucleotides used were designed to also introduce a new restriction site and were as follow: S37A, 5'-

CAGTGTGCGCATACTACAAGG-3', *Bst*UI; S37T, 5'-CAGTGTGACTCATACTACAAGG-3', *Hinf*I and; S37Y, 5'-CAGTGTGTACCATACTACAAGG-3', *Rsa*I. The resulting mutations were confirmed by DNA sequencing and the plasmids designated pETHT:mgmk-S37A, pETHT:mgmk-S37T, and pETHT:mgmk-S37Y. Sequencing was performed at the core sequencing facility at Washington State University.

#### *Genetic complementation*

For complementation studies, *E. coli* strain TS202A(DE3) harboring pETHT, pETHT:mgmk, pETHT:mgmk-S37A, pETHT:mgmk-S37T or pETHT:mgmk-S37Y were grown at 37°C on selection media as previously described (Stolworthy *et al.*, 2003). Briefly, all transformants were grown under non-selective conditions on minimal medium [For 1L - 15g Bacto Agar, 100µl 1M CaCl<sub>2</sub>, 1mM MgSO<sub>4</sub>, 11mM glucose, 22mM KH<sub>2</sub>PO<sub>4</sub>, 9mM NaCl, 19mM NH<sub>4</sub>Cl, 47mM Na<sub>2</sub>HPO<sub>4</sub>, 3 mM L-isoleucine, 3 mM L-valine] containing carbenicillin (carb) and kanamycin (kan) each at 50µg/ml and supplemented with 0.2% L-arabinose (+ARA) to provide expression of an endogenous guanylate kinase from an arabinose promoter. For selective conditions (genetic complementation by guanylate kinase), arabinose was omitted from the minimal medium (-ARA). For drug sensitivity assays, -ARA medium was supplemented with 300µg/ml of 6-thioguanine (-ARA+6-TG).

#### *Growth curves*

*E. coli* strain TS202A(DE3) harboring pETHT, pETHT:mgmk, pETHT:mgmk-S37A, pETHT:mgmk-S37T or pETHT:mgmk-S37Y were grown at 37°C on +ARA media. Single colony from each sample was grown over night. Five ml of overnight cultures (+ARA) of TS202A(DE3) cells harboring pETHT, pETHT:mgmk, pETHT:mgmk-S37A, pETHT:mgmk-S37T or pETHT:mgmk-S37Y were used to inoculate 50ml of +ARA, -ARA, or -ARA+6TG media to an initial OD<sub>600</sub> of ~0.05-

0.07. Cultures were then grown at 37°C with vigorous shaking and monitored for growth by reading the OD<sub>600</sub> every 30 min using a Bio-Rad Smart Spec 3000 (Hercules, CA). The growth experiments were repeated at least three times and similar results were obtained.

#### *Protein overexpression and purification*

*E. coli* TS202A(DE3) harboring pETHT:mgmk, pETHT:mgmk-S37A, pETHT:mgmk-S37T or pETHT:mgmk-S37Y were grown at 30°C in M9ZB [For 1L – 10g Bacto tryptone, 5g NaCl, 100µl CaCl<sub>2</sub>, 1mM MgSO<sub>4</sub>, 11mM glucose, 22mM KH<sub>2</sub>PO<sub>4</sub>, 9mM NaCl, 19mM NH<sub>4</sub>Cl, 47mM Na<sub>2</sub>HPO<sub>4</sub>] containing carbenicillin (carb) and kanamycin (kan) at 50µg/ml and supplemented with 0.2% L-arabinose (M9ZB+ARA). Five ml of overnight culture was transferred to 500ml of M9ZB +ARA and the cultures grown at 30°C until an OD<sub>600</sub> of 0.2 – 0.25 was reached. Protein overexpression was induced by the addition of 0.4mM isopropyl-1-thio-β-D-galactopyranoside (IPTG).

Proteins were purified using a Qiagen Ni-NTA Spin Kit (Valencia, CA) under native conditions as specified by the manufacturer. Three hrs following IPTG induction, cells were cooled on ice for 15-30 min and then centrifuged at 4000rpm for 10 min at 4°C (Beckman JLA-10.500). Cells were lysed by adding 17.5mL lysis buffer (50mM NaH<sub>2</sub>PO<sub>4</sub>, 300mM NaCl, 10mM imidazole at pH 8.0) and lysozyme at 1mg/mL and incubated on ice for 30 min and further subjected to sonication with six-10 sec bursts with a 10 sec cooling period between bursts. To pellet cellular debris, the lysate was centrifuged at 9000rpm (Beckman JA-17) for 20-30 min at 4°C. Cleared lysate was produced by filtering the lysate through 0.2µM Supor<sup>®</sup> Membrane Low Protein Binding (PALL-Life Sciences, East Hills, NY). For affinity purification, 1mL of Ni-NTA slurry was added to 4mL cleared lysate and gently mixed by shaking at 4°C for 60 min. The Ni-NTA resin/cleared lysate mixture was added

into a column and flow through fractions were collected. The resin was subjected to washing by adding 8mL of wash buffer (50mM NaH<sub>2</sub>PO<sub>4</sub>, 600mM NaCl, and 20mM imidazole at pH 8.0) three times. Bound protein was eluted by adding 4 aliquots of 500µl elution buffer (50mM NaH<sub>2</sub>PO<sub>4</sub>, 300mM NaCl, and 250mM imidazole at pH 8.0). The elution fractions were dialyzed against dialysis buffer (50mM NaCl, 50mM Tris at pH 7.5) at 4°C. After dialysis, the samples were collected and stored at -20°C. A small sample (1µg) of each purified protein was subjected to electrophoresis in a 12% polyacrylamide-SDS containing gel. Protein concentrations were quantified by the Bradford method using reagents supplied by Bio-Rad (Hercules, CA). Known concentrations of bovine serum albumin were used as standards and used to generate calibration curves according to the manufacturer's instructions.

#### *Spectrophotometric assay*

Enzyme activities towards the substrates GMP and 6-thioguanine-monophosphate (6-TGMP) were measured using a lactate dehydrogenase-pyruvate kinase coupled assay (Agarwal *et al.*, 1978). Briefly, 1µg or 7µg of enzyme, for GMP or 6-TGMP assays, respectively, was mixed with 500µl guanylate kinase assay cocktail reaction (1M Tris pH 7.5, 2.5M KCl, 1M MgCl<sub>2</sub>, 1M NaPEP, 10mM NADH, 100mM ATP, 8.5µl pyruvate kinase, 8.5µl lactate dehydrogenase in 5ml). The reaction was started by the addition of either various concentrations of GMP or 6-TGMP. The A<sub>340</sub> was measured at 2 sec intervals over 1800 sec using an HP™ 8452 Olis SpectralWorks diode array spectrophotometer. For kinetic analysis studies, the A<sub>340</sub> was measured at 10 sec intervals over 900 sec (GMP) or at 60 sec intervals over 1800 sec (6-TGMP) using a Shimadzu UV-1700 PharmaSpec UV-VIS Spectrophotometer. Each enzyme assay experiment was repeated at least three times.



## RESULTS

### *Construction of mutants and genetic complementation*

Using site-directed mutagenesis, single amino acid substitutions were introduced at S37 to create the MGMK mutants S37A, S37T, and S37Y as described in *Materials and Methods*. To ascertain whether these mutants displayed GMK activity, pETHT, pETHT:mgmk, pETHT:mgmk-S37A, pETHT:mgmk-S37Y and pETHT:mgmk-S37T were used to transform a previously established conditional guanylate kinase deficient *E. coli* strain, TS202A(DE3) and plated onto selection medium in the presence or absence of arabinose (Figure 3.2). *E. coli* strain TS202A(DE3) was created by integration of the mouse gmK gene downstream of the bacterial chromosomal arabinose promoter and disruption of the endogenous bacterial gmK gene by insertion of a kanamycin resistant gene into the bacterial gmK locus. Because GMK is an essential enzyme, the growth of *E. coli* TS202A(DE3) requires the presence of arabinose to induce expression of the integrated mgmk gene. In the absence of arabinose, the cells are not viable on selective medium unless a functional GMK is expressed from an introduced gmK-encoded plasmid (Stolworthy *et al.*, 2003).

Growth of individual transformants was assessed visually following streaking onto minimal selection plates containing arabinose (+ARA) or without arabinose (-ARA) and incubation at 37°C for 36-48 hours (Figure 3.2). All transformants grew on the +ARA plates as expected since no selection is imposed (Figure 3.2B). The ability of transformants to grow on selection media lacking arabinose (-ARA) indicates that the transformants express sufficient functional guanylate kinase activity to complement the conditionally GMK-deficient *E. coli*. Figure 3.2C shows that on -ARA media, pETHT (empty vector) was unable to complement the conditional GMK-deficient *E. coli*, whereas cells expressing the wild type and the three mutant

MGMKs, S37A, S37T and S37Y, were viable. This indicates that the S37 substitutions retain activity towards GMP.

To assess whether these substitutions impact the ability of GMK to phosphorylate 6-TG and thereby restrict cell growth, transformants were streaked onto -ARA plates containing a concentration of 6-TG (300µg/ml) that prevents growth of cells expressing wild type GMK (pETHT:mgmk). As shown in Figure 3.2D, cells harboring wild type mgmk were not able to grow on -ARA+6-TG plates. Surprisingly, all three S37 mutants were viable in the presence of 6-TG and display a resistant phenotype.

#### *Growth in selective media*

As a means to better understand the impact of the different S37 substitutions on substrate activity and specificity, we evaluated the ability of wild type and mutant mgmk containing strains on TS202A(DE3) growth over time on non-selective, selective and 6-TG containing media. Results of representative growth curves in these media are shown in Figure 3.3. Doubling times of each sample in different media were calculated and are shown in Table 3.1. When +ARA medium was used, all MGMK expressing transformants grew approximately at the same rate as shown in Figure 3.3A. Cells harboring pETHT grew somewhat slower than the S37 mutants with a doubling time of 125.6 min. We speculate that this reduced growth rate may be due to the reliance of arabinose induction of the chromosomal integrated guanylate kinase gene. Doubling times for cells harboring wild type MGMK and MGMK mutants S37A and S37T were in the range of 100-108 min in +ARA media. Cells harboring MGMK mutant S37Y, however, showed the highest doubling time of 118.2 min ( $P > 0.05$ ). In the absence of arabinose (-ARA), no growth is observed with pETHT (TS202A(DE3)). However, cells harboring wild type MGMK and MGMK mutants initially grew at comparable rates as shown in Figure 3.3B but at later time

points diverged slightly. It is unclear why this occurred but accumulation of some enzymes with time may be responsible. Doubling times were 104.5 min (wild type), 114.4 min (S37A), 106.5 min (S37T) and 155.7 min (S37Y) with a P value > 0.05, indicating the difference in growth is not statistically significant. Figure 3.3C shows a representative graph of cells incubated in -ARA medium supplemented with 300µg/mL 6-TG (-ARA+6TG). As demonstrated in Figure 3.2D, pETHT:mgmk (TS202A(DE3)) is unable to grow under these conditions and demonstrates sensitivity to 6-TG. Doubling times for cells harboring mutant MGMKs were fairly comparable to each other for S37A and S37Y (211.6 min and 204.6 min, respectively) and slightly higher for S37T (242.6 min) although the growth rate is somewhat impaired (2-3 fold) in -ARA+6-TG compared to their growth in the absence of 6-TG (-ARA). The results shown in Figure 3.3 provide further evidence that the substitutions at S37 not only yield enzymes with activity towards GMP but that this activity has shifted away from 6-TGMP.

#### *Enzyme assays*

Induction of the pETHT:mgmk constructs with IPTG led to high levels of MGMK protein expression. All proteins were purified to near homogeneity (data not shown) with concentrations obtained at 609mg/L (wild type MGMK), 114.2 mg/L (S37A), 746.6 mg/L (S37T) and 386mg/L (S37Y). To extend the complementation studies and growth curve results, we performed enzyme assays using purified enzymes and the substrates, GMP and 6-TGMP. All assays were performed at least three times and similar results were obtained. As shown in Figure 3.4A, the ability of mutant guanylate kinases (S37A, S37T and S37Y) to phosphorylate GMP was altered with respect to the wild type guanylate kinase activity. S37A activity was the most dramatically altered and retained only very low to modest activity. Two mutants, S37T and S37Y, displayed impaired but significant activities towards GMP.

Compared to wild type GMK activity at 420 sec (set at 100%), S37Y had the highest guanylate kinase activity at ~70%, S37T at ~35% and S37A at ~7%. Interestingly, this difference in activities is not apparent in the biological systems examined (plate and growth assays).

To better understand the influence of the different substitutions at S37, kinetic analyses were performed using purified enzymes. These studies show that wild type MGMK displays a  $K_m$  value towards GMP of 59.0 $\mu$ M (Table 3.2). Mutant S37Y has a slightly better  $K_m$  values at 48.7 $\mu$ M. As suggested by the impaired growth rate, both mutants S37A and S37T display reduced binding ability to GMP, as indicated by a 6.5 to 9.5-fold increase in  $K_m$  as compared to wild type MGMK. All three mutant MGMK's however, have much reduced turnover rates ( $k_{cat}$ ) relative to wild type MGMK, ranging from 32.5-fold lower for S37A to 12- and 9-fold lower for S37T and S37Y, respectively (Table 3.2). Overall, wild type MGMK has the highest relative catalytic efficiency ( $k_{cat}/K_m$ ) toward GMP. Corresponding to enzyme assay results, mutant S37A shows the greatest reduction in relative catalytic activity at about 318-fold lower than that of the wild type enzyme. Mutant S37T also shows significant reduction in catalytic efficiency (~81-fold less efficient) whereas mutant S37Y displays a modest reduction in catalytic efficiency (7-fold) (Table 3.2).

When 6-TGMP is used as the substrate in crude lysate assays (Figure 3.4B), the only detectable phosphorylation was observed with wild type MGMK. Wild type MGMK displays a clear preference for GMP since 6-TGMP activity is much reduced even with use of seven fold more enzyme and twice as much substrate (6-TGMP). When 6-TGMP was used as a substrate with wild type MGMK, only 15% of the activity observed with GMP as the substrate, was detected. Kinetic analyses lend further support that only wild type enzyme retains the ability to phosphorylate 6-TGMP. When the overall wild type enzyme catalytic efficiencies ( $k_{cat}/K_m$ ) between 6-TGMP and GMP are compared, a 8140-fold reduction in catalytic efficiency toward 6-

TGMP is observed (2%  $k_{cat}$  and 2.9-fold higher  $K_m$ ). This is in line with earlier reports that human guanylate kinase is the rate limiting enzyme activity in the phosphorylation pathway of 6-TG and displays a  $K_m$  over 2mM for 6-TGMP and a maximal velocity of 3% of that with GMP (Miller *et al.*, 1977; Sekulic *et al.*, 2002). When 6-TGMP was used as the substrate in kinetic studies, none of the three S37 mutants display any detectable activity towards 6-TGMP even at high enzyme (35 $\mu$ g or 5-fold higher than the amount of wild type MGMK used) and high substrate concentrations (up to 2000 $\mu$ M 6-TGMP or 12-fold higher than the wild type  $K_m$  for 6-TGMP (171.5 $\mu$ M)). All assays were performed at least three times and similar results were observed (Table 3.2). These results lend further support to the data shown in Figures 3.2 and 3.3 that indicate that wild type MGMK is capable of phosphorylating GMP and to a lesser extent, 6-TGMP while the S37 mutants are capable of phosphorylating GMP but lack detectable activity towards 6-TGMP, i.e., are resistant to 6-TGMP.

## **DISCUSSION**

Guanylate kinase (GMK) is an essential enzyme in the purine nucleotide biosynthesis pathway and plays a key role in generating GDP and dGDP precursors for RNA and DNA metabolism, respectively. In addition, GMK is also responsible for the activation of several antiviral and anti-neoplastic drugs, including the chemotherapeutic drug, 6-thioguanine, which has been used as the first line of treatment for leukemia for five decades (Karran and Attard, 2008). Unfortunately, treatment failure due to the development of 6-TG resistance has been widely reported (Aubrecht *et al.*, 1997). Loss of activity of the key enzyme, HGPRT, is the best characterized resistance mechanism and, more recently, inactive MMR and impaired 6-TG transport systems have also been reported to be responsible for 6-TG resistance in cancer cells (Lennard, 1992; Morgan *et al.*, 1994; Fotoohi *et al.*, 2006).

Because not all 6-TG resistance can be accounted for by these mechanisms we sought to evaluate whether mutations in GMK, the rate limiting step in the activation of 6-TG, could lead to drug resistance.

We have focused this study on the mouse rather than the human guanylate kinase primarily because, in our hands, the mouse enzyme is soluble in *E. coli* whereas the human enzyme is not (Brady *et al.*, 1996). Since the mouse enzyme shares high sequence similarity to human GMK (88% identity, 93% homology, information learned about MGMK is likely to be directly transferable to the human enzyme (Brady *et al.*, 1996). Furthermore, the crystal structure of mouse guanylate kinase was solved in 2002 (no structure of the human enzyme has been forthcoming) and facilitates visualization of important molecular interactions (Sekulic *et al.*, 2002). Indeed, structural studies by Sekulic *et al.* (2002) suggest substrate discrimination between the two purine nucleotides, AMP and GMP, in GMK occurs in part at the interactions between S37 and the C6 position on guanine with additional hydrogen bonding with threonine 83 (T83). From their report of the yeast guanylate kinase structure, Stehle and Schulz (1992) suggest the S37 analogous serine (S34) and the T83 analogous residue (S80) in yeast are important in substrate specificity. Furthermore, modeling of the interactions between MGMK and 6-TG indicates that the formation of bonds with S37 and T83 occurs in a similar fashion to when GMP is bound but that steric clashes between these groups and the substrate might occur and diminish enzyme activity (Sekulic *et al.*, 2002).

In this study, we sought to evaluate the role of S37 to discriminate between the oxygen or sulfur in GMP or 6-TGMP substrate interactions, respectively, as well as to provide evidence that this proposed discrimination could result in drug resistance in a biological setting. Three site-directed mutants of MGMK were created at serine 37 (S37A, S37T and S37Y) and their activities towards the native substrate or the anti-leukemic drug 6-TG were assessed in a conditional-guanylate kinase

deficient *E. coli* strain using genetic complementation in both plate assays and growth curve experiments (Figures 3.2 and 3.3). While the growth of wild type and mutant MGMK expressing *E. coli* under non-permissive conditions (-ARA) was robust, it contrasted sharply with the growth pattern exhibited in the presence of 6-TG. On drug containing plates, wild type mgmk expressing cells were non-viable whereas all three S37 mutants grew well (Figure 3.2D). In 6-TG containing cultures, a similar pattern emerged; all S37 mutants grew whereas no growth was observed with the wild type mgmk-expressing cells (Figure 3.3C). While the growth rate under selective pressure and in the presence of 6-TG (-ARA+6-TG) of all mutants is diminished compared to that in the absence of 6-TG (-ARA), this may be partly attributable to reduced production of GMP as a result of competition between 6-TG and guanine with HGPRT. These data indicate that mutations at S37 display sufficient GMP activity for growth but result in a resistance phenotype to 6-TG.

Initial enzyme assays using GMP as the substrate also confirms that all three mutants display guanylate kinase activity although activity was reduced in all mutants compared to that of wild type MGMK. Kinetic analyses of the three MGMK mutants and wild type confirm that the overall enzyme catalytic efficiency ( $k_{cat}/K_m$ ) toward GMP is reduced varying degrees from the wild type value and ranges from 7- to 318-fold. For S37T and S37A with GMP as the substrate both  $K_m$  and  $k_{cat}$  values are significantly impaired (6.5 to 9.5-fold and 12 to 32.5-fold, respectively). However, for S37Y the  $K_m$  is slightly improved while the  $k_{cat}$  is reduced 8.9-fold compared to wild type values. Alanine and threonine bind with similarly poor affinity whereas tyrosine binds GMP slightly better than the wild type serine. When serine is substituted by any of the three residues examined,  $k_{cat}$  values are substantially reduced, indicating that a hydroxyl group may be facilitate catalytic turnover ( $k_{cat}$ ) if it is at an appropriate distance from the oxygen moiety at the C6 position of guanine such as with the wild type serine. Hydroxyl groups on the slightly longer threonine

and aromatic ring of tyrosine may not be positioned sufficiently well to allow phosphorylation to occur efficiently.

Only the wild type GMK displays detectable activity towards 6-TGMP although the  $K_m$  is almost three-fold higher and the  $k_{cat}$  2810-fold lower than when GMP is the substrate. Even when 5-fold more enzyme (35 $\mu$ g) and 12-times the wild type  $K_m$  concentration (2000 $\mu$ M) are used with the S37 mutants, no 6-TGMP activity is detected. While a hydroxyl group at the correct distance from the C6 position might be advantageous for catalysis, steric hindrance may play a larger role for S37Y or S37T when 6-TGMP is bound. Catalysis may also be impaired because the substrate is unable to be correctly positioned or binds in a 'sloppy' fashion for efficient phosphorylation to occur. S37A displays the worst binding and catalysis and this may be a result of a very loose/sloppy active site afforded by the presence of a small side chain. These data suggests that there is a level of discrimination between the side chain at S37 and the ability of the enzyme to interact with the substrate and that the rules that govern this distinction differ when there an oxygen or a sulfur at the carbon 6 position. Crystal structure determinations of the S37 variants with 6-TGMP and GMP may provide further insight to the nature of the impact of these substitutions on the kinetic parameters described here.

The emergence of resistance to chemotherapeutic agents is a key cause of treatment failure. A better understanding of the molecular factors that result in the loss of drug potency may lead to the development of improved dosing regimens and treatment options for patients. A complete list of the potential mechanism(s) of drug resistance to 6-TG remains elusive because not all cases of resistance can be explained by mutational events in known targets. In this report we sought to demonstrate that mutations in guanylate kinase could reveal a previously undescribed 6-TG resistance mechanism. Our results demonstrate that MGMK containing amino acid substitutions at S37 (S37A, S37T and S37Y) retain varying



degrees of essential GMP activity but do not display detectable activity towards 6-TGMP. Furthermore, the S37 mutants provide sufficient guanylate kinase activity in a genetic complementation system for robust cell viability and also confer resistance to otherwise lethal doses of 6-TG. Taken together, these data suggest that the substitutions examined at S37 in MGMK are biologically relevant and display critical and appropriate discrimination in substrate specificity/recognition that results in drug resistance.

### **FUNDING**

This work was supported by the National Institutes of Health [CA 85939 to M.E.B.].

### **ACKNOWLEDGEMENTS**

We thank Shannon Winn for technical assistance on the initial aspects of this study.

## References

- Agarwal,K.C., Miech,R.P., and Parks,R.E. (1978) *Methods Enzymol.*, **51**, 483-490.
- Aubrecht,J., Goad,M.E., and Schiestl,R.H. (1997) *J. Pharmacol. Exp. Ther.*, **282**,1102-1108.
- Boehme,R.R. (1984) *J. Biol. Chem.*, **269**, 12346-12349.
- Bohon,J. and de los Santos,C.R. (2003) *Nucl Acids Res.*, **31**, 1331-1338.
- Brady,W.A., Kokoris,M.S., Fitzgibbon,M., and Black,M.E. (1996) *J. Biol. Chem.*, **271**, 16734-16740.
- Elion,G.B. (1989) *Science*, **244**, 41-47.
- Gaidarov,I.O., Suslov,O.N., and Abdulev,N.G. (1993) *FEBS Lett.*, **335**, 81-84
- Davies,M.J., Lovell,D.P. and Anderson,D. (1992) *Mutation Res.*, **265**, 165-171.
- Fukuchi,K., Tanaka,K., Kumahara,Y., Marumo,K., Pride,M.B., Martin,G.M., and Monnat,R.J. (1990) *Hum. Genet.*, **84**, 249-252.
- Fotoohi,A.K., Lindqvist,M., Peterson,C., and Albertioni,F. (2006) *Biochem. Biophys. Res. Commun.*, **343**, 208-215.
- Karran,P. (2006) *Br. Med. Bull.*, **79-80**, 153-170.
- Karran,P., and Attard,N. (2008) *Nat. Rev. Cancer.*, **8**, 24-36.
- Kunkel,T. (1985) *Proc. Natl. Acad. Sci. USA*, **82**, 488-492.
- Lennard,L. (1992) *Eur. J. Clin. Pharmacol.*, **43**, 329-339.
- Ling,Y.H., Chan,J., Beattie,K.L., and Nelson,J.A. (1992) *Mol Pharmacol.*, **42**, 802-807.
- Miller,R.L., Adamczyk, D.L., and Spector,T. (1977) *Biochem. Pharmacol.*, **26**, 1573-1576
- Miller, W.H., and Miller,R.L. (1980) *J. Biol. Chem.*, 255, 7204-7207.
- Morgan,C.J., Chawdry,R.N., Smith,A.R., Siravo-Sagraves,G., and Trewyn,R.W. (1994) *Cancer Res.*, **54**, 5387-5393.
- Sekulic,N., Shuvalova,L., Spangenberg,O., Konrad,M., and Lavie,A. (2002) *J. Biol. Chem.*, **277**, 30236-30243.
- Stehle,T., and Schulz,G.E. (1992) *J. Mol. Biol.*, **224**, 1127-1141.
- Stolworthy,T.S., and Black,M.E. (2001) *Protein Eng. Des. Sel.*, **14**, 903-909.

Stolworthy,T.S., Krabbenhoft,E., and Black,M.E. (2003) *Anal. Biochem.*, **322**:40-47.

Swann,P.F., Waters,T.R., Moulton,D.C., Xu,Y.Z., Zheng,Q., Edwards,M., and Mace,R. (1996) *Science*, **273**,1109-1111.

Woods,D.F., and Bryant,P.J. (1991) *Cell*, **66**, 451-464.

Yamanaka,H., Kamatani,N., Nishoka,K., Kobayashi,M., Wada,Y., Ohtani,T., and Mikanagi,K. (1985) *Hum.Hered.*, **35**, 358-363.

Yan,T., Berry,S.E., Desai,A.B., and Kinsella,T.J. (2003) *Clin. Cancer Res.*, **9**, 2327-2334.

## FIGURE LEGENDS

**Figure 3.1.** Schematic of active site with the location of S37 and T83 with respect to guanine in MGMK. These residues are analogous to S34 and S80 in yeast GMK. (Adapted from Sekulic et al. (2002) and Stehle and Shultz (1992)).

**Figure 3.2.** Functional complementation of the conditional guanylate kinase strain *E. coli* TS202A(DE3) by wild type and mutant mouse guanylate kinases. **(A)** *E. coli* TS202A(DE3) strains harboring the expression vector (pETHT) or the vector containing the wild type mgmk (pETHT:mgmk) or mgmk mutants (pETHT:S37A, pETHT:S37T, pETHT:S37Y) were grown at 37°C for 36-48 hours on **(B)** mgmk selection medium with arabinose (+ARA), **(C)** without (-ARA), or **(D)** in the absence of arabinose with the addition of 300µg/ml 6-TG (-ARA+6-TG).

**Figure 3.3.** Growth of conditional guanylate kinase deficient strain TS202A(DE3) harboring vector (□ - pETHT), wild type mgmk (○ - pETHT:mgmk), and mgmk mutants (■ - S37A, ▲ - S37T, and ● - S37Y) at 37°C in mgmk selection medium **(A)** with arabinose (+ARA), **(B)** in the absence of arabinose (-ARA) and **(C)** in the absence of arabinose with the addition of 300µg/ml 6-TG (-ARA+6TG) was monitored over 10 to 13 hours by OD<sub>600</sub> readings. This experiment was repeated at least three times with similar results. Representative plots are shown.

**Figure 3.4.** Guanylate kinase enzyme assays of purified wild type (○ - MGMK) and mutant guanylate kinases (■ - S37A, ▲ - S37T and ● -S37Y). **(A)** One µg of each purified enzyme was used with 30µM GMP in a lactate dehydrogenase – pyruvate kinase coupled enzyme assay described in Agarwal *et al.* (1978). **(B)** Seven µg of each purified enzyme was subjected to coupled enzyme assays in the presence of

60 $\mu$ M 6-TGMP. The enzyme assays were repeated at least three times with similar results observed. Representative plots are shown.

**Table 3.1.** Growth pattern profile in *E. coli*

	Doubling Time (min)		
	+ARA	-ARA	-ARA + 300µg/mL 6-TG
<b>pETHT</b>	125.62 (23.05) <sup>a</sup>	N.D.	N.D.
<b>pETHT:mgmk</b>	104.42 (8.50)	104.51 (9.11)	N.D.
<b>pETHT:S37A</b>	108.28 (13.22)	114.41 (5.31)	211.6 (7.56)
<b>pETHT:S37T</b>	100.51 (2.39)	106.53 (3.22)	242.56 (7.46)
<b>pETHT:S37Y</b>	118.23 (11.51)	155.71 (16.26)	204.6 (18.42)

<sup>a</sup> Standard error

N.D. – Not Detected

**Table 3.2.** Kinetic parameters of wild-type MGМК and S37 mutants

	GMP			6-TGMP		
	$K_m$ (µM)	$k_{cat}$ <sup>a</sup> (s <sup>-1</sup> )	$k_{cat} / K_m$ (s <sup>-1</sup> /µM)	$K_m$ (µM)	$k_{cat}$ (s <sup>-1</sup> )	$k_{cat} / K_m$ (s <sup>-1</sup> /µM)
<b>MGМК</b>	59.02 (0.23) <sup>b</sup>	20.8 (2.1)	0.35 (0.033)	171.5 (11.65)	0.0074 (0.00055)	$4.3 \times 10^{-5}$ ( $8.22 \times 10^{-7}$ )
<b>S37A</b>	558.6 (18.37)	0.64 (0.05)	0.0011 ( $5 \times 10^{-5}$ )	N.D.	N.D.	N.D.
<b>S37T</b>	381.7 (3.64)	1.7 (0.09)	0.0043 (0.00019)	N.D.	N.D.	N.D.
<b>S37Y</b>	48.7 (0.26)	2.35 (0.36)	0.048 (0.0065)	N.D.	N.D.	N.D.

<sup>a</sup> The  $k_{cat}$  values were calculated using the equation  $V_{max} = k_{cat} / [E]$  where [E]=total enzyme concentration and is based on one active site per monomer. Assay conditions are described in Materials and Methods.

<sup>b</sup> Standard error

N.D. – Not Detected

**Figure 3.1**

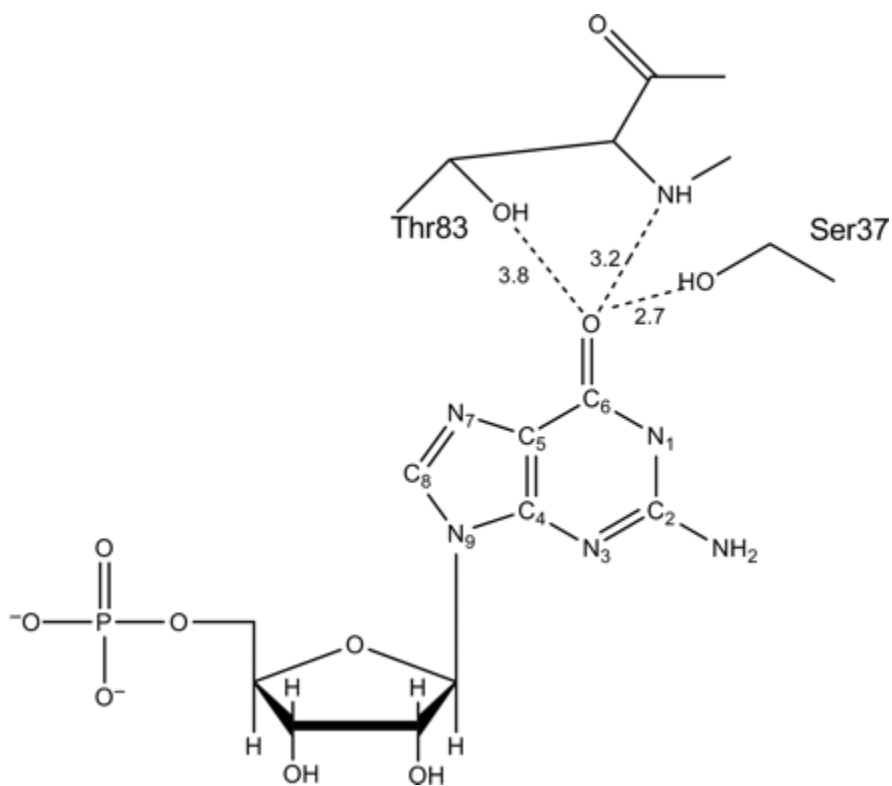


**Figure 3.2**

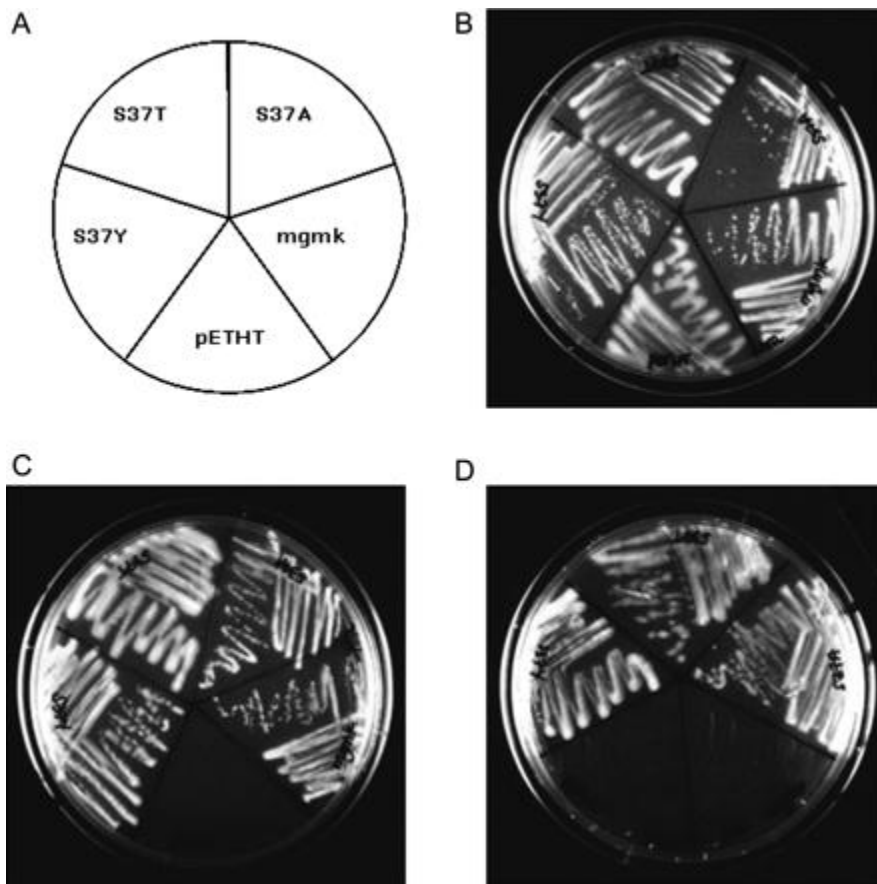




Figure 3.3

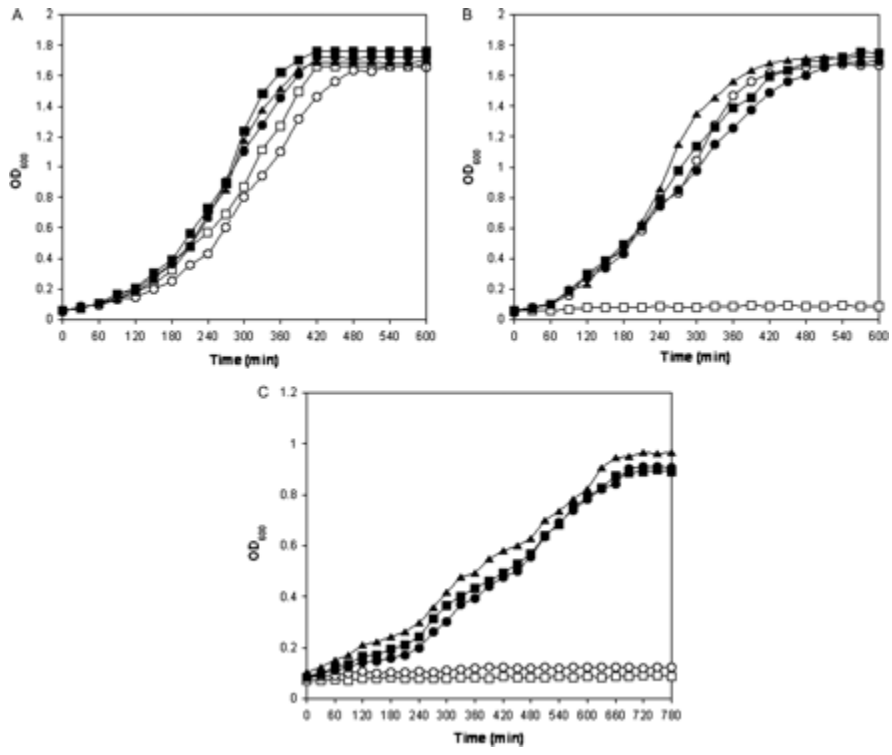
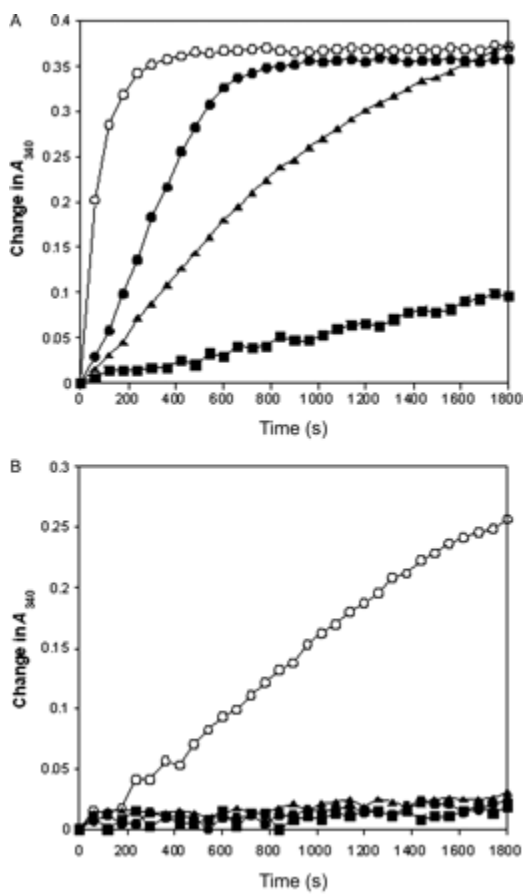


Figure 3.4



## CHAPTER FOUR

### **Bacterial Cytosine Deaminase Mutants Created by Molecular Engineering Demonstrate Improved 5FC-Mediated Cell Killing *In Vitro* and *In Vivo***

#### **ABSTRACT**

Cytosine deaminase is used in combination with 5-fluorocytosine as an enzyme-prodrug combination for targeted genetic cancer treatment. This approach is limited by inefficient gene delivery and poor prodrug conversion activities. Previously, we reported individual point mutations within the substrate binding pocket of bacterial cytosine deaminase (bcd) that result in marginal improvements in the ability to sensitize cells to 5FC. Here we describe an expanded random mutagenesis and selection experiment that yielded enzyme variants which provide significant improvement in prodrug sensitization. Three of these mutants were evaluated using enzyme kinetic analyses and then assayed in three cancer cell lines for 5FC sensitization, bystander effects and formation of 5FU metabolites. All variants displayed 18 to 19-fold shifts in substrate preference toward 5FC, a significant reduction in IC<sub>50</sub> values and improved bystander effect compared to wild-type bcd. In a xenograft tumor model the best enzyme mutant was shown to prevent tumor growth at much lower doses of 5FC than is observed when tumor cells express wild-type bcd. Crystallographic analyses of this construct demonstrates the basis for improved activity towards 5FC, and also how two different mutagenesis strategies yield closely related, but mutually exclusive mutations that each result in a significant alteration of enzyme specificity.

---

This manuscript was accepted by *Cancer Research* in the following manuscript: Fuchita, M\*, **Ardiani, A\***, Zhao, L., Serve, K., Stoddard, B.L., and Black, M.E. Bacterial Cytosine Deaminase Mutants Created by Molecular Engineering Demonstrate Improved 5FC-Mediated Cell Killing *In Vitro* and *In Vivo*. - **\*joint 1<sup>st</sup> authorship.**

## **INTRODUCTION**

Cytosine deaminase (CD; EC 3.5.4.1) is responsible for the conversion of cytosine to uracil and ammonia, providing an important mechanism for pyrimidine salvage in microbes. Because this activity is not found in mammalian cells(1, 2), CD is being explored for use in suicide gene therapy (SGT) due to its ability to also convert the antifungal agent 5-fluorocytosine (5FC) to the potent antimetabolite, 5-fluorouracil (5FU)(3-6). Intracellularly, 5FU is subsequently metabolized by endogenous enzymes to 5FdUMP, an irreversible inhibitor of thymidylate synthetase (TS) thereby restricting the production of dTMP and downstream phosphorylated products. Depletion of dTTP pools results in inhibition of DNA synthesis and leads to apoptosis(7-9). A phenomenon known as the bystander effect (BE) provides an extension of cell killing beyond the cells expressing the suicide gene to neighboring cells(10-13). A combination of factors is thought to participate in the BE including transfer of antimetabolites and/or suicide enzymes through gap junctions, diffusion and apoptotic vesicles. An immune-related response also contributes to the BE although in a delayed fashion. A potent BE is critical to successful tumor ablation especially in light of the inefficient viral and non-viral gene delivery systems currently available. In order to support an effective BE, sufficient antimetabolites must be generated in suicide enzyme-expressing cells.

Unfortunately, wild-type CD displays relatively poor turnover of 5FC, thus limiting the overall therapeutic response. As such, high doses of 5FC are necessary and result in undesirable side effects primarily due the presence of microbes in the intestinal tract that encode CD. The rapid half-life of 5FC in blood serves to further limit the availability of 5FC at the tumor site. To overcome the constraints associated with poor 5FC activation, we sought to optimize the activity of bCD towards 5FC using regio-specific random mutagenesis by targeting two key regions of the active site. From earlier studies, residue D314 in wild-type bCD was shown to

play a key role in substrate recognition(14, 15). In particular, the D314G and D314S substitutions display a shift in substrate preference towards 5FC. However, these variants provide only a modest 2-4-fold decrease in  $IC_{50}$  for 5FC *in vitro* as compared to wild-type bCD-expressing tumor cells.

Using structural information as well as previous mutagenesis results, two regions lining the active site of bCD (residues 149-159 and 310-320; Fig.1) were targeted for random mutagenesis to identify mutants with further enhanced 5FC sensitivity *in vitro* and *in vivo* (16, 17). Such optimized CD variants that allow lower, less toxic 5FC doses to achieve efficient cell killing and an enhanced BE will likely provide meaningful and significant clinical benefit when used in SGT protocols for the treatment of a variety of cancers.

## **MATERIALS AND METHODS**

*Materials.* Oligonucleotides were obtained from IDT (Coralville, IA). Enzymes were purchased from New England Biolabs (Beverly, MA). Polyclonal bCD-antibody was generated by Harlan (Harlan, Indianapolis, IN). DNA purification was done using Wizard-PCR kit (Promega, Madison, WI), HiSpeed-Plasmid Mini Kit (Qiagen, Valencia, CA), and StrataPrep EF-Plasmid Midikit (Stratagene, La Jolla, CA). Alamar Blue was purchased from Serotec (Oxford, UK). Nickel affinity chromatography reagents were purchased from Qiagen. All cell culture reagents were purchased from Gibco (Carlsbad, CA). All other reagents were purchased from Sigma (St. Louis, MO) unless otherwise noted.

*Bacterial strains.* *Escherichia coli* strain GIA39(DE3), which is deficient in CD and orotidine 5'-phosphate decarboxylase activities, was used in the genetic complementation assays for CD activity(15). The *E. coli* strains NM522 and XL1-Blue

were used as recipients for certain cloning and mutagenesis procedures. *E. coli* BL21(DE3) and BL21-RIL (Novagen, Madison, WI) were used for protein purification. *Cell lines.* Rat C6 glioma cells (C6) were purchased from ATCC (Manassas, VA). Human colorectal carcinoma cells (HCT116) and human prostate carcinoma cells (DU145) were provided by Dr. Neal Davies (Washington State University, Pullman, WA). Growth conditions for the cells lines are described in detail by ATCC. Transfected cells were cultured in media supplemented with blasticidin at 4 $\mu$ g/ml (C6 and DU145) or 6 $\mu$ g/ml (HCT116).

*Library construction and selection of 5FC active clones.* A bCD expression library encoding variants randomized across residues 149-159 was constructed, followed by insertion of randomized sequences spanning residues 310-320 (Table S4.1). Six overlapping oligonucleotides (MB271-MB276) were used to synthesize a 256bp DNA fragment including the 11 codons (149-159) that were randomized at 9% mutation frequency. The codons for the 310-320 residues were also randomized at 9% and the 238bp DNA fragment was synthesized using the six oligonucleotides, MB384-MB387 and MB267-MB268. Plasmid DNA purified from the 149-159 mutagenesis selection and the randomized 310-320 region fragment were digested with complementary restriction enzymes and ligated together. Transformation and selection for 5FC active mutants were performed as described previously using lower 5FC concentrations (10-0.5 $\mu$ g/ml) in plate assays (14, 15).

*Enzyme assays.* The activity of wild-type and variant bCD lysates was assayed by monitoring the absorbance change due to the consumption of cytosine at 286nm and the production of 5FU at 316nm using an HP8452A Diode Array Spectrophotometer (Olis, Bogart, GA) at room temperature for 10min following a protocol adapted from Hayden *et al.* (18). Cleared cell lysates were prepared as described previously (14).

Selected bCDs were expressed in *E. coli* BL21(DE3) and enzymes were purified by Ni-NTA chromatography and quantified as described(14). The kinetic constants were determined by plotting initial reaction rates fitted to the Michaelis-Menten equation using KaleidaGraph software (Synergy Software, Reading, PA).

*Construction of mammalian expression vectors.* The wild-type and mutant bCD were subcloned as *Nco*I(blunt-ended)/*Xho*I fragments into pCDNA6/*myc*-HisB (Invitrogen, Carlsbad, CA) digested with *Eco*RV and *Xho*I. Site-directed mutagenesis was performed to overlay D314S mutation into pCDNA:1525 using QuikChange mutagenesis according to the manufacturer's protocol (Stratagene, La Jolla, CA).

*In vitro cytotoxicity assays.* One  $\mu$ g of each plasmid DNA was used to transfect  $1 \times 10^5$  C6, HCT116 and DU145 cells by lipofection using FuGENE 6 transfection reagent (Roche, Penzberg, Germany) at a 3:1 ratio according to the manufacturer's instructions. Protein expression level was determined by immunoblot analysis as previously described(19). For *in vitro* cytotoxicity assays pools of transfectants were transferred to 96-well microtiter plates at an initial density of 500 (C6) or 1000 cells/well (HCT116/DU145). Following cell adherence overnight, 5FC (0-30mM) was added and the cells were incubated for 6 days, at which time the redox indicator dye Alamar Blue was added. Cell survival was determined by fluorescence recorded at a 530/590nm as described by the manufacturer and data were plotted with the SD. At least three replicates were performed.

*In vitro Bystander Effect (BE) assays.* C6, HCT116 and DU145 cells stably transfected with pCDNA were mixed at different ratios with stable transfectants harboring either pCDNA:bCD, pCDNA:1246, pCDNA:1525 or pCDNA:1779. The mixed cells were transferred to 96-well microtiter plates at final density as described

above. Following cell adherence overnight, 5FC (4mM (C6) or 10mM (HCT116/DU145) was added and the cells were incubated for 6 days. Cell viability was determined as described above. At least three replicates were performed.

*HPLC metabolite analysis.* Stably transfected cells (HCT116) were plated in 6-well dishes (Corning, New York, NY) at a concentration of  $4 \times 10^4$  cells/well. The reaction was stopped at various hours post-dose (2.5mM 5FC) by adding 200 $\mu$ l/well of 94:6 (v/v) acetonitrile/glacial acetic acid and the level of 5FU in cell lysates was detected using an isocratic, reverse-phase high performance liquid chromatography (HPLC) method(20). Metabolite separation was carried out on a Phenomenex Luna C18(2) analytical column (250mm x 4.6mm, 5 $\mu$ m particle size) (Phenomenex, Torrence, CA) at a flow rate of 1ml/min. The mobile phase was formic acid and water (1:99, v/v). 5FU was detected at an ultraviolet wavelength of 285nm and eluted at 5.8min. Total metabolite levels were calculated relative to a known concentration of an internal standard (5-chlorouracil).

*Introduction of individual mutations at residues 316 and 317.* The QuikChange kit was used to create amino acid substitutions F316C (MB480-481), F316L (MB482-MB483), F316V (MB484-MB485), D317G (MB478-MB479) F316C/D317G (MB490-MB491), F316L/D317G (MB492-MB493), F316V/D317G (MB494-MB495). After DNA sequence confirmation, the resulting plasmids were designated pETHT:F316C, pETHT:F316L, pETHT:F316V, pETHT:D317G, pETHT:F316C/D317G, pETHT:F316L/D317G and pETHT:F316V/D317G.

*Xenograft tumor model.* Pools of HCT116 cells stably transfected with pCDNA, pCDNA:bCD or pCDNA:1525 ( $0.5 \times 10^6$  cells in 200 $\mu$ l of PBS (pH 7.2)) were injected subcutaneously into the flanks of 5-6 week old female nude mice



(n=5)(BALB/cAnNCr-nu/nu; National Cancer Institute, Fredrick, MD). When tumors reached 3-4mm (day 0), PBS or 5FC (375mg/kg) was administered by intraperitoneal injection twice/day for 21 days. Starting at day 0, the tumor volume was monitored using caliper measurement every other day, calculated using the formula:  $4/3\pi((\text{width} \times \text{length} \times \text{height})/2)$  and analyzed for statistical significance using Student's t-test.

*X-ray crystallography.* Three sequential mutations (V152A, F316C and D317G) were introduced by site-directed mutagenesis into the wild-type bCD. The expression and purification of the resulting construct (1525) was carried out as previously described(21). Crystals of 1525 were grown in sitting drops by vapor phase equilibration against reservoirs containing 10%-15% PEG 6K, 200mM MgCl<sub>2</sub> and 100mM HEPES (pH 7~8). Crystals were grown using microseeds of wild-type enzyme crystals (transferred by streaking drops with a fiber) and grew within one week to approximately 500µm in each dimension. Crystals were cryo-preserved as previously described and found to be isomorphous with crystals of wild-type enzyme(16). Data were collected on a Rigaku RAXIS IV<sup>++</sup> area detector, using X-rays produced by a Rigaku MicroMax<sup>TM</sup>-007 HighFlux(HF) microfocus X-ray generator ( $\lambda=1.54\text{\AA}$ ). Data collection and reduction were performed using the CrystalClear<sup>TM</sup> software package (Rigaku, The Woodlands, TX). The structures were refined using the CCP4 crystallographic software suite(22).

## **RESULTS AND DISCUSSION**

Many factors limit the overall efficacy of current SGT approaches for cancer when CD and 5-FC are used. These include rapid turnover and clearance of 5FC in serum, inefficient gene delivery efficiency such that only a small population of tumor

cells expresses the suicide gene, and poor enzyme activity towards the prodrug coupled with efficient competition for the enzyme's active site by the cells' endogenous pool of cytosine(1, 23-25). As a means to overcome these obstacles, we sought to create novel CD variants with significantly improved kinetic preferences towards 5FC. We employed random mutagenesis to introduce multiple amino acid substitutions in two regions lining the active site of bCD and used both positive and negative selection in *E. coli* to identify variants with the ability to confer enhanced 5FC sensitivity to three cancer cell lines *in vitro* and *in vivo*. A similar strategy was used to identify several Herpes Simplex Virus thymidine kinase (HSVTK) mutants with enhanced tumor ablation capabilities(26, 27). One such variant, SR39, is currently being used in a phase III clinical trial for prostate cancer. While HSVTK is widely used, there are two key reasons for optimizing additional suicide genes: 1) not all cancers are equally responsive to the same drug and 2) should treatment with one suicide gene fail, alternate suicide genes that the immune system has not been exposed to previously, could be used in additional rounds of therapy to ablate tumors.

*Construction of random library and mutant selection.* Previous studies revealed that individual point mutations in the substrate binding pocket of bCD, that confer sensitivity to *E. coli* at 1µg/ml 5FC, do not achieve substantial *in vitro* activity. We therefore aimed to direct the bCD variants to evolve more efficiently towards 5FC by heavily randomizing the two regions lining the active site in a stepwise approach (Fig 4.1). A single-targeted library randomized at the 149-159 residue region was initially generated and ~590 *E. coli* that harbored functional CD were pooled. A second randomized coding region, corresponding to the incorporation of mutations across residues 310 to 320, was then introduced and approximately 3700 enzymatically active variants were identified from an estimated  $1.35 \times 10^6$  total

number of transformants. Of those, 849, 365, 62, 20 and 12 clones conferred sensitivity at 20, 10, 2, 1 and 0.5 $\mu$ g/ml 5FC, respectively. This lowest 5FC dose is 40-fold lower than the sublethal dose for *E. coli* expressing wild-type bCD.

*Sequence analysis.* Sequences of 47 variants sampled from each round of screening (data not shown) revealed that all targeted codons had at least one amino acid substitution. The average number of substitutions was 2.6, close to the theoretical average number of 2.1 for 9% randomization. Sequences of the 12 variants identified at 0.5 $\mu$ g/ml 5FC were somewhat unexpected (Supplementary Table S4.2) because substitutions in the 149-159 residue region occurred infrequently and appeared unrelated to the degree of 5FC activity, and many of the same substitutions were observed in mutants with less or no 5FC activity. In contrast, the substitutions at the 310-320 residue region showed a strong relationship with 5FC sensitivity: in particular, substitutions at positions D317 and F316 with smaller hydrophobic residues were observed for the most active constructs. Few substitutions were observed at F310, G311, P318, W319 and Y320, suggesting these sites are important for overall catalytic activity or for structural stabilization. Sequence analysis reveals that the most active 12 mutants all have substitutions at D314, F316 and/or D317. -As described in detail below, three mutants (referred to as constructs 1246, 1525 and 1779) were identified as conferring sensitivity at significantly lower concentrations of 5FC, and were chosen for further characterization. To elucidate the participation of individual amino acid substitutions at F316 and D317 found in all three constructs (1246=D314E/F316L/D317G, 1525=V152A/F316C/D317G and 1779=V315L/F316V/D317G), site-directed mutagenesis was used to generate the substitutions: F316L, F316C, F316V, D317G, F316L/D317G, F316C/D317G and F316V/D317G. Results from *E. coli* complementation assays indicate that all mutants display CD activity and that the individual D317G substitution and the

double F316C/D317G substitutions found in 1525 appears to be responsible for conferring the greatest degree of sensitivity to 5FC.

*Enzyme assays of select mutants.* To further characterize the 12 mutants identified by growth inhibition on plates containing 0.5µg/ml 5FC, cell lysates were used initially to assess cytosine and 5FC conversion levels. Lysates of the mutants 1246, 1525 and 1779 showed the largest 5FC conversions of the variants and the wild-type, while the other variants displayed weak or no activity (data not shown). These three mutants and wild-type bCD were then purified to near homogeneity using a Ni-NTA chromatography column and their kinetic constants for cytosine and 5FC conversion were determined. All three random mutants display reduced kinetic parameters towards cytosine (Table 4.1). Mutant  $K_m$  values are increased 3.7-10.7-fold relative to wild-type bCD and  $k_{cat}$  values for the mutants range from 16.6-29-fold lower, corresponding to a 82.2-305.4-fold reduction in catalytic efficiency ( $k_{cat}/K_m$ ). When 5FC is used as the substrate,  $K_m$  values are modestly increased 1.8-3.3-fold and  $k_{cat}$  values are increased 4.3-5.9-fold, to yield an overall improvement in  $k_{cat}/K_m$  for 5FC of 1.5-2.9-fold as compared to wild-type bCD. The combination of reduced activity towards cytosine, and increased  $k_{cat}$  for 5FC, results in a significant (18.2 to 19.2-fold) shift in the relative substrate specificity towards 5FC relative to wild-type bCD.

*In vitro analysis of mutant bCDs.* Mutant and wild-type bCD genes were cloned into the expression vector, pCDNA, and used to stably transfect C6, HCT116 and DU145 cell lines. Results from prodrug sensitivity assays demonstrate that all three variant bCD constructs confer increased sensitivity to 5FC, albeit to varying degrees in the different cell lines (Fig 4.2A). In C6 transfectants, only a modest reduction in  $IC_{50}$  was observed compared to wild-type bCD-transfected cells (1.3-2.7-fold). The  $IC_{50}$  values of mutant bCD-transfected DU145 cells were 2.1-5-fold lower than wild-type bCD-transfectants. The mutants displayed the greatest

reduction in  $IC_{50}$  values in HCT116 transfectants at 2.4-17-fold lower values than bCD. In all cell lines examined, 1525 consistently displayed the lowest  $IC_{50}$  values of the three mutants with the best response observed in HCT116 cells. We observed some cell line variance in the degree of 5FC sensitivity. Clinical studies indicate 5FU is an effective chemotherapeutic agent for colorectal, pancreatic and breast cancer, but is less effective for other types of cancers(28). Therefore, the observed cell line differences may simply be a reflection of inherent variations in drug sensitivity exhibited by individual cell types.

Previously we reported the construction and characterization of single site mutations at residue 314 (D314)(14). Here we sought to compare these D314 variants (D314G, D314A and D314S) to the randomly derived mutants (1246, 1525 and 1779) and to explore the possibility that combinations of the best mutants from both series would yield an additive effect. Initially D314G, D314A and D314S and wild-type bCD-transfected HCT116 cells were evaluated for 5FC sensitivity (Fig 4.2B). Of the three D314 substitutions, D314S displays the greatest response to 5FC with an  $IC_{50}$  approximately 3.4-fold lower than that of wild-type bCD and ~5-fold higher than 1525-transfected cells. To assess the impact of the combination mutant, cells transfected with pCDNA, pCDNA:bCD, pCDNA:1525, pCDNA:D314S and pCDNA:1525/D314S were subjected to *in vitro* 5FC sensitivity assays as described above. Results from this comparison indicate that the 1525/D314S overlay does not yield an increase in 5FC sensitivity over 1525 or the individual D314S mutant or wild-type bCD-transfected cells (Fig 4.2C). Thus, the mutational routes towards optimal 5FC activation, generated by site-directed or randomizing mutagenesis, yield mutually exclusive sets of mutations that do not act synergistically. Below we provide a possible explanation for this lack of additive response based on details that emerged from 1525 structure determinations.

*Bystander effect.* The three key mutants were further characterized for their

ability to influence the killing of non-bCD expressing cells via the BE. Towards that end, populations of vector and bCD-transfected cells were mixed at various ratios and subjected to either 4mM (C6) or 10mM (HCT116 and DU145) 5FC for six days. The percentage of bCD-expressing cells needed to achieve 50% cell killing ranges from 20-50%, 20-60% and 10-80% for C6, DU145 and HCT116 cells, respectively, when mutant bCDs were examined (Fig 4.3A-C). In contrast, mixed populations containing wild-type bCD-transfectants displayed no cell killing effect in HCT116 cells and slight to modest effects in DU145 and C6 cells, respectively, and were unable to achieve 50% cell killing in any of the cell lines tested. Mutant 1525 displayed the greatest BE in every cell line examined. In HCT116 cells this is most evident; when only 10% of 1525-expressing cells are present, 50% of the population is killed at a 5FC concentration at which 100% wild-type bCD population remains fully viable.

*HPLC analysis of 5FU metabolites.* Low transfection efficiencies in SGT impose a reliance on a robust BE for tumor ablation. While results from our kinetic studies suggest an improvement in 5FC deamination activity, we sought to more directly assess the production of 5FU by bCD-transfected cells by high performance liquid chromatography (HPLC). Starting on day 3 the level of 5FU begins to accumulate in lysates from 1525-transfected cells and continues to increase from about 100µg/ml at day 3 to ~400µg/ml on day 7 (last time point) and reflects a 35.8-fold difference in 5FU levels between 1525 and wild-type bCD (Fig 4.3D). This is in contrast to vector and bCD-transfected cell lysates that show no significant change in 5FU levels over the time course. Bystander experiments with 5FC revealed that all three variant bCDs demonstrated a more robust cell killing in all three transfected cell lines as compared to wild-type bCD-transfected cells. We suggest this is a direct reflection of the amount of 5FU produced in the transfected cells.

*In vivo xenograft tumor model.* Mutant 1525 demonstrates the best cell

killing and BE *in vitro* and was selected for further analysis in an *in vivo* xenograft tumor model for human colorectal cancer. Tumor growth in all groups treated with PBS was indistinguishable with the exception of later points (Fig 4.4B). This statistically insignificant difference in the tumor volume near the end of the time course is likely due to the amorphous nature of the large tumors that made it difficult to obtain consistent measurements. While no difference in tumor volume was observed between mice bearing vector or wild-type bCD tumors throughout or following the 5FC treatment period, the lack of significant tumor growth observed in mice bearing 1525 tumors is in stark contrast (Fig 4.4A). From the time 5FC administration began to the maximum size, wild-type bCD tumors increased in volume from 34.4mm<sup>3</sup> to 1154 mm<sup>3</sup> (30.8-fold) whereas the 1525 tumors increased only from 32.5mm<sup>3</sup> to maximum of 185mm<sup>3</sup> (5.7-fold). Other studies using wild-type bCD show a reduced tumor growth rate using comparable doses of 5FC(29-31). In our hands, no significant antitumor response with wild-type bCD is observed at 375mg/kg twice a day whereas this dose provides a substantial growth restriction in 1525 bearing tumors. As such, 1525 provides significant improvement in tumor growth inhibition using a 5FC dose at which wild-type bCD tumors is completely unresponsive to.

*Crystallographic analysis of bCD 1525.* Crystals containing the enzyme in complex with the mechanism-based inhibitors 4-(R)-hydroxyl-3,4-dihydropyrimidine (DHP) or 5-fluoro-4-(S)-hydroxyl-3,4-dihydropyrimidine (5F-DHP) were generated out by soaking crystals in buffer containing 10mM 2-hydroxypyrimidine or 5-fluoro-2-hydroxypyrimidine (Aldrich, St. Louis, MO), respectively. In these experiments, the pyrimidine compounds are converted enzymatically to a tightly-bound hydrated adduct that mimics the enzyme transition state. The statistics for data collection and refinement are summarized in Supplementary Table S4.3.

Unbiased Fourier difference ( $F_{\text{obs}}-F_{\text{calc}}$ ) maps were calculated using diffraction data of 1525 soaked in DHP and 5F-DHP (Fig 4.5A), respectively, using the phase information calculated from a protein model consisting of the wild-type bCD enzyme (PDB accession code 1K70) with residues 152, 316 and 317 changed to alanine and the bound ligand DHP removed. The density of the bound compounds clearly demonstrated the presence of bound compounds in positions nearly identical to those observed in the wild-type enzyme. The orientation of the pyrimidine ring within the density maps is confirmed by the presence of additional density in the 5F-DHP complex, corresponding to the additional fluorine substituent. However, as compared to the wild-type enzyme, the compounds appear to exhibit significant conformational heterogeneity in the active site, particularly evident as disorder and minimal density at the C1 carbon position of both compounds. As a result, coordinates of the bound compounds were not included in the final refined models of 1525. These structural models, along with the X-ray diffraction amplitudes, have been deposited in the RCSB structural database (accession code 3G77) in order to allow independent calculation of difference maps by interested investigators.

In the previously described structure of D314A mutant, the D314A substitution creates a hydrophobic pocket to accommodate the fluorine atom of 5F-DHP(16). This mutation not only eliminates a spatial clash with the fluorine atoms, but also provides a favorable van der Waals contact with the bound 5F-DHP. In contrast, none of the three side chains mutated in the active site of 1525 are in direct contact with bound substrate. However, as a result of the mutation of D317 (which eliminates a carboxylate side chain), the wild type residue D314, which is the side chain nearest to the 5'-position of the substrate, swings away from the active site (Fig 4.5B), creating a neighboring cavity and reducing the local negative charge. This movement produces a similar chemical and structural effect as observed in D314A mutant.



Two other mutations (V152A and F316C) do not seem to affect the active site directly. This is further supported by experiments in which the substitutions found at F316 and D317 in 1246, 1525 and 1779 were individually examined for the ability to confer 5FC sensitivity in complementation assays. Close examination of the sequences at position D314 and D317 of the 12 bCD variants identified from the genetic complementation studies reveals D317G substitutions (but no D314A, S or G substitutions) in nine of the isolates, whereas the remaining three clones have A or G substitutions at D314 but none at D317. Combining 1525 (V152A/F316C/D317G) and D314S substitutions resulted in a reversal of 5FC sensitivity rather than an additive effect. Taken together, these results support the notion that enhancement of 5FC activity occurs when mutations exist at D314 or the D317G substitution is present but that these substitutions are mutually exclusive.

Cancer chemotherapy treatments can result in significant and often debilitating side effects due to the absence of distinct biochemical differences that occur between normal and neoplastic cells. SGT provides an exceptional opportunity to introduce unique biochemical characteristics to cancer cells that can then be exploited for a safer, less toxic and more effective treatment. Two suicide gene/prodrug systems have garnered significant attention and are undergoing preclinical and clinical evaluations; the widely used HSVTK/ganciclovir and the CD/5FC systems(30). Despite initial enthusiasm for the use of these suicide gene/prodrug approaches, limitations such as insufficient gene delivery to the tumor site and poor prodrug conversion properties of the suicide enzymes have restricted the full potential of SGT. From over a million bCD mutants we have identified one bCD variant (1525) that displays superior 5FC kinetic, cell killing, bystander and tumor growth restriction activities. Collaborative studies using adenoviral vectors expressing mutant D314A in combination with radiotherapy to treat pancreatic cancer suggested that even the slight improvement of D314A provided enhancement

of 5FC-mediated cytotoxicity *in vitro* and *in vivo*(32). Therefore, mutant 1525 will likely provide a significant advantage over wild-type bCD or D314A in at least three important ways: 1) by enhancing 5FC-mediated cell killing through both direct and bystander mechanisms; 2) by allowing the use of lower, less debilitating doses of 5FC to achieve effective cell killing and; 3) by providing an optimized alternative to the use of wild-type CD or HSVTK suicide gene therapy approaches. Furthermore mutant 1525 may be used in a variety of different applications including for restenosis, non-invasive tumor imaging and in negative selection systems.

## References

1. Nishiyama T, Kawamura Y, Kawamoto K, et al. Antineoplastic effects in rats of 5-Fluorocytosine in combination with cytosine deaminase capsules. *Cancer Res* 1985;45:1753-61.
2. Katsuragi T, Sakai T, and Tonomura K. Implantable enzyme capsules for cancer chemotherapy from bakers' yeast cytosine deaminase immobilized on epoxy-acrylic resin and urethane prepolymer. *Appl Biochem Biotechnol* 1987;16:61-69.
3. Springer CJ, Niculescu-Duvaz I. Gene-directed enzyme prodrug therapy (GDEPT): choice of prodrugs. *Adv Drug Deliv Rev* 1996;22:351-64.
4. Austin EA, Huber BE. A first step in the development of gene therapy for colorectal carcinoma: cloning, sequencing, and expression of *Escherichia coli* cytosine deaminase. *Mol Pharmacol* 1993;43:380-7.
5. Mullen CA, Kilstrup M, Blaese RM. Transfer of the bacterial gene for cytosine deaminase to mammalian cells confers lethal sensitivity to 5-fluorocytosine: a negative selection system. *Proc Natl Acad Sci USA* 1992;89:33-37.
6. Dong Y, Wen P, Manome Y, et al. In vivo replication-deficient adenovirus vector-mediated transduction of the cytosine deaminase gene sensitizes glioma cells to 5-fluorocytosine. *Hum Gene Ther* 1996;7:713-20.
7. Huber BE, Austin EA, Richards CA, Davis ST, Good SS. Metabolism of 5-fluorocytosine to 5-fluorouracil in human colorectal tumor cells transduced with the cytosine deaminase gene: significant antitumor effects when only a small percentage of tumor cells express cytosine deaminase. *Proc Natl Acad Sci USA* 1994;91:8302-06.
8. Mullen CA, Coale MM, Lowe R, Blaese RM. Tumors expressing the cytosine deaminase suicide gene can be eliminated in vivo with 5-fluorocytosine and induce protective immunity to wild type tumor. *Cancer Res* 1994;54:1503-06.
9. Haberkorn U, Oberdorfer F, Gebert J, et al. Monitoring gene therapy with cytosine deaminase: in vitro studies using tritiated-5-fluorocytosine. *J Nucl Med* 1996;37:87-94.
10. Lawrence TS, Rehemtulla A, Ng EY, Wilson M, Trosko JE, Stetson PL. Preferential cytotoxicity of cells transduced with cytosine deaminase compared to bystander cells after treatment with 5-fluorocytosine. *Cancer Res* 1998;58:2588-93.
11. Freeman SM, Abboud CN, Whartenby KA, et al. The "bystander effect": tumor regression when a fraction of the tumor mass is genetically modified. *Cancer Res* 1993;53:5274-83.
12. Moolten FL. Tumor sensitivity conferred by inserted herpes thymidine kinase genes: paradigm for a prospective cancer control strategy. *Cancer Res* 1986;46:5276-81.

13. Kuriyama E, Masui K, Sakamoto T, et al. Bystander effect caused by cytosine deaminase gene and 5-fluorocytosine in vitro is substantially mediated by generated 5-fluorouracil. *Anticancer Res* 1998;18:3399-406.
14. Mahan SD, Ireton GC, Stoddard BL, Black ME. Alanine-scanning mutagenesis reveals a cytosine deaminase mutant with altered substrate preference. *Biochemistry* 2004;43:8957-64.
15. Mahan SD, Ireton GC, Knoeber C, Stoddard BL, Black ME. Random mutagenesis and selection of *Escherichia coli* cytosine deaminase for cancer gene therapy. *Prot Eng Des Sel* 2004;17:625-33.
16. Ireton GC, McDermott G, Black ME, Stoddard BL. The structure of *Escherichia coli* cytosine deaminase. *J Mol Biol* 2002;315:687-97.
17. Ireton GC, Black ME, Stoddard BL. The 1.14 Å crystal structure of yeast cytosine deaminase: evolution of nucleotide salvage enzymes and implications for genetic chemotherapy. *Structure* 2003;11:961-72.
18. Hayden MS, Linsley PS, Wallace AR, Marquardt H, Kerr DE. Cloning, overexpression, and purification of cytosine deaminase from *Saccharomyces cerevisiae*. *Protein Expr.Purif* 1998;12:173-84.
19. Stolworthy TS, Aaron MK, Candice LW, Ardiani A, Cundiff J, Stoddard BL, Black ME. Yeast cytosine deaminase mutants with increased thermostability impart sensitivity to 5-fluorocytosine. *J Mol Biol* 2008;377:854-69.
20. Serve K, Yanez JA, Remsburg CM, Davies NM and Black ME. Development and validation of a rapid and sensitive HPLC method for detection of 5-fluorocytosine and its metabolites. Submitted 2009.
21. Ireton GC, Black ME, Stoddard B. Crystallization and preliminary X-ray analysis of bacterial cytosine deaminase. *Acta Crystallogr D Biol Crystallogr* 2001;57:1643-45.
22. Collaborative Computational Project, Number 4. The CCP4 Suite: Programs for Protein Crystallography. *Acta Cryst* 1994;D50:760-3.
23. Trinh QT, Austin EA, Murray DM, Knick VC, Huber BE. Enzyme/prodrug gene therapy: comparison of cytosine deaminase/5-fluorocytosine versus thymidine kinase/ganciclovir enzyme/prodrug systems in a human colorectal carcinoma cell line. *Cancer Res* 1995;55:4808-12.
24. Malet-Martino M, Jolimaitre P, Martino R. The prodrugs of 5-fluorouracil. *Curr Med Chem Anticancer Agents* 2002;2:267-310.
25. Kievit E, Bershad E, Ng E, et al. Superiority of yeast over bacterial cytosine deaminase for enzyme/prodrug gene therapy in colon cancer xenografts. *Cancer Res* 1999;59:1417-21.
26. Black ME, Newcomb TG, Wilson HM, Loeb LA. Creation of drug-specific herpes simplex virus type 1 thymidine kinase mutants for gene therapy. *Proc Natl Acad Sci USA* 1996;93:3525-29.

27. Kokoris MS, Black ME. Characterization of herpes simplex virus type 1 thymidine kinase mutants engineered for improved ganciclovir or acyclovir activity. *Protein Sci* 2002;11:2267-72.
28. Harris BE, Manning BW, Federle TW, Diasio RB. Conversion of 5-fluorocytosine to 5-fluorouracil by human intestinal microflora. *Antimicrob Agents Chemother* 1986;29:44-8.
29. Kievit E, Nyati MK, Ng E, et al. Yeast cytosine deaminase improves radiosensitization and bystander effect by 5-fluorocytosine of human colorectal cancer xenografts. *Cancer Res* 2000;60:6649-55.
30. Greco O, Dachs G. Gene directed enzyme/prodrug therapy of cancer: historical appraisal and future prospective. *J Cell Physiol* 2001;187:22-36.
31. Niculescu-Duvaz I, Springer CJ. Gene-directed enzyme prodrug therapy: a review of enzyme/prodrug combinations. *Expert Opin Investig Drugs* 1997;6:685-703.
32. Kaliberova LN, Della Manna DL, Krendelchtchikova V, Black ME, Buchsbaum DJ, Kaleberov SA. Molecular chemotherapy of pancreatic cancer using novel mutant bacterial cytosine deaminase gene. *Mol Cancer Ther* 2008;7:2845-54.

## FIGURE LEGENDS

**Figure 4.1.** Cartoon diagram of wild-type bCD monomer. The 22 residues that were subjected to randomization and selection for 5FC sensitization are in blue. The location and identity of mutations (V152A, F316C and D317G; 1525) that gave rise to highest specificity and activity toward 5FC are labeled.

**Figure 4.2.** 5FC sensitivity assays of cells stably transfected with wild-type or mutant bCDs. Pools of stably transfected **(A)** C6, DU145 and HCT116 cells containing pCDNA, pCDNA:bCD, pCDNA:1246, pCDNA:1525 and pCDNA:1779 were evaluated for 5FC sensitivity. Pools of stably transfected HCT116 cells containing pCDNA, pCDNA:bCD, **(B)** pCDNA:D314G, pCDNA:D314A and pCDNA:D314S; or **(C)** pCDNA:1525, pCDNA:D314S and pCDNA:1525/D314S were evaluated for 5FC sensitivity. After 6 days of 5FC treatment, cell survival was determined using Alamar Blue according to the manufacturer's instructions. Each data point (mean  $\pm$  SEM; n=3; performed with 24 replicates) is expressed as a percentage of the value for control wells with no 5FC treatment. Student's t-test analysis determined that the differences in IC<sub>50</sub> values between mutant bCD-and wild-type bCD-transfectants are statistically significant (P $\leq$ 0.05).

**Figure 4.3.** Bystander analysis of stable transfectants exposed to 5FC. Pools of **(A)** C6, **(B)** DU145, **(C)** HCT116 cells containing pCDNA were mixed with cells harboring either pCDNA:bCD, pCDNA:1246, pCDNA:1525 or pCDNA:1779 at different ratios and were subjected to 4mM (C6) or 10mM (DU145 and HCT116) 5FC for a period of 6 days and cell survival was determined using Alamar Blue. Each data point (mean  $\pm$  SEM; n=3; performed with 24 replicates) is expressed as a percentage of the value for control wells with vector-transfected cells. Student's t-test analysis determined that the differences between percentage of mutant bCD-and wild-type

bCD-transfectants needed to achieve 50% tumor cell killing are statistically significant ( $P \leq 0.05$ ). **(D)** HPLC analysis of 5FU levels in transfected cells. Stably transfected HCT116 cells were incubated with 2.5mM 5FC for up to seven days and metabolite levels calculated relative to a known concentration of an internal standard. Student's t-test was done to compare 1525 versus wild-type bCD transfected cell lysates. Asterisks denote  $p \leq 0.005$  (days 3-4) and  $P \leq 0.0003$  (days 5-7).

**Figure 4.4.** Tumor growth during and after 5FC treatment in a xenograft model. Pools of HCT116 cells transfected with pCDNA, pCDNA:bCD or pCDNA:1525 were used to seed tumors in nude mice ( $n=5$ ). When tumor size reached 3-4mm (day 0), **(A)** 5FC (375mg/kg) or **(B)** PBS was intraperitoneally administered twice a day for 21 days. Tumor growth was measured every other day for the duration of the experiment. Tumor volume was calculated using the formula  $4/3\pi ((\text{width} \times \text{length} \times \text{height})/2)$ , plotted and analyzed for statistical significance using Student's t-test. Asterisks denote statistical significance ( $p \leq 0.05$ ) in tumor sizes between mice harboring 1525-expressing tumor cells and those that received either empty vector- or wild-type bCD-expressing tumor cells in the presence of 375mg/kg 5FC.

**Figure 4.5. (A)** Electron density for bound substrate analogue 2-hydroxypyrimidine (or dihydroxypyrimidine, DHP) (left) and 5-fluoro-DHP (right) bound in the active site of bCD. As noted in the text, the density for the bound compound indicates disorder, particularly near the C1 carbon. However, the appearance of additional difference density corresponding to the 5-fluoro substituent (arrow) unambiguously confirms the orientation of the inhibitor.

**(B)** Comparison of the active sites of wild-type and mutant bCD enzymes. Superposition of the active sites of wild-type bCD in complex with DHP (PDB

accession code-1K70), D314A mutant in complex with 5F-DHP (PDB accession code-1RA5) versus 1525 soaked with 5F-DHP. The motion of residue D314 (arrow), into the cavity vacated by removal of a side chain in the D317G mutation, mimics the structural effect of the previously described D314A and D314G mutations.

#### **ACKNOWLEDGMENTS**

This work was supported by NIH grants CA85939 (MEB) and CA97380 (BLS and MEB).



**Table 4.1.** Enzyme Kinetics of wild-type bCD and bCD mutants

	WT - bCD		1246		1525		1779	
	cytosine	5FC	cytosine	5FC	cytosine	5FC	cytosine	5FC
$K_m$ (mM)	0.46 (0.05) <sup>b</sup>	3.76 (0.4)	1.65 (0.34)	6.73 (2.07)	4.9 (1.11)	12.69 (4.53)	3.16 (1.8)	7.55 (0.84)
$k_{cat}$ (sec <sup>-1</sup> )	49.68 (2.14)	19.71 (0.74)	2.13 (0.26)	83.68 (12.16)	1.69 (0.45)	101.74 (21.72)	2.98 (0.72)	115.24 (6.28)
$k_{cat} / K_m$ (mM <sup>-1</sup> sec <sup>-1</sup> )	106.85 (39.3)	5.24 (1.87)	1.29 (0.76)	12.44 (5.88)	0.35 (0.4)	8.02 (4.8)	0.94 (0.46)	15.27 (7.47)
Relative efficiency to the wild type	1	1	0.01	2.37	0.003	1.53	0.009	2.91
Relative substrate specificity <sup>a</sup>	0.95	0.05	0.09	0.91	0.04	0.96	0.06	0.94
Relative substrate specificity to the wild type	1	1	0.09	18.2	0.04	19.2	0.06	18.8

<sup>a</sup> Cytosine:  $[k_{cat} / K_m(\text{cytosine})] / [k_{cat} / K_m(\text{cytosine}) + k_{cat} / K_m(5\text{FC})]$ ; 5FC:  $[k_{cat} / K_m(5\text{FC})] / [k_{cat} / K_m(\text{cytosine}) + k_{cat} / K_m(5\text{FC})]$

<sup>b</sup> Standard error

**Figure 4.1**

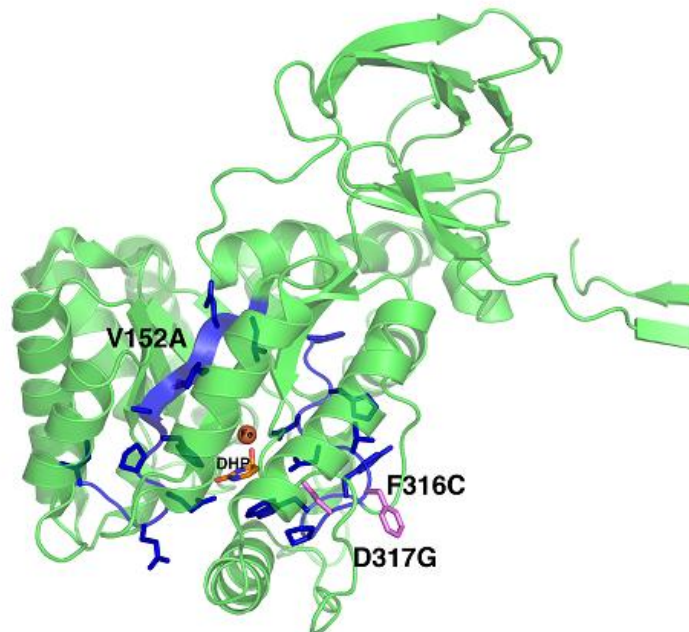


**Figure 4.2**

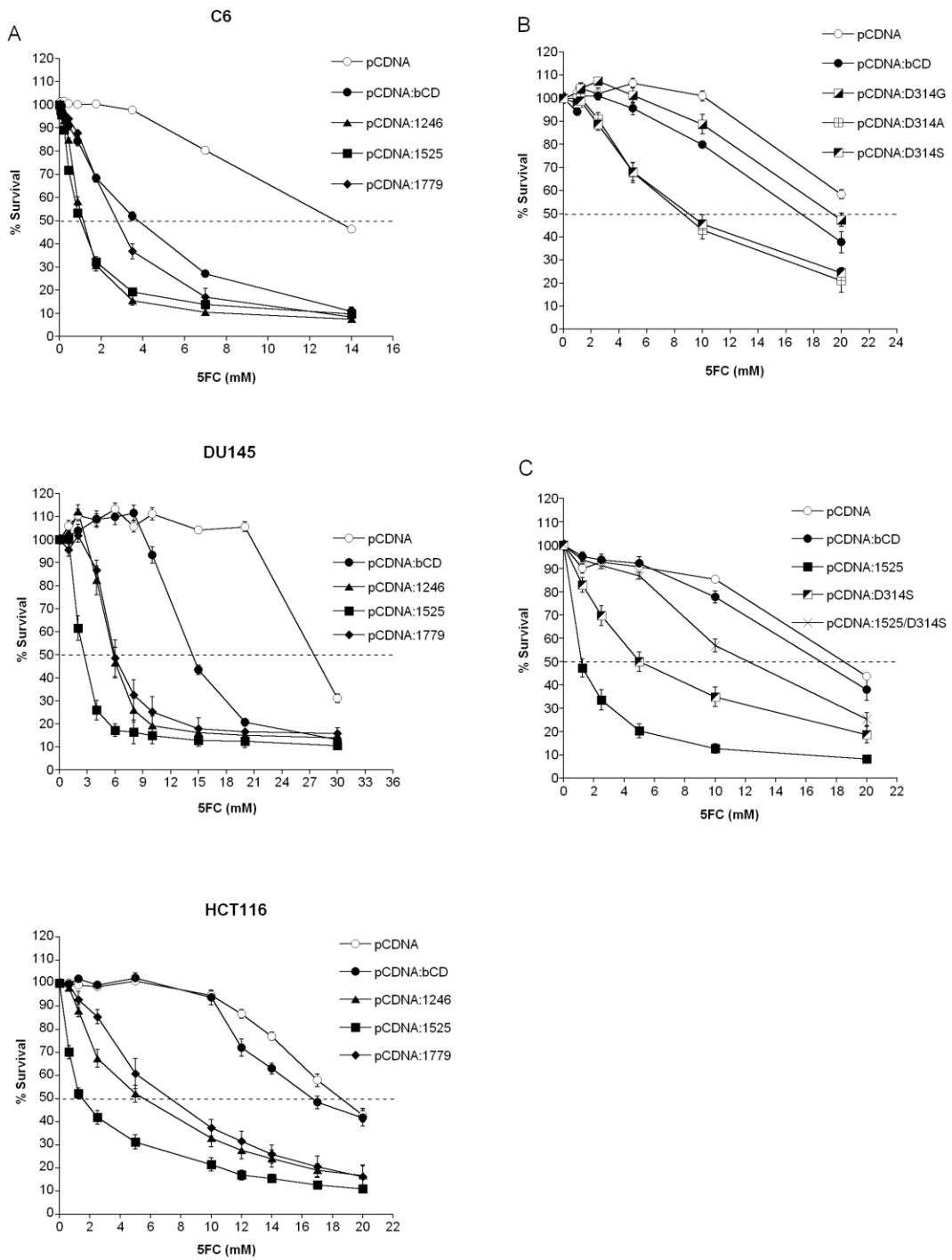


**Figure 4.3**

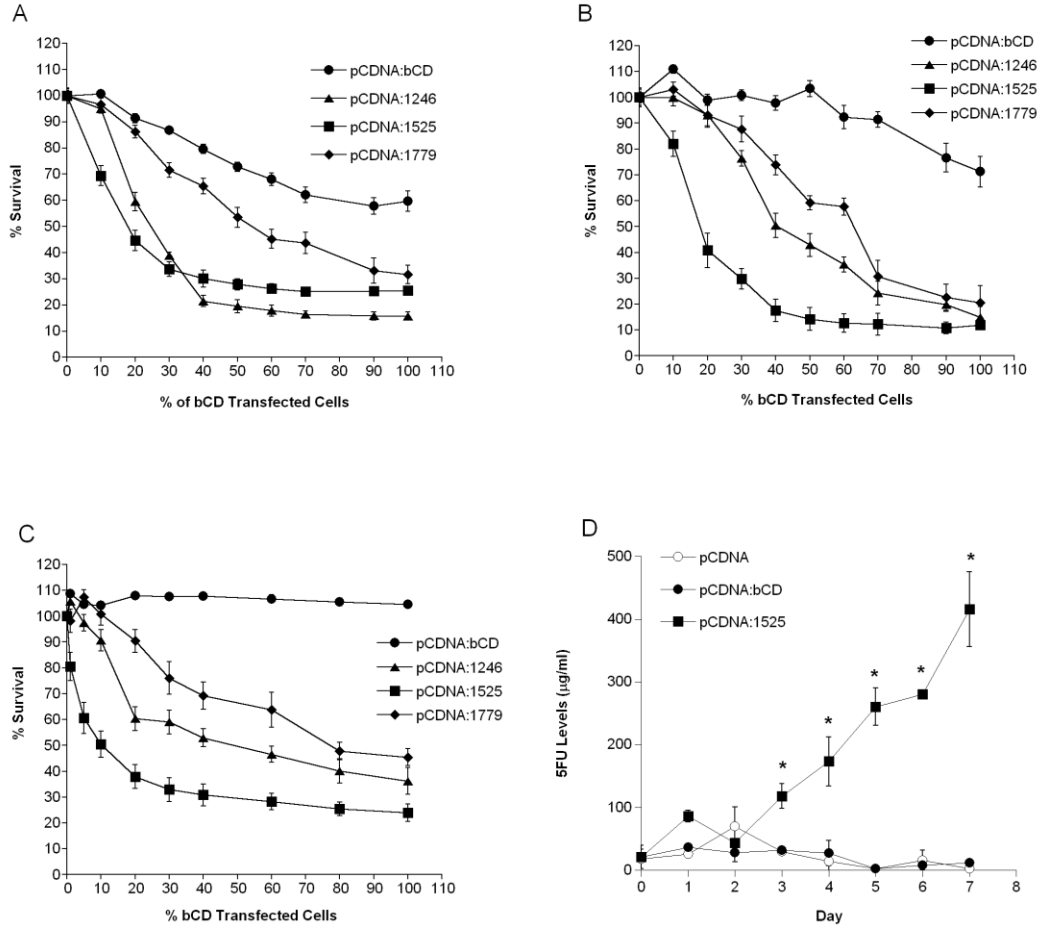


Figure 4.4

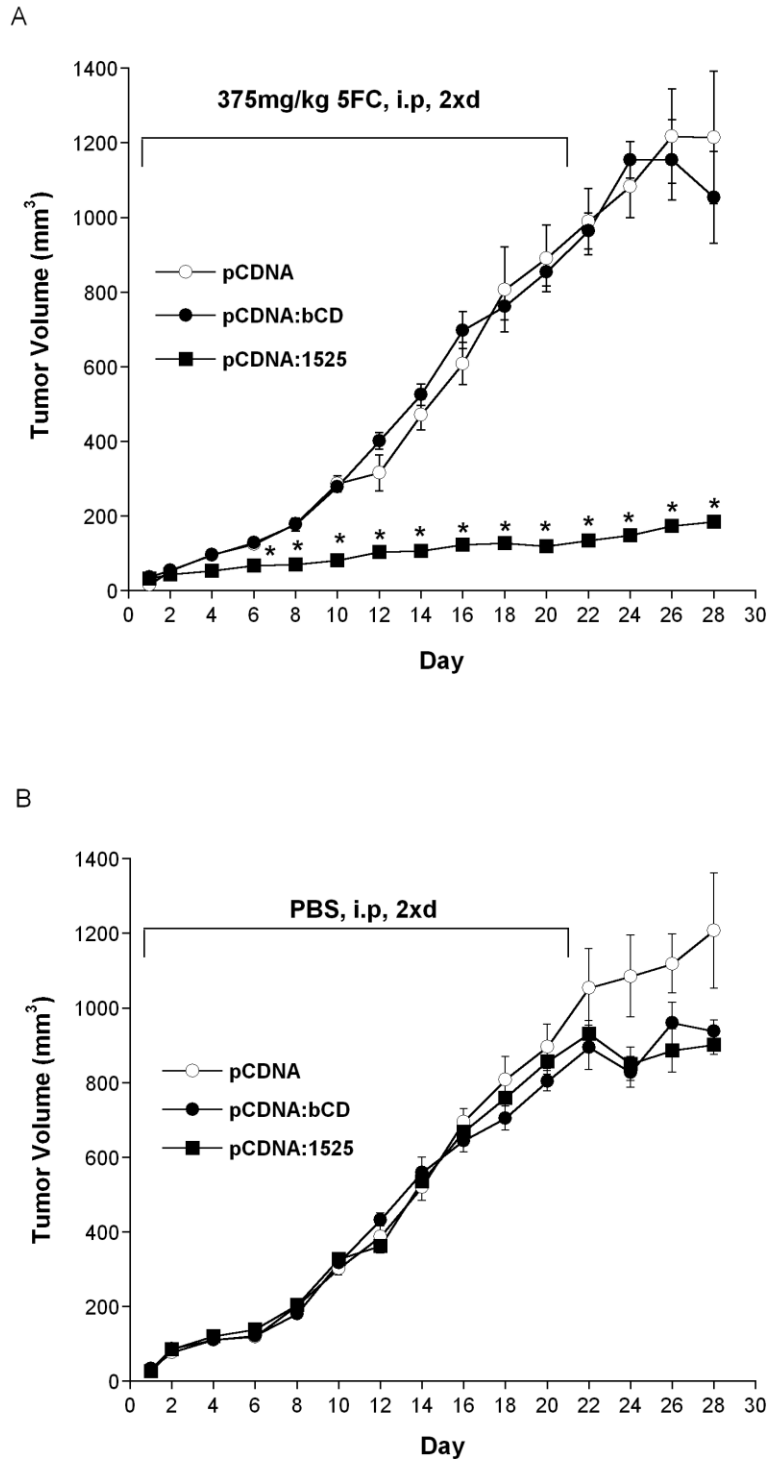
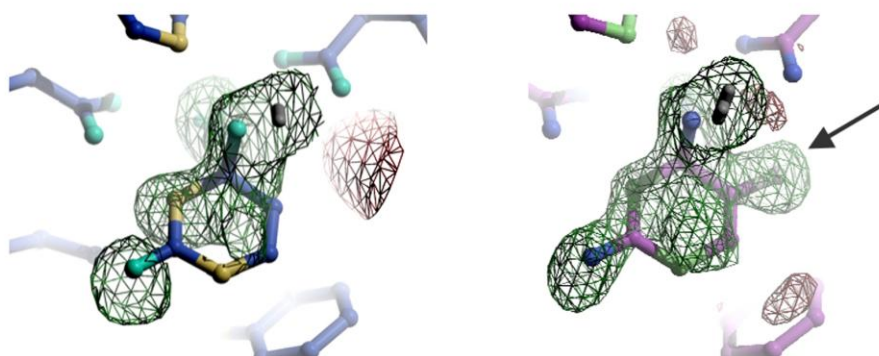
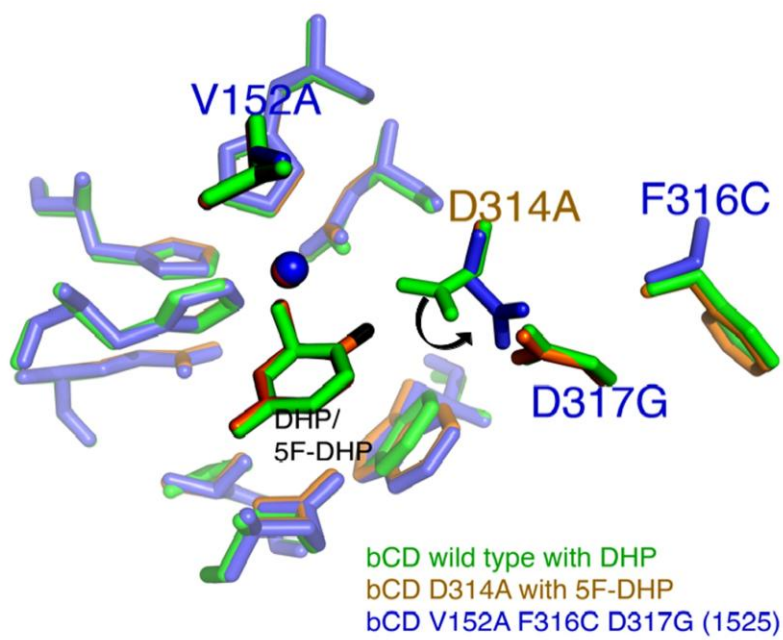


Figure 4.5

a



b



## Supplementary Table 4.1

Oligonucleotides used to generate randomized DNA fragment<sup>a</sup>

MB267: 5'-GACGTTAATGCCGGACTCCAGCATCTCTTTAACGGCGGTGATGCCGCGACG-3'  
MB268: 5'-CCGGCATTAAAGTCTGCT**TTTGGTCACGATGATGTCTTCGATCCCGTGGTAT**CCCGCTGGGAACGGCG-3'  
MB271: 5'-CGACATGGGTACGCACATGCTGGATCCCGTTGGCAATC-3'  
MB272: 5'-GCGTACCCATGTCGATGTTTCGGATGCAACGCTAACTGCCGTGAAAG-3'  
MB273: 5'-CAATCCACGGCGCGACTCCTGCTTCACTTCCAGCATTGCTTTCAGGCGCAG-3'  
MB274: 5'-CGCGCCGTGGATTGAT**CTGCAAATCGTCGCCTTCCCTCAGGAAGGGATT**TTTGTCTATCCCAACGGTG-3'  
MB275: 5'-CTGCCCTAAGCGTAACGCCTCTCCAGCAACGCTTCCCGTTGGGATACG-3'  
MB276: 5'-CGCTTAGGGGACAGATGATGTTGGGGCGATTCCGCATTTT(GAATTC)ACCCGTG-3'  
MB361: 5'-GCCGTATTCACGGGTGAATTCAAAATGCG-3'  
MB384: 5'-CGAAACGTCCCTGCAGATGAATATTGACCAGCGGGTGGCGACAAAGTTAATACC-3'  
MB385: 5'-CATCTGCAAGGACGTTTCGATACGTATCCAAAACGTCCGGGCATCACGCGCG-3'  
MB386: 5'-CATGCAGCCC(CATGTG)CAGCACTTGCAGCATATTCCCGTTCCCGAGC-3'  
MB387: 5'-G(CACATG)GGGCTGCATGTTG(CCAGTTGATGGG)CTACGGGCAGATTAACG-3'  
MB388: 5'-GGTATTAACCTTTGTCGCCAACCCGCTGG-3'  
MB389: 5'-CGTTAATCTGCCCGTAGCCCATCAACTGG-3'

Oligonucleotides used to perform general sequencing, introduce amino acid substitutions, introduce or eliminate restriction sites<sup>b</sup>

MB262: 5'-CACATGCTG**GAT**CCCGTTGGC-3'  
MB263: 5'-ACGGGT**G**AATTCAAAATGCG-3'  
MB349: 5'-GAAATGGCAGATTG**CCAACGGGAT**CCAG-3'  
MB364: 5'-GGACAACCGAACTGGAATCAG-3'  
MB438: 5'-GCTTTGGCCACGAT**AG**CGTCTGCGGTCCG-3'  
MB439: 5'-CGGACCGCAGACG**CT**ATCGTGCCAAAGC-3'  
MB478: 5'-GGTCACGATGATGTCTTCG**G**TCCGTGGTATCCGCTG-3'  
MB479: 5'-CAGCGATACCCAGGAC**CGA**AAGACATCATCGTGACC-3'  
MB480: 5'-GGTCACGATGATGTCT**CGAT**CCCGTGGTATCCGCTG-3'  
MB481: 5'-CAGCGATACCCAGGATCG**G**AGACATCATCGTGACC-3'  
MB482: 5'-GGTCACGATGATGT**CT**CGATCCCGTGGTATCCGCTG-3'  
MB483: 5'-CAGCGATACCCAGGATCG**AG**GACATCATCGTGACC-3'  
MB484: 5'-GGTCACGATGATGT**CT**CGATCCCGTGGTATCCGCTG-3'  
MB485: 5'-CAGCGATACCCAGGATCG**AG**GACATCATCGTGACC-3'  
MB490: 5'-GGTCACGATGATGTCT**CGG**TCCGTGGTATCCGCTG-3'  
MB491: 5'-CAGCGATACCCAGGAC**CGC**AGACATCATCGTGACC-3'  
MB492: 5'-GGTCACGATGATGT**CT**CGG**T**CCCGTGGTATCCGCTG-3'  
MB493: 5'-CAGCGATACCCAGGAC**CGA**GACATCATCGTGACC-5'  
MB494: 5'-GGTCACGATGATGT**CT**CG**G**TCCCGTGGTATCCGCTG-3'  
MB495: 5'-CAGCGATACCCAGGAC**CGA**GACATCATCGTGACC-5'

<sup>a</sup> Nucleotide shown in bold are mixtures of wild-type nucleotides (91%) and the three non-wild type nucleotides (9%).

<sup>b</sup> Underlined nucleotides indicate changes in amino acid sequences or change in restriction site.

## Supplementary Table S4.2

WT	L	Q	I	V	A	F	P	Q	E	G	I	F	G	H	D	D	V	F	D	P	W	Y
	149	150	151	152	153	154	155	156	157	158	159	310	311	312	313	314	315	316	317	318	319	320
238														N			V	G				
1246												I			E		L	G				
1525				A													C	G				Y
1779																L	V	G				Y
2014		H												D		G						Y
2186																G						Stop
2533						L								Y		A						
2720		K								K								I	G			
3153																	G		G			
3286																	G		G			
3532													A	F				V	G			Y
3534																		L	G			

## Supplementary Table S4.3

Crystal complex	bCD1525 with DHP	bCD1525 with 5F-DHP
<b><u>Crystallographic data</u></b>		
Resolution (Å)	45-1.8 (1.86-1.80)	37-1.9(1.97-1.90)
Space group	R32	R32
Cell parameters (Å)	a=b=108.9 c=240.8	a=b=109.0 c=239.8
	$\alpha=\beta=90^\circ \gamma=120^\circ$	$\alpha=\beta=90^\circ \gamma=120^\circ$
Completeness (%)	98.7 (99.2)	96.3 (93.5)
$R_{\text{sym}}$ (%)	8.8 (26.1)	6.4 (23.9)
$I/\sigma$	24.9 (13.0)	16.2 (3.5)
Redundancy	4.0(3.9)	13.8 (4.8)
<b><u>Refinement</u></b>		
Resolution (Å)	1.8	1.9
R-factor (%)	17.2	18.2
R-free (%)	20.0	21.0
R.m.s bond length (Å)	0.012	0.009
R.m.s bond angle (°)	1.325	1.0755
Ramachandran distribution	99.2 % allowed 0.8 % disallowed	99.5% allowed 0.5 % disallowed
Mean B factor (Å <sup>2</sup> )	11.5	15.6

## CHAPTER FIVE

### **Engineering Novel Fusion Enzyme Cytosine Deaminase/Uracil Phosphoribosyltransferase for Improved Cancer Gene Therapy**

#### **ABSTRACT**

Cytosine deaminase (CD) is an enzyme responsible for deaminating cytosine to form uracil. It is also able to deaminate the anti-fungal drug, 5-fluorocytosine (5FC), to the potent anti-cancer drug, 5-fluorouracil (5FU). UPRT is an important enzyme involved in the pyrimidine salvage pathway, catalyzing the transfer of a ribosyl-phosphate group to uracil to form uridine-monophosphate. The enzyme also converts 5FU to 5FU-monophosphate (5FUMP), which is then further catalyzed to antimetabolites by endogenous enzymes. Previously, we reported the generation and characterization of bCD variants with increased activity towards 5FC. One bCD mutant, 1525, was shown to have the greatest increase in tumor cytotoxicity and bystander killing activity *in vitro* and *in vivo*. Earlier reports demonstrated that the fusion of CD with UPRT (CD/UPRT) along with 5FC imparts a greater tumor killing activity than CD alone. Therefore, to further enhance the production of cytotoxic compounds, we sought to incorporate improvements previously identified in bCD 1525 into new fusion constructs containing both bCD and UPRT activities. The fusion construct 1525/UPRT was evaluated for its tumor cell killing and bystander effects *in vitro*. Because mutant fusion enzymes offered only a modest increase in cell sensitivity toward 5FC and displayed no significant improvement in bystander killing effect, we hypothesized that the conversion of 5FU to 5FUMP by UPRT became the rate limiting step in this pathway. To overcome this limitation, we performed region-specific random mutagenesis to generate UPRT mutants and, coupled with genetic complementation in *E. coli*, identified variants with increased activity toward 5FU.



Three UPRT mutants were identified to have enhanced activity towards 5FU using negative complementation in *E. coli*. These three mutants were further analyzed biochemically and in rat C6 glioma cell lines. Although kinetic analyses indicated that two UPRT mutants (3802 and 4312) displayed a modest shift in substrate preference towards 5FU, *in vitro* data suggested that the kinetics of the combination of 1525 and UPRT mutant 3802 or were not sufficiently improved to enhance their tumor killing activity. Future work to address this problem as well as to create mutants with further enhanced activity towards 5FU will be performed. Toward that end, the use of such novel mutant fusion constructs will advance suicide gene therapy treatment for cancer and improve the likelihood of complete tumor ablation in cancer patients.

---

This manuscript will be submitted in the following manuscript: **Ardiani, A** and Black, M.E. Engineering Novel Fusion Enzyme Cytosine Deaminase/Uracil Phosphoribosyltransferase for Improved Cancer Gene Therapy.

## **INTRODUCTION**

Cytosine deaminase (CD; EC 3.5.4.1) is an important enzyme involved in pyrimidine salvage pathway catalyzing the deamination of cytosine to uracil and ammonia<sup>1</sup>. CD is uniquely present in fungi and bacteria and is absent in mammalian cells. Bacterial CD (bCD), originated from *Escherichia coli*, is a hexamer of approximately 300 kDa comprised of identical subunits<sup>2</sup>. It is being used in suicide gene therapy protocols because of its ability to deaminate 5-fluorocytosine (5FC), an anti-fungal drug, to 5-fluorouracil (5FU), a potent anti-cancer drug. Upon successful delivery of bCD to cancer cells followed by systemic administration of 5FC, transfected cancer cells become sensitized to the prodrug and result in cytotoxicity. Intracellularly, 5FC is initially deaminated by CD to form 5FU, which is then further converted to several active antimetabolites, 5-fluoro-2'-deoxyuridine 5'-monophosphate (5FdUMP), 5-fluorodeoxyuridine triphosphate (5FdUTP) and 5-fluorouridine-triphosphate (5FUTP), by endogenous enzymes (Figure 5.1)<sup>3</sup>. Cytotoxicity is mainly due to the action of 5FdUMP, which is a reversible inhibitor of thymidylate synthase (TS). Inhibition of TS results in the depletion of dTMP and subsequently dTTP pools, which ultimately leads to cell death. The active antimetabolites, 5FdUTP and 5FUTP, can cause toxicity by inhibiting DNA and RNA synthesis, respectively. Because low gene transfer is a key limitation in gene therapy, the success of suicide gene therapy relies heavily on a phenomenon known as the bystander effect, which is an extension of cell killing beyond the cells expressing the suicide gene to neighboring cells<sup>4,5</sup>. A combination of factors is thought to participate in the bystander effect including transfer of antimetabolites and/or suicide enzymes through gap junctions, diffusion and apoptotic vesicles. An immune-related response also contributes to the bystander effect although in a delayed fashion. Previous studies reported that significant tumor ablation *in vivo* could be achieved in the presence of 5FC even when only a small percentage of

tumor cells express CD<sup>6</sup>. Implicit in the bystander effect is that sufficient active prodrug is transferred to neighboring cells to elicit cell killing.

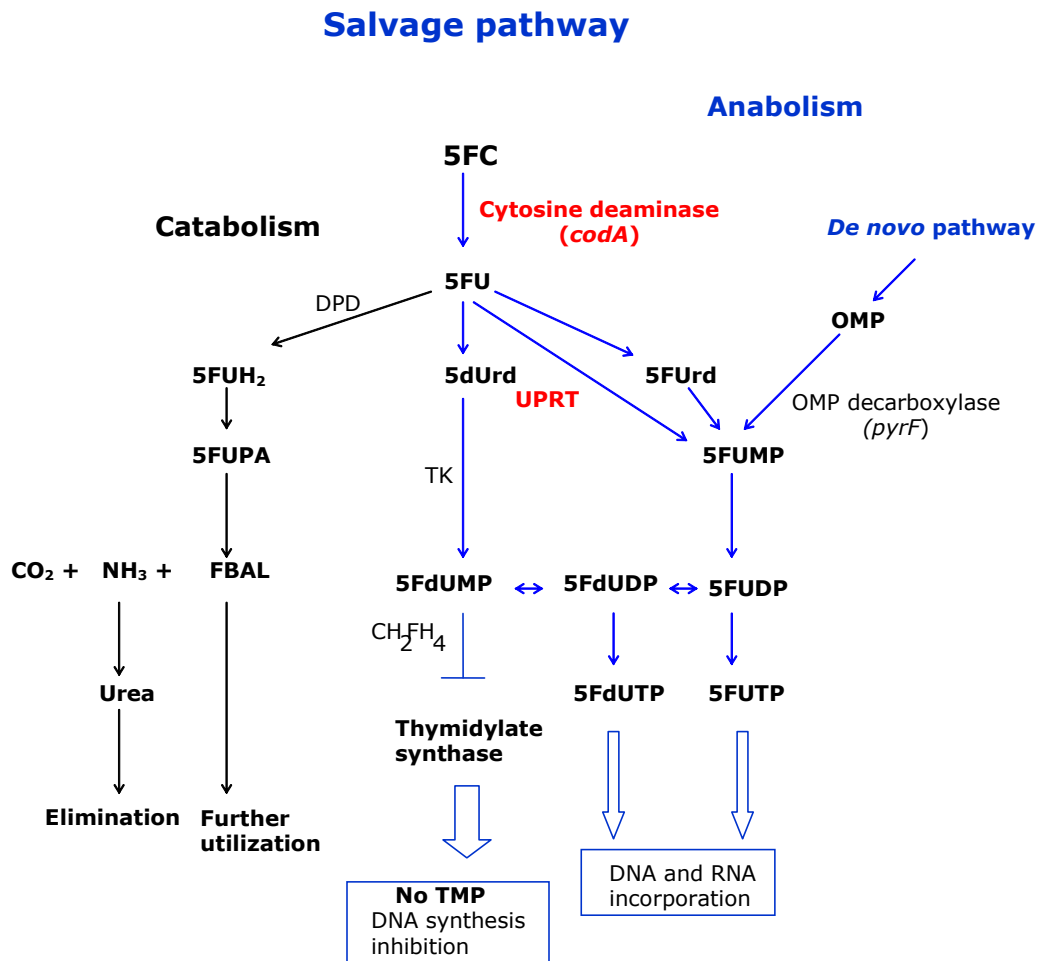


**Figure 5.1.** 5FC metabolites and their fates in the pyrimidine metabolism pathway. DPD: dihydropyrimidine dehydrogenase, TK: thymidine kinase, UPRT: uracil phosphoribosyltransferase, OMP: orotidine-5'-monophosphate, CH<sub>2</sub>FH<sub>4</sub>: N<sup>5</sup>,N<sup>10</sup>-methylenetetrahydrofolate, 5FUH<sub>2</sub>: 5,6-dihydro-5-fluorouracil, 5FUPA: 5- $\alpha$ -fluoro- $\beta$ -ureidopropionic acid, 5- $\alpha$ -fluoro- $\beta$ -alanine. Enzymes highlighted in red and bold (CD and UPRT) is absent in mammals.

Although the bystander effect provides significant benefit to suicide gene therapy, inefficient activation of 5FC by bCD impedes this advantage and limits the overall therapeutic response. When this problem is combined with the low gene transfer and the rapid half life of 5FC in blood, high doses of 5FC are required to achieve substantial anti-tumor responses. However, high doses of 5FC generally

results in undesirable side effects, primarily due to the presence of microbes in the gastrointestinal tract that naturally encode CD. Frequently, patients treated with high doses of 5FC suffer from bone marrow depression and gastrointestinal complications<sup>7</sup>.

One approach to improve prodrug activation, which may consequently reduce the dose of 5FC required to kill tumor cells and thereby limit the 5FC-associated negative side effects, is to use bCD mutants with increased activity and/or substrate specificity toward the prodrug (Fuchita *et al.*, submitted)<sup>8,9</sup>. We previously reported the construction and characterization of one superior bCD mutant, mutant 1525, that exhibits not only an improvement in kinetic properties towards 5FC, but also *in vitro* tumor killing and *in vivo* tumor growth inhibition when compared to wild-type bCD. Another strategy to improve tumor killing activity of CD/5FC system is by creating a fusion enzyme containing activity CD and uracil phosphoribosyltransferase (UPRT). UPRT is an important enzyme involved in the pyrimidine salvage pathway, catalyzing the transfer of a ribosyl-phosphate group to uracil to form uridine-monophosphate. Similar to CD, UPRT is absent in mammalian cells and present in protozoa, fungi and bacteria. Bacterial UPRT is considered attractive in gene therapy field because of its ability to carry out the second step in 5FC pathway, converting 5FU to 5FU-monophosphate (5FUMP). Earlier reports demonstrated that the fusion of bCD with UPRT (bCD/UPRT) along with 5FC administration imparts a greater tumor killing activity than bCD alone<sup>10</sup>. Therefore, to further enhance the production of cytotoxic compounds, we sought to incorporate mutant 1525 into the fusion construct bCD/UPRT. The fusion construct (1525/UPRT) was evaluated for cell killing and bystander effects *in vitro*. Results from those studies indicated that 1525/UPRT offered only a slight increase in sensitivity toward 5FC and exhibited no improvement in bystander killing effect. We hypothesized that the conversion of 5FU to 5FUMP by UPRT was the rate limiting step in this pathway when 1525/UPRT is used. To

overcome this limitation, we performed regio-specific random mutagenesis to generate UPRT mutants and, coupled with genetic complementation in *E. coli*, identified variants with increased activity towards 5FU. Three UPRT mutants, constructs 3662, 3802, and 4312, were identified to confer 5FU sensitivity to *E. coli*. All three mutants were further analyzed biochemically and our kinetic analyses data suggest that two of the mutants (3802 and 4312) displayed 2- to 3-fold increases in substrate preferences towards 5FU. *In vitro* cytotoxicity analyses revealed that the combination of bCD mutant 1525 with either of the UPRT mutants identified in this study resulted in no improvement in killing activity as shown by higher or similar IC<sub>50</sub> values compared to that of fusion 1525/UPRT. Circular dichroism and x-ray crystallography will be done in the future, as an attempt to provide answers and explanations to this problem. Radioactive reagents were purchased from Moravek Biochemicals (Brea, CA).

## **MATERIALS and METHODS**

### **Materials**

Oligonucleotides used to mutate and sequence bCD and UPRT were obtained from Integrated DNA Technologies (Coralville, IA). Restriction endonucleases and T4 DNA ligase were purchased from New England Biolabs (Beverly, MA). DNA purification was done using several kits: Wizard PCR prep kits from Promega (Madison, WI), HiSpeed Plasmid Mini Kit from Qiagen (Valencia, CA), and StrataPrep EF Plasmid Midikit from Stratagene (La Jolla, CA). Polyclonal UPRT antibody was generated by Harlan using purified wild-type UPRT enzyme (Harlan Laboratories, Indianapolis, IN). All PCR reagents were either purchased from Invitrogen (Carlsbad, CA) or New England Biolabs (Beverly, MA). Alamar Blue was purchased from Serotec Limited (Oxford, UK). All cell culture reagents were purchased from Gibco (Carlsbad,

CA). All other reagents were purchased from Sigma (St. Louis, MO) unless otherwise noted.

### **Bacterial strains**

*Escherichia coli* strain NM522 [ $F^+$   $lacI^q\Delta(lacZ)$ -M15 $proA^+B^+/supE$   $thi\Delta(lac-proAB)\Delta(hsdMS-mcrB)5(r_k^-m_k^-McrBC^-)$ ] and *E. coli* strain XL1-Blue [ $F'::Tn10$   $proA^+B^+ lacI^q$  D( $lacZ$ ) M15/ $recA1$   $endA1$   $gyrA96$  (Nal<sup>r</sup>)  $thi$   $hsdR17$  ( $r_k^-m_k^+$ )  $supE44$   $relA1$   $lac$ ] were used as recipients in certain cloning procedures. *E. coli* BM604 (HfrH  $thi$   $galE$   $\Delta$  ( $att\lambda$ -*bio*)  $deoA103$   $deoC$   $argA$   $lysA$   $cytR$   $upp$   $udp$   $pyrF30$ ) was lysogenized with DE3 according to the manufacturer's instructions (Novagen, Madison, WI). The resulting strain BM604(DE3) was used in genetic complementation assay to assess UPRT activity and 5FU sensitivity. *E. coli* GIA39, a strain deficient in CD and orotidine 5'-phosphate decarboxylase, was obtained from the *E. coli* Genetic Stock Center (CGSC no. 5594:  $thr^-$   $dadB3$   $fhuA21$   $codA1$   $lacY1$   $tsk-95$   $glnV44$ (AS)  $\lambda$ - $pyrF101$   $his-108$   $argG6$   $ilvA634$   $thi-1$   $deoC1$   $glt-15$ ). *E. coli* GIA39 was lysogenized with DE3 according to the manufacturer's instructions. The derived strain, GIA39(DE3), was used in the genetic complementation assays for CD activity. *E. coli* BL21(DE3) (Novagen, Madison, WI) was used for large-scale protein purification.

### **Cell lines**

Cell lines were maintained in a humidified incubator at 37°C in 5% CO<sub>2</sub>. Rat C6 glioma cells (C6) were purchased from ATCC (Manassass. VA) and were grown in Dulbecco's Modified Essential Medium containing 5% fetal bovine serum, 1mM sodium pyruvate, 10mM HEPES, 10μM nonessential amino acids, 100U/ml penicillin G, 10μg/ml streptomycin sulfate, 292μg/ml L-glutamine, 100μM sodium citrate and 0.0014% NaCl. Transfected cells were cultured in media supplemented with blasticidin at concentration 4μg/ml for the selection of stable transfectants.

### **PCR amplification and cloning of *E. coli* UPRT gene**

PCR amplification of the *E. coli* UPRT gene was performed using two PCR oligonucleotides, MB488 and MB489 (Table 5.1), in 5 $\mu$ L 10X Taq buffer (supplied by the manufacturer), 5 $\mu$ L 2.5mM dNTPs, 1 $\mu$ L MB488, 1 $\mu$ L MB489, 1.5 $\mu$ L 1M MgCl<sub>2</sub>, 0.5 $\mu$ L Taq Polymerase, 33 $\mu$ L H<sub>2</sub>O, and 3 $\mu$ L of a 1:100 dilution of an overnight culture of BL21(DE3). The primer MB488 was specifically designed to introduce *Nco*I site upstream the start codon and the primer MB489 was designed to introduce *Eco*RI downstream the stop codon. The above reaction was initiated at 94°C for 3min, followed by 30 cycles of 94°C for 30s, 55°C for 30s, 72°C for 40s. The final step was a 20min extension at 72°C. The resulting 627-bp fragment was gel purified and ligated to pCR2.1 TOPO (Invitrogen, Carlsbad, CA). The UPRT gene was then further subcloned into pETHT as *Nco*I/*Eco*RI fragment and the resulting plasmid was designated pETHT:UPRT.

### **Construction of mammalian expression vectors**

The plasmid pORF-codA::upp carrying functional bacterial CD and bacterial UPRT was purchased from Invivogen (San Diego, CA). The bCD/UPRT gene was cloned into the mammalian expression vector pCDNA6/myc-HisB (Invitrogen, Carlsbad, CA) digested with *Eco*RV/*Xho*I as *Nco*I(blunt-ended)/*Xho*I fragments. After restriction enzyme verification, DNA sequencing analysis confirmed the presence of in-frame bCD/UPRT gene. Site-directed mutagenesis was performed on pCDNA:bCD/UPRT to introduce mutations derived from mutant bCD 1525 using the QuikChange site-directed mutagenesis kit from Stratagene (La Jolla, CA) according to the manufacturer's protocol. Two pairs of oligonucleotides, MB455, MB456, MB457, and MB458 (Table 5.1), were used to introduce amino acid substitutions at V152A, F316C and D317G. DNA sequencing analysis was done to verify the correct mutations of mutant 1525 onto the fusion construct. The UPRT gene was cloned into

pCDNA6/myc-HisB digested with *Bam*HI(blunt-ended)/*Eco*RI as *Nco*I(blunt-ended)/*Eco*RI fragments. The resulting plasmids were designated pCDNA:bCD/UPRT, pCDNA:1525/UPRT, and pCDNA:bUPRT respectively. The construction of pCDNA:bCD and pCDNA:1525 were as previously described by Fuchita *et al.* (submitted, 2009).

### ***In vitro* cytotoxicity assay**

One  $\mu$ g of each DNA: pCDNA (empty vector), pCDNA:bCD, pCDNA:1525, pCDNA:bUPRT, pCDNA:bCD/UPRT and pCDNA:1525/UPRT was used to transfect  $1 \times 10^5$  rat C6 glioma cells by lipofection using FuGENE 6 transfection reagent (Roche Diagnostic, Penzberg, Germany) at a 3:1 ratio as described by the manufacturer. Protein expression levels were determined by immunoblot analyses as previously described<sup>11</sup>. The membrane was probed with rabbit polyclonal UPRT antibody and followed by goat anti-rabbit-AP-conjugated antibody. The color reaction was developed using the AP Conjugate Substrate Kit (Bio-Rad, Hercules, CA). *In vitro* cytotoxicity assays were performed using stable transfectants confirmed by immunoblot. Pools of transfectants were transferred to 96-well microtiter plates at an initial density of 500 cells per well. Upon cell adherence overnight, 5FC (0-20mM) was added in sets of eight wells for each concentration tested. The cells were subjected to 5FC for 7 days, at which time the redox indicator dye Alamar Blue was added. Cell survival was determined by fluorescence recorded at 530/590nm, using a multi detector microplate reader Biotek Synergy HT, several hours later as described by the manufacturer and data were plotted with the standard deviation. At least three replicates were performed.



### ***In vitro* bystander experiment**

Rat glioma C6 cells stably transfected with pCDNA (empty vector) were mixed at different ratios with stable transfectants harboring either pCDNA:bCD, pCDNA:1525, pCDNA:bUPRT, pCDNA:bCD/UPRT or pCDNA:1525/UPRT. The mixed cells were then transferred to 96-well microtiter plates at a final density of 500 cells per well and following cell adherence overnight, a 5FC concentration of 10mM was added into the cells. Cell survival was determined as described above.

### **Construction of the UPRT regio-specific random library**

#### *Preparation of random insert*

The basic protocol of regio-specific random mutagenesis was performed as previously outlined<sup>12</sup>. Table 5.1 lists the oligonucleotides to synthesize a 153-bp double-stranded DNA fragment that spans 17 codons (Y192, I193, I194, P195, G196, L197, G198, D199, A200, G201, D202, K203, I204, F205, G206, T207, K208) and contains 15% randomness at those positions (MB571-MB572). Briefly, the 153-bp double-stranded DNA fragment was synthesized by annealing 50pmol each of MB571 and MB572 with 10×annealing buffer (70mM Tris-HCl, pH7.5, 60mM MgCl<sub>2</sub>, and 200mM NaCl) in a final volume of 50μL at 95 °C for 5min, at 65 °C for 20min, and at room temperature for 10min. Next, the annealed product was extended with the Klenow fragment of *E. coli* DNA polymerase in an 80μL reaction mixture consisting of the 40μL annealed product, 4μL 10×annealing buffer, 5.6μL 10mM deoxyribonucleotide triphosphates, 1.6μL 0.1M DTT, and 4.8μL Klenow fragment (5U/μL) at 37°C for 30min, at 65°C for 10min, and at room temperature for 10min.

#### *Amplification of the random insert*

A master mix was prepared consisting of 110μL of 10×PCR buffer (200mM Tris-HCl, pH 8.3, 250mM KCl, 15mM MgCl<sub>2</sub>, and 0.5% Tween-20), 200pmol each of

MB567 and MB489, 4.4 $\mu$ L of 10mg/mL bovine serum albumin, 5.5 $\mu$ L of 10mM deoxyribonucleotide triphosphates, and 4.4 $\mu$ L of Taq polymerase (5U/ $\mu$ L). The extended product (16 $\mu$ L or 5 $\mu$ L) and 27.8 $\mu$ L of the master mix were mixed to a final volume of 200 $\mu$ L and split into four tubes containing 50 $\mu$ L each. The 50 $\mu$ L mixtures were subjected to amplification by 30 cycles, with 1 cycle at 94°C for 1min, at 34°C for 2min, and followed with a 7min extension at 72°C. Amplification of the 153-bp insert was confirmed by gel electrophoresis.

#### *Construction of recombinant UPRT variants*

The original *Xho*I site in the vector backbone was removed by digestion with *Xho*I, blunt ended and re-ligated to construct the vector carrying the inactive or dummy gene. Site directed mutagenesis using two oligonucleotides, MB567 and MB568 (Table 5.1), was used to introduce another *Xho*I site upstream the randomized regions. The UPRT gene was inactivated by introducing double stop codons and an *Mlu*I site in the middle of the uracil active site using two oligonucleotides (MB569 and MB570 – Table 5.1). This was done to reduce the presence of wild-type UPRT in the selection. The resulting inactivated UPRT was designated as 'pETHT:UPRT-dummy'. Following digestion with *Xho*I and *Eco*RI, the gel-purified insert was cloned into the dummy vector digested with the same restriction enzymes.

#### *Transformation of E. coli BM604(DE3) and positive selection*

The ligated product was subjected to ethanol precipitation and approximately 5 $\mu$ L of the ligated product was electroporated into 40 $\mu$ L of electrocompetent *E. coli* BM604(DE3) and then shaken at 37 °C for 1h in 1mL of SOC medium (3g of bactopectone, 2.5g of yeast extract, 1M NaCl, 1M KCl, 5mM MgSO<sub>4</sub>, 5mM MgCl<sub>2</sub>, and 1.8% glucose per liter). The transformation mixture was concentrated by pelleting, resuspended in 100 $\mu$ L of 0.9% NaCl, and plated at various volumes onto 2 $\times$ YT rich medium and UPRT selection media [For 1L – 1.92g yeast synthetic (-

uracil), 100µl CaCl<sub>2</sub>, 1mM MgSO<sub>4</sub>, 11mM glucose, 22mM KH<sub>2</sub>PO<sub>4</sub>, 9mM NaCl, 19mM NH<sub>4</sub>Cl, 47mM Na<sub>2</sub>HPO<sub>4</sub>, uracil (10mg/l), thiamin (1mg/l), biotin (1mg/l)] containing carbenicillin (carb) at 50µg/ml]<sup>13</sup>. Growth on UPRT selection media requires the presence of a functional UPRT, while 2×YT medium was used to determine the total number of transformants. The 2×YT plates were incubated at 37°C overnight, and UPRT selection plates were incubated at 37°C for approximately 36h. Transformants from the UPRT selection plates were picked and re-streaked onto fresh UPRT selection plates to confirm the phenotype.

#### *Selection of 5FU sensitive mutants*

Functional UPRT variants identified by the positive selection described above were streaked onto UPRT selection media supplemented with 5FU at 40µg/mL, a sublethal dose for wild-type UPRT, and incubated for approximately 36h at 37°C to determine the ability of the mutants to confer 5FU sensitivity. Colonies unable to grow on the 5FU plates were selected from the control plates and subjected to additional rounds of negative selection at decreasing 5FU concentrations (20, 2 and 0.5µg/mL). Plasmid DNA of the UPRT variants was isolated, and the randomized region was sequenced using the MB560 oligonucleotide at the core sequencing laboratory of Washington State University.

#### **Protein expression and purification**

*E. coli* BL21(DE3) harboring pETHT:UPRT, pETHT:3662, pETHT:3802 or pETHT:4312 were grown at 30°C in M9ZB [For 1L – 10g Bacto tryptone, 5g NaCl, 100µl CaCl<sub>2</sub>, 1mM MgSO<sub>4</sub>, 11mM glucose, 22mM KH<sub>2</sub>PO<sub>4</sub>, 9mM NaCl, 19mM NH<sub>4</sub>Cl, 47mM Na<sub>2</sub>HPO<sub>4</sub>] containing carbenicillin (carb) at 50µg/ml. Five ml of overnight culture was transferred to 500ml of M9ZB media and the cultures grown at 30°C until an OD<sub>600</sub> of 0.2 – 0.25 was reached. Cells were collected and cooled on ice for 15-30min and then centrifuged at 4000rpm for 10min at 4°C (Beckman JLA-10.500).

Cells were lysed by adding 17.5mL lysis buffer (50mM NaH<sub>2</sub>PO<sub>4</sub>, 300mM NaCl, 10mM imidazole at pH 8.0) and lysozyme at 1mg/mL and incubated on ice for 30min and further subjected to sonication with six-10sec bursts with a 10sec cooling period between bursts. To pellet cellular debris, the lysate was centrifuged at 9000rpm (Beckman JA-17) for 20-30min at 4°C. Cleared lysate was produced by filtering the lysate through 0.2µM Supor<sup>®</sup> Membrane Low Protein Binding (PALL-Life Sciences, East Hills, NY). Protein was purified using a Qiagen Ni-NTA Spin Kit (Valencia, CA) under native conditions as specified by the manufacturer. For affinity purification, 1mL of Ni-NTA slurry was added to 4mL cleared lysate and gently mixed by shaking at 4°C for 60min. The Ni-NTA resin/cleared lysate mixture was added to a column and flow-through fractions were collected. The resin was subjected to washing by adding 8mL of wash buffer (50mM NaH<sub>2</sub>PO<sub>4</sub>, 600mM NaCl, and 20mM imidazole at pH 8.0) three times. Bound protein was eluted by adding 4 aliquots of 500µl elution buffer (50mM NaH<sub>2</sub>PO<sub>4</sub>, 300mM NaCl, and 250mM imidazole at pH 8.0). The elution fractions were dialyzed against dialysis buffer (50mM NaCl, 50mM Tris at pH 7.5) at 4°C. After dialysis, the samples were collected and stored at -20°C. Protein concentrations were quantified by the BCA method using reagents supplied by Bio-Rad (Hercules, CA). Known concentrations of bovine serum albumin were used as standards and used to generate calibration curves according to the manufacturer's instructions.

### **Enzyme assays**

The standard assay was used to measure UPRTase activity in the direction of UMP synthesis as adapted from Lundegaard *et al.*,<sup>14</sup>. Briefly, the assay mixture (15µl) contained 20mM Tris/HCl pH 8.5, 5mM MgCl<sub>2</sub>, 1mM GTP, 1mM phosphoribosyl pyrophosphate (PRPP) and a specified amount of wild-type or mutant UPRT enzyme. The mixture was incubated at 37°C for 5min, and the reaction was started by the

addition of various concentration of [<sup>14</sup>C]-Uracil (specific activity, 52mCi/mmol) or [<sup>14</sup>C]-5FU (specific activity, 57.2mCi/mmol) (time = 0). The reaction mixture was then incubated for 30min and then stopped by adding 5µl of 0.33M formic acid. The entire samples were applied to the center of DE81 whatman filter paper. The discs were washed with running deionized water to remove unbound [<sup>14</sup>C]-Uracil or [<sup>14</sup>C]-5FU for at least 10min. The discs were then dried completely and the amount of radioactive retained, i.e., phosphorylated radiolabeled substrates [<sup>14</sup>C]-UMP or [<sup>14</sup>C]-5FUMP, was detected using a scintillation counter. Data were plotted as the double reciprocal of velocity versus substrate concentration and the intercepts values used to determine  $K_m$  and  $V_{max}$ . These values were used to calculate the  $k_{cat}$  from the double reciprocal plot data as per active site (one active site per monomer).

### **Introducing UPRT mutants into bCD/UPRT or 1525/UPRT fusion constructs**

Site-directed mutagenesis was done to introduce amino acid substitutions from UPRT mutants 3662, 3802 and 4312 into pCDNA:1525/UPRT. To introduce amino acid substitutions from mutant 3662, 3802, and 4312 into pCDNA:1525/UPRT, oligonucleotides MB626-627, MB628-629, and MB632-635 (Table 5.1) were used, respectively. DNA sequence analysis confirmed the presence of correct mutations. The resulting plasmids were designated pCDNA:1525/3662, pCDNA:1525/3802, and pCDNA:1525/4312. These plasmids were used to generate stable transfectants in a rat C6 glioma cell line as described above. The stable transfectants were then subjected to *in vitro* 5FC sensitivity assay and bystander experiments as described above.

**Table 5.1.** List of oligonucleotides

MB455	5'-GG ATT GAT CTG CAA ATC GCC GCT TTC CCT CAG G-3'
MB456	5'-C CTG AGG GAA AGC GGC GAT TTG CAG ATC AAT CC-3'
MB457	5'-C TTT GGT CAC GAT GAT GTC TGC GGT CCG TGG TAT-3'
MB458	5'-ATA CCA CGG ACC GCA GAC ATC ATC GTG ACC AAA G-3'
MB488	5'-CAA AGG AGA AAG ACC ATG GAG ATC GTG GAA GTC AAA C-3'
MB489	5'-CTT AAA GTC GGC TTT AAT GAA TTC TAT TCT TTA TTT CGT ACC-3'
MB560	5'-GAG CGT ATG GCG CTG ATC GTT G-3'
Mb567	5'-GGT ATC GCT GCG CTC GAG AAA GCG CAC-3'
MB568	5'-GTG CGC TTT CTC GAG CGC AGC GAT AAC-3'
MB569	5'-GAG CAC GGA TAA ATT ATT ACG CGT CTC GGC TAG GCC GGT G-3'
MB570	5'-C ACC GGC CTA GCC GAG ACG CGT AAT AAT ATT TCC GTG CTC-3'
MB571	5'-GGT ATC GCT GCG CTC GAG AAA GCG CAC CCG GAC GTC GAA CTG TAT ACC GCA TCG ATT GAT CAG GGA CTG AAC GAG CAC GGA-3'
MB572	5'-GAG CTC GAA TTC TAT TCT TTA TTT CGT ACC AAA GAT TTT GTC ACC GGC ATC GCC GAG GCC CGG AAT AAT GTA TCC GTG CTC GTT CAG TCC-3'
MB626	5'-GGA TAC ATT AAT TCG AGC CTA GGC GAT GCC GGT GAC-3'
MB627	5'-GTC ACC GGC ATC GCC TAG GCT CGA ATT AAT GTA TCC-3'
MB628	5'-GGA TAC ATT GTT CCT GGC CTT GGA GAT GCC GGT TAC AAA ATA TTG GGT ACG AAA TAA-3'
MB629	5'-TTA TTT CGT ACC CAA TAT TTT GTA ACC GGC ATC TCC AAG GCC AGG AAC AAT GTA TCC-3'
MB632	5'-C GAG CAC GGA TCC ATT GTT CCG GGC CTC GGC-3'
MB633	5'-GCC GAG GCC CGG AAC AAT GGA TCC GTG CTC G-3'
MB634	5'-GGC GAT GCC GTT GAA AAT ATC CTT GGT ATC AAA TAA GCT TGC-3'
Mb635	5'-GCA AGC TTA TTT GAT ACC AAG GAT ATT TTC AAC GGC ATC GCC-3'

## RESULTS

### *In vitro* prodrug-sensitivity assay of bCD/UPRT and mutant fusion 1525/UPRT

Mammalian expression vectors (pCDNA backbone) encoding bCD, 1525, UPRT, bCD/UPRT, and 1525/UPRT were constructed as previously described and used to transfect rat C6 glioma cells. Immunoblots of stable transfectants revealed the presence of bCD at around 48kDa when the anti-bCD serum was used, and UPRT at around 27kDa when anti-UPRT serum was used. These results are in accord with the predicted molecular masses for each protein. The fusion proteins cross-reacted with both anti-sera at the predicted molecular mass of approximately 75kDa and relatively equivalent protein levels were observed (data not shown). Pools of stable transfectants were exposed to 5FC ranging from 0-20mM. Representative results of the 5FC sensitivities displayed by the wild-type and mutant fusion constructs are shown in Figure 5.2. Little to no toxicity was observed with empty vector at lower 5FC doses, however, above 10mM 5FC, an inherent cytotoxicity is observable in the glioma cell line. As expected, mutant 1525 exhibited strong tumor killing activity, as shown by a low  $IC_{50}$  value of approximately 0.5mM. The  $IC_{50}$  for the wild-type fusion bCD/UPRT was 1mM 5FC and the wild-type fusion thus conferred 5FC sensitivity in this cell line as indicated by a reduction in  $IC_{50}$  of approximately 5-fold compared to the wild-type bCD  $IC_{50}$  value at 4mM 5FC. Mutant fusion 1525/UPRT displayed the lowest  $IC_{50}$  value of approximately 0.1mM 5FC, this was approximately 4-, 10-, and 90-fold lower compared to mutant 1525, wild-type bCD/UPRT, and wild-type bCD, respectively.

### *In vitro* bystander activity analysis of bCD/UPRT and 1525/UPRT

*In vitro* bystander analysis was performed as described in the Materials and Methods section. Figure 5.2 shows representative results as percent survival from one experiment. This experiment was performed at least three times using different

pools of transfectants with similar results. In the presence of 5mM 5FC, results indicate that mutant 1525 demonstrated the strongest bystander activity as only ~10% of tumor cells expressing 1525 were sufficient to induce 40% cell killing. This is a significant improvement over wild-type bCD alone, where bystander killing activity was non-existent at this lower dose of 5FC. The 1525/UPRT fusion demonstrated little to no bystander activity as ~50% cells expressing fusion proteins only induced about 50% of tumor cell killing. Similar to 1525/UPRT, the bCD/UPRT fusion appeared to also have bystander activity as approximately 70% cell transduction only resulted in 50% tumor ablation.

#### *Construction of random library and mutant selection*

To create UPRT variants with increased activity to 5FU, 17 codons (Y192, I193, I194, P195, G196, L197, G198, D199, A200, G201, D202, K203, I204, F205, G206, T207, K208) were subjected to regio-specific, partially randomizing mutagenesis as described in the Materials and Methods section. Identification of functional UPRT variants with enhanced 5FU activity involved a two-step selection procedure. First, functional UPRT mutants were selected for preservation of catalytic activity, based on their ability to confer growth on UPRT plates, under conditions that require functional UPRT activity for viability. Second, the functional variants were screened on UPRT plates supplemented with various concentrations of 5FU. The sublethal dose, or the highest concentration that restricts the growth of wild-type UPRT is 40 $\mu$ g/mL 5FU. Any mutant with increased 5FU activity will not be viable on UPRT plates supplemented with the sublethal concentration of 5FU. Colonies were sequentially streaked onto plates containing 40 to 0.5 $\mu$ g/mL 5FU to identify the best variants within the library pool. From an estimated total of one million transformants, approximately 4500 colonies were identified as UPRT-positive based on their ability to grow uracil-containing plates. Of the 4500 UPRT-positive clones,



40, 3, and 1 variants conferred sensitivity at 20, 2, and 0.5 $\mu$ g/mL 5FU, the lowest effective 5FU concentration used in the negative selection, respectively. Plasmid DNA from colonies from the nonselective and selective plates was isolated and sequenced in order to evaluate the library diversity, along with identifying which substitutions are tolerated. Sequence analysis of the two variants (designated 3662 and 3802) that conferred sensitivity at 2 $\mu$ g/mL 5FU revealed that mutant 3662 had three substitutions at I194N, P195S, and G196S and that mutant 3802 also had three substitutions at I194V, D202Y and F205L. DNA sequence analysis of the third mutant, mutant 4312 which conferred the greatest sensitivity at 0.5 $\mu$ g/mL 5FU, revealed that this mutant had five amino acid substitutions at Y192S, I194V, D202Q, K203N, F205L, and T207I.

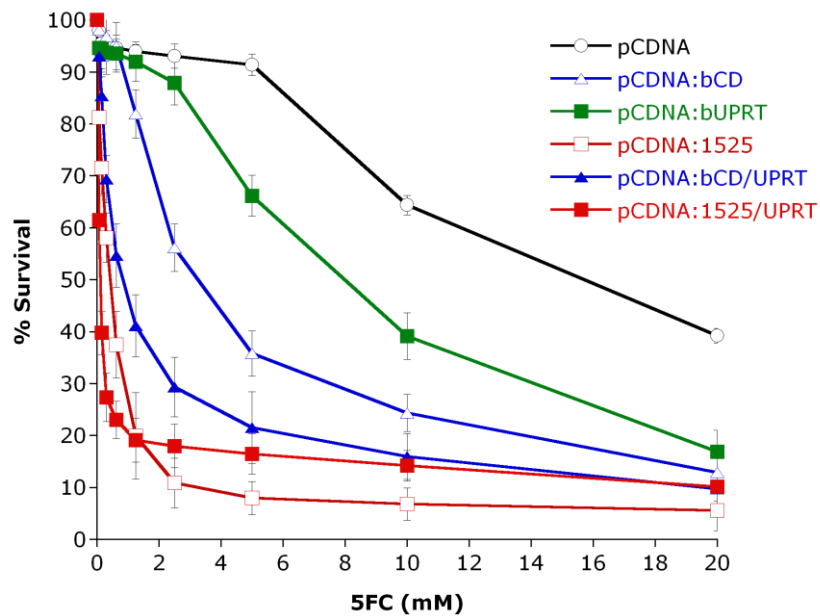


**Figure 5.2.** *In vitro* response of fusion CD/UPRT to 5FC in rat C6 glioma cells. Pools of stable transfectants containing empty vector (pCDNA), pCDNA:bCD, pCDNA:bUPRT, pCDNA:1525, pCDNA:bCD/UPRT, and pCDNA:1525/UPRT were evaluated for 5FC sensitivity as described in the Materials and Methods section. After seven days of 5FC treatment, growth inhibition was determined by staining with Alamar Blue and fluorescence recorded at 530/590nm. Each data point (mean $\pm$ SEM, n=3 performed with at least 16 replicates) is expressed as a percentage of the value for control wells with no 5FC treatment.

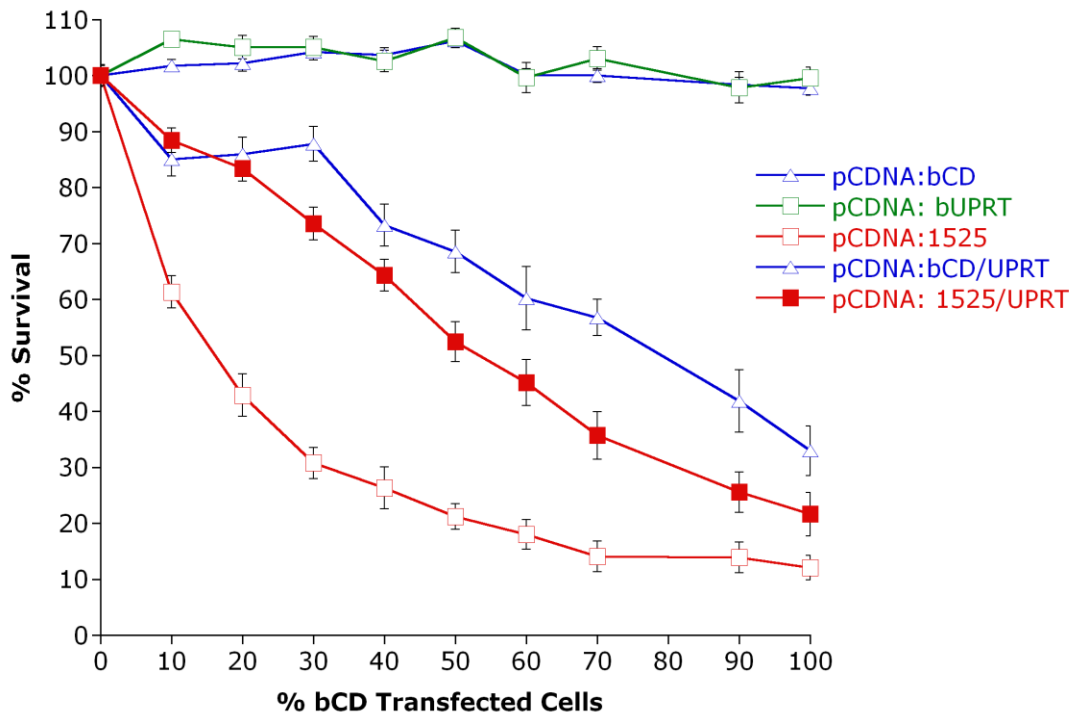


**Figure 5.3.** *In vitro* bystander response of fusion CD/UPRT to 5FC in rat C6 glioma cells. Pools of stable transfectants containing empty vector (pCDNA) were mixed at different ratios with cells harboring pCDNA:bCD, pCDNA:bUPRT, pCDNA:1525, pCDNA:bCD/UPRT, or pCDNA:1525/UPRT. Mixed cells were evaluated for 5FC sensitivity as described in Materials and Methods section. After seven days of 5FC treatment, the growth inhibition was determined by staining with Alamar Blue and fluorescence recorded at 530/590nm. Each data point (mean±SEM, n=3 performed with at least 16 replicates) is expressed as a percentage of the value for control wells with no 5FC treatment.

#### Enzyme kinetics

All proteins were purified by nickel affinity chromatogram to near homogeneity (data not shown). Purified wild-type and mutant UPRT enzymes were characterized for their kinetic parameters towards uracil and 5FU using a filter binding assay adapted from Erbs *et al.*<sup>15</sup>. The optimal substrate concentration and enzyme amounts were determined for each substrate. With uracil as substrate, mutant 3662, 3802 and 4312 displayed 51-, 128.2- and 161-fold increases in  $K_m$ , respectively, compared to wild-type UPRT (Table 5.2). However, the turnover number ( $k_{cat}$ ) for mutant 3662 was decreased by 0.6-fold and for mutant 3802 and 4312 was increased by 18- and 1.57-fold, respectively, compared to wild-type UPRT.

The increase  $K_m$  and decrease in  $k_{cat}$  values towards uracil that mutant 3662 displayed translates to approximately 73.5-fold lower overall enzyme catalytic efficiency ( $k_{cat}/K_m$ ). The  $k_{cat}/K_m$  values towards uracil for mutant 3802 and 4312 were also decreased by approximately 7.35- and 105-fold, respectively, when compared to wild-type enzyme. When 5FU was used as substrate, mutant 3662 displayed very poor activity as indicated by a 48.5-fold increase and a 2.6-fold decrease in  $K_m$  and  $k_{cat}$  values, respectively, totaling in about a 130-fold decrease in  $k_{cat}/K_m$ . The two other variants, 3802 and 4312, demonstrated higher  $K_m$  and  $k_{cat}$  values, translating to a modest improvement in overall enzyme catalytic efficiency towards 5FU as shown by 1.7- and 1.3-fold increases in  $k_{cat}/K_m$  when compared to wild-type enzyme value (Table 5.2).

#### *In vitro prodrug-sensitivity assay of UPRT mutants*

The double mutant fusion constructs, consisting mutant bCD 1525 and mutant UPRTs (3662, 3802, and 4312) were constructed using QuikChange site directed mutagenesis and were used to create stably transfectants in rat C6 glioma cells. *In vitro* 5FC-mediated cytotoxic assays in rat C6 glioma cells by all samples are shown Figure 5.4. Little to no toxicity was observed with empty vector at lower 5FC doses, however, above 10mM 5FC, an inherent cytotoxicity is observable in the glioma cell line. As expected and in line with previous reports, mutant 1525 exhibited significant tumor killing activity, as seen by the lowest  $IC_{50}$  value. The 1525/UPRT fusion conferred 5FC sensitivity in this cell line as indicated by a reduction in  $IC_{50}$  value between 4- and 5-fold compared to mutant 1525 alone. Surprisingly, the mutant fusion constructs, 1525/3662, 1525/3802, and 1525/4312, did not show any enhancement in tumor killing activity when compared to 1525/UPRT or mutant 1525 alone. The 1525/3662 from displayed an  $IC_{50}$  value of

approximately 5mM 5FC and both 1525/3802 and 1525/4312 exhibited IC<sub>50</sub> values of approximately 2.5mM 5FC.

**Table 5.2.** Kinetic parameters of wild-type and mutant UPRTs.

	<b>WT</b>	<b>3662</b>	<b>3802</b>	<b>4312</b>
<b>Uracil</b>				
K <sub>m</sub> (μM)	2.405 (0.19) <sup>a</sup>	123.1 (36.5)	308.3 (54.65)	388.4 (19.18)
k <sub>cat</sub> (s-1)	0.035 (0.0036)	0.0212 (0.005)	0.65 (0.243)	0.055 (0.0144)
k <sub>cat</sub> /K <sub>m</sub> (μM <sup>-1</sup> /s <sup>-1</sup> )	0.0147 (0.0014)	0.0002 (9x10 <sup>-5</sup> )	0.002 (0.004)	0.00014(3x10 <sup>-5</sup> )
<b>5FU</b>				
K <sub>m</sub> (μM)	1.246 (0.19)	60.5 (2.17)	14.9 (3.17)	3.524 (0.96)
k <sub>cat</sub> (s-1)	0.014 (0.00065)	0.0054 (0.003)	0.33 (0.1)	0.056 (0.023)
k <sub>cat</sub> /K <sub>m</sub> (μM <sup>-1</sup> /s <sup>-1</sup> )	0.012 (0.0014)	9.2x10 <sup>-5</sup> (4.7x10 <sup>-5</sup> )	0.02 (0.0045)	0.014 (0.0021)
<b>Relative specificity<sup>b</sup></b>	<b>0.45</b>	<b>0.29</b>	<b>0.89</b>	<b>0.99</b>

<sup>a</sup> Standard error mean is in parenthesis

<sup>b</sup> Relative specificity = k<sub>cat</sub>/K<sub>m</sub> (5FU) / [k<sub>cat</sub>/K<sub>m</sub>(5FU) + k<sub>cat</sub>/K<sub>m</sub>(U)]

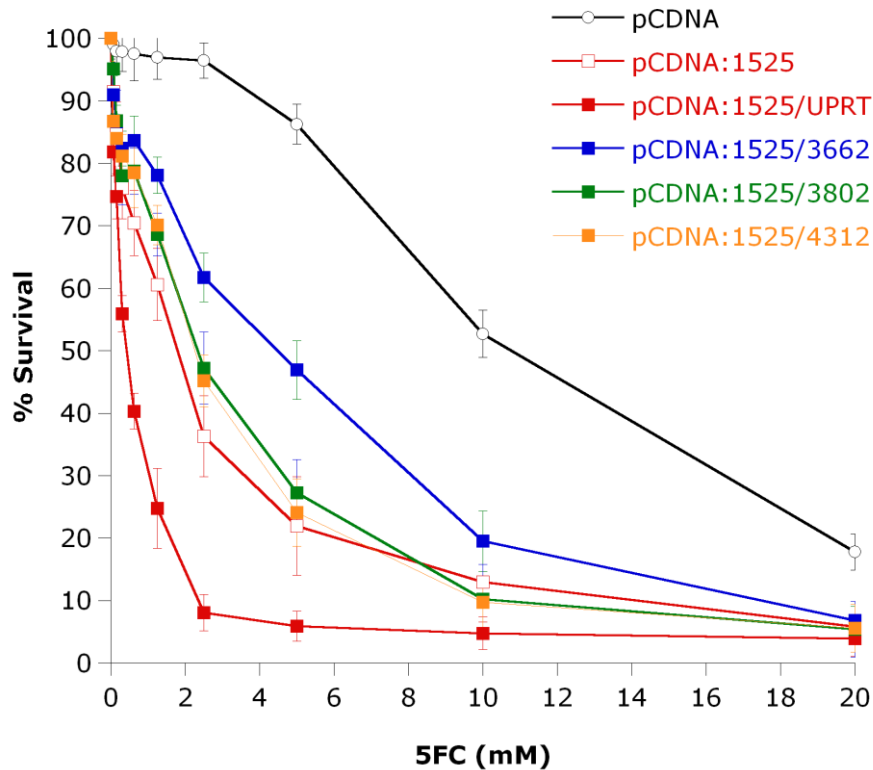


**Figure 5.4.** *In vitro* cytotoxic assays of UPRT mutants. Pools of stable transfectants containing empty vector (pCDNA), pCDNA:1525, pCDNA:1525/UPRT, pCDNA:1525/366, pCDNA:1525/3802, and pCDNA:1525/4312 were evaluated for 5FC sensitivity in rat C6 glioma cells as described in the Materials and Methods section. After seven days of 5FC treatment, the growth inhibition was determined by staining with Alamar Blue and fluorescence recorded at 530/590nm. Each data point (mean±SEM, n=3 performed with at least 16 replicates) is expressed as a percentage of the value for control wells with no 5FC treatment.

## Discussion

Suicide gene therapy offers a more selective targeting treatment for cancer cells and is more attractive than systemic administration of chemotherapy that often results in undesired negative side effects. One of the most widely studied and used suicide enzyme/prodrug system is bCD with 5FC. The enzyme bCD is able to deaminate 5-FC to form the toxic anticancer drug 5FU. However, many factors limit the efficacy of this therapy including rapid turnover and clearance of 5FC in serum, inefficient gene delivery efficiency such that only a small population of tumor cells expresses the suicide gene, and poor enzyme activity towards the prodrug coupled with efficient competition for the enzyme's active site by the intracellular pool of cytosine<sup>6,16,17</sup>. Due to these limitations, high doses of 5FC are needed to achieve clinically beneficial results in cancer patients and often cause unwanted side effects, such as gastrointestinal complication and severe bone marrow depression, primarily due the presence of microbial flora in the intestinal tract that encode CD<sup>7</sup>. As a means to overcome these obstacles, we have previously created novel bCD variants with significantly improved kinetic preferences towards 5FC (Fuchita *et al.*, submitted). We employed regio-specific random mutagenesis to introduce multiple amino acid substitutions in two regions lining the active site of bCD and used both positive and negative selection in *E. coli* to identify variants with the ability to confer enhanced 5FC sensitivity and bystander killing effect to three cancer cell lines *in vitro* and *in vivo*.

Another strategy to enhance therapeutic response of bCD towards 5FC is by performing pathway engineering, where two enzymes in one particular drug activation pathway are combined together as one functional fusion protein. Bacterial UPRT can be utilized in such a strategy or as a single suicide gene because of its ability to convert 5FU to 5FUMP. The premise behind pathway engineering is to guarantee that the activation of 5FC does not lead to an accumulation of ineffective compounds because of the low activity of endogenous enzymes responsible for complete activation of the drug. This is particularly important in the 5FC pathway because of the absence of UPRT in mammalian cells. In human cells, without the presence of exogenous CD and/or UPRT, 5FU is converted to toxic antimetabolites via an indirect pathway and must bypass several steps (Figure 5.1). In a previous pathway engineering approach, we successfully combined HSVTK and mouse GMK (MGMK/HSVTK) activities in a fusion protein and were able to achieve significantly improved reduction in the IC<sub>50</sub> value (~175-fold) for GCV in tumor cell killing<sup>11</sup>. Utilizing the same strategy, other studies have also shown that fusion CD/UPRT demonstrated a significant improvement in tumor killing activity *in vitro* and in an animal tumor model compared to the use of CD alone when 5FC was administered<sup>10,15</sup>.

The purpose of this study is to further augment 5FC-mediated toxicity of wild-type fusion CD/UPRT by replacing the wild-type bCD enzyme with the previously characterized bCD mutant 1525. We constructed fusion 1525/UPRT and analyzed its tumor killing activity *in vitro* in rat glioma cells (Figure 5.2). Results from *in vitro* cytotoxicity assays indicated that a slight improvement in cell killing was seen in cells stably transfected with 1525/UPRT when compared to cells harboring 1525, as indicated by approximately a 4-fold reduction of IC<sub>50</sub> value for 5FC. Approximately 10- and 90-fold reductions in IC<sub>50</sub> values for 5FC were also observed in cells harboring wild-type bCD/UPRT and wild-type bCD, respectively,

when compared to cells expressing 1525/UPRT. Although 1525 mediated cytotoxicity achieved a 9-fold reduction in IC50 compared to wild-type bCD, when fused to UPRT only a modest further improvement (4-fold) was observed. This observation led us to suggest that the rate limiting step in this drug activation pathway may have shifted from the initial step carried out by bCD to the introduced second step, UPRT. Because mutant 1525 generates higher levels of 5FU compared to wild-type bCD enzyme (Fuchita *et al.*, submitted), we suspect the escalated levels of 5FU might overwhelm UPRT and consequently result in inefficient conversion of 5FU to 5FUMP (i.e., a bottleneck). In addition, the modest improvement in tumor killing of 1525/UPRT did not translate to improved bystander activity. Surprisingly, the 1525/UPRT fusion exhibited a weaker bystander killing activity when compared to mutant 1525 (Figure 5.3). One possible explanation for this relies on the mode of action of 5FC-mediated bystander effect. Unlike the GCV-mediated bystander effect where gap junctions are necessary to transfer phosphorylated GCV to neighboring cells, the transfer of 5FU does not depend on gap junctions as it can passively diffuse across cell membranes. This is a huge advantage because broader and greater bystander effect can still be achieved in certain types of tumors that have been reported to down regulate intracellular gap junction communication and thus have disorganized and non-functional gap junctions<sup>5,18,19</sup>. However, when UPRT is present, it allows direct conversion of 5FU to 5FUMP and, because 5FUMP cannot passively diffuse cell membrane, the bystander effect becomes reliant on gap junctions.

One way to overcome the reduced bystander effect and the inefficient conversion of 5FU to 5FUMP observed is to generate UPRT mutants with enhanced activity towards 5FU. Mutants with superior 5FU activity may eliminate the bottleneck problem resulting from higher levels of 5FU generated by mutant 1525 by producing higher amounts of 5FUMP and this in turn may provide a broader

bystander effect as well. Towards that end, we employed regio-specific random mutagenesis and, coupled with genetic complementation in *E. coli*, identified UPRT variants with increased activity towards 5FU. Three UPRT mutants, constructs 3662, 3802, and 4312, were identified to enhanced confer 5FU sensitivity to *E. coli*. Kinetic analyses of these three mutants suggest that only two mutants (3802 and 4312) displayed a modest shift in substrate preferences toward 5FU (Table 5.2). Mutant 3802 and 4312 exhibited about 2- to 3-fold increases in relative specificity towards 5FU. Mutant 3662, surprisingly, displayed lower activity towards uracil and 5FU compared to wild-type enzyme. Site-directed mutagenesis kit was used to introduce mutant 3662, 3802, and 4312 into the 1525/UPRT construct and the resulting plasmids were used to stably transfect rat C6 glioma cells. When tested for 5FC-mediated toxicity, however, no improvement in tumor killing was observed. Because kinetic analyses suggested that mutant 3662 displayed weak activity to 5FU, we did not expect to see any improvement in tumor killing. However, a higher IC<sub>50</sub> value (5mM 5FC) was observed from cells expressing fusion 1525/3662. Interestingly, although kinetic analyses suggested that both mutants 3802 and 4312 appeared to have a slight shift in substrate preferences towards 5FU, *in vitro* data showed that no improvement in 5FC-mediated toxicity was detected in cells stably transfected with 1525/3802 and 1525/4312 (Figure 5.4). It is possible that the slight kinetic improvements seen in mutant 3802 and 4312 were not sufficient to enhance 5FC-mediated cell killing. Other insights to this problem and future work that may provide answers will be discussed in the next section.

## **Future Work**

Our *in vitro* data suggested that replacing wild-type UPRT with mutant UPRT was not advantageous. By introducing mutations in UPRT gene, changes in the architecture and the folding of the protein may have occurred. When UPRT variants



are used in combination with mutant 1525 in a fusion construct, inappropriate protein folding problem may result in reduced prodrug activity. One way to confirm the possibility of problem folding problem is by performing circular dichroism to evaluate protein folding properties of these mutants. Another strategy is by solving the X-ray crystal structure of the novel fusion enzymes, particularly the fusion 1525/3802 and 1525/4312, which should allow us to observe the consequences of amino acids substitutions that were introduced to UPRT gene and how the two enzymes interact/fold together. Another indirect way to verify that the reduced prodrug activity only occurs when UPRT mutants are used in the fusion constructs is by analyzing single gene construct of 3802 and 4312 in combination with 5FU. Future work to generate mammalian expression vector expressing mutant 3802 and 4312 will be performed. Once stable transfectants are created, *in vitro* cytotoxic assays will be done to ascertain whether single UPRT mutant constructs (pCDNA:3802 and pCDNA:4312) confer enhanced sensitivity to 5FU in rat C6 glioma cells. In addition, because we only saw a modest improvement in relative specificity from mutant 3802 and 4312, there is clearly room for improvement. X-ray crystal structures of mutant 3802 and 4312, in particular, may provide further insight into which amino acids play a major role in substrate/prodrug binding. In turn we can also speculate what amino acid substitutions may favorably result in the enhancement of prodrug binding ability. Moreover, we can also introduce single amino acid substitution into residues that may be important in substrate binding and catalysis. Furthermore, by closer examination of UPRT crystal structure, we can locate more appropriate regions/sites to mutate so that UPRT mutants with even greater activity to 5FU can be generated. Molecular modeling of UPRT crystal structure may also be used to predict the impact of key mutations on substrate specificity. Enzymes with high catalytic activity can impact cell killing efficacy directly by generating more active prodrug or indirectly through a broader bystander

effect. Ultimately, the use of enzymes with high catalytic activity allows lower prodrug doses to be administered and, therefore, reduces side effects.

## References

1. Austin, E. A. & Huber, B. E. A first step in the development of gene therapy for colorectal carcinoma: cloning, sequencing, and expression of *Escherichia coli* cytosine deaminase. *Mol Pharmacol* **43**, 380-387 (1993).
2. Ireton, G. C., McDermott, G., Black, M. E. & Stoddard, B. L. The structure of *Escherichia coli* cytosine deaminase. *J Mol Biol* **315**, 687-697 (2002).
3. Longley, D. B., Harkin, D. P. & Johnston, P. G. 5-Fluorouracil: mechanisms of action and clinical strategies. *Nat Rev Cancer* **3**, 330-338 (2003).
4. Moolten, F. L. Tumor sensitivity conferred by inserted herpes thymidine kinase genes: paradigm for a prospective cancer control strategy. *Cancer Res* **46**, 5276-5281 (1986).
5. Greco, O. & Dachs, G. Gene directed enzyme/prodrug therapy of cancer: historical appraisal and future prospective. *J Cell Physiol* **187**, 22-36 (2001).
6. Trinh, Q. T., Austin, E. A., Murray, D. M., Knick, V. C. & Huber, B. E. Enzyme/prodrug gene therapy: comparison of cytosine deaminase/5-fluorocytosine versus thymidine kinase/ganciclovir enzyme/prodrug systems in a human colorectal carcinoma cell line. *Cancer Res* **55**, 4808-4812 (1995).
7. Vermes, A., Guchelaar, H. J. & Dankert, J. Flucytosine: a review of its pharmacology, clinical indications, pharmacokinetics, toxicity and drug interactions. *J Antimicrob Chemother* **46**, 171-179 (2000).
8. Mahan, S. D., Ireton, G. C., Stoddard, B. L. & Black, M. E. Alanine-scanning mutagenesis reveals a cytosine deaminase mutant with altered substrate preference. *Biochemistry* **43**, 8957-8964 (2004).
9. Mahan, S. D., Ireton, G. C., Knoeber, C., Stoddard, B. L. & Black, M. E. Random mutagenesis and selection of *Escherichia coli* cytosine deaminase for cancer gene therapy. *Prot Eng Des Sel* **17**, 625-633 (2004).
10. Tiraby, M. *et al.* Concomitant expression of *E. coli* cytosine deaminase and uracil phosphoribosyltransferase improves the cytotoxicity of 5-fluorocytosine. *FEMS Microbiology Letters* **167**, 41-49 (1998).
11. Willmon, C. L., Krabbenhoft, E. & Black, M. E. A guanylate kinase//HSV-1 thymidine kinase fusion protein enhances prodrug-mediated cell killing. *Gene Ther* **13**, 1309-1312 (2006).
12. Devanathan S, Willmon, C. L., Mahan, S. D. & Black, M. E. Engineering enzymes for improved cancer gene therapy. *Res. Adv. In Cancer* 315-326 (2002).
13. Andersen, P. A., Smith, J. M. & Mygind, B. Characterization of the upp gene encoding uracil phosphoribosyltransferase of *Escherichia coli* K12. *European Journal Biochemistry* **204**, 51-56 (1992).

14. Lundegaard, C. & Jensen, K. F. Kinetic mechanism of uracil phosphoribosyltransferase from *Escherichia coli* and catalytic importance of the conserved proline in the PRPP binding site. *Biochemistry* **38**, 3327-3334 (1999).
15. Erbs, P. *et al.* *In vivo* cancer gene therapy by adenovirus-mediated transfer of a bifunctional yeast cytosine deaminase/uracil phosphoribosyltransferase fusion gene. *Cancer Res* **60**, 3813-3822 (2000).
16. Nishiyama, T. *et al.* Antineoplastic effects in rats of 5-Fluorocytosine in combination with cytosine ceaminase capsules. *Cancer Res* **45**, 1753-1761 (1985).
17. Kievit, E. *et al.* Superiority of yeast over bacterial cytosine deaminase for enzyme/prodrug gene therapy in colon cancer xenografts. *Cancer Res* **59**, 1417-1421 (1999).
18. Carystinos, G. D. *et al.* Cyclic-AMP induction of gap junctional intercellular communication increases bystander effect in suicide gene therapy. *Clin Cancer Res* **5**, 61-68 (1999).
19. Vrionis, F. D. *et al.* The bystander effect exerted by tumor cells expressing the herpes simplex virus thymidine kinase (HSVtk) gene is dependent on connexin expression and cell communication via gap junctions. *Gene Ther* **4**, 577-585 (1997).

## CHAPTER SIX

### Summary

Although tremendous hurdles in the feasibility and therapeutic response of gene therapy have gradually been overcome in the past two decades, further advances to improve suicide gene therapy must be achieved before suicide gene therapy becomes a mainstream therapeutic approach for treating cancer. One key problem in gene therapy is achieving a delivery method that is tumor specific, efficient in delivering suicide gene(s), safe and not immunogenic. The task of perfectly targeting every cancerous cell in a complex system can be quite an undertaking and is yet to be fully realized with current delivery methods. To exacerbate this problem, wild-type suicide enzymes are known to display low activity towards their prodrugs and thus high doses of drugs must be administered to achieve clinically beneficial results and may consequently result in undesired negative side effects. One approach to alleviate this problem is to improve the suicide enzyme itself and this is the focus of the work described in the preceding chapters. When engineered suicide enzymes with improved activity towards their prodrugs are used to replace wild-type enzymes, lower doses of prodrugs could be administered to obtain the same or even better tumor cytotoxicity and subsequently unwanted side effects in patients could be greatly minimized. Additionally, with the generation of more active antimetabolites, greater and broader bystander effects should take place and ultimately leading to an enhanced tumor cell ablation.

In our laboratory, we employed three means to engineer suicide enzymes: regio-specific mutagenesis, pathway engineering and the combination of two. Wild-type Herpes Simplex Virus thymidine kinase (HSVTK) has poor activity towards its

prodrug, ganciclovir (GCV), and therefore high and toxic doses of GCV are needed to achieve significant tumor cell killing. Previously, mutant HSVTK enzymes, with exceptional GCV converting properties, were generated using regio-specific mutagenesis and were extensively evaluated *in vitro* and *in vivo*<sup>1-3</sup>. An additional aspect of engineering enzymes is by pathway engineering to ensure activation of the product does not lead to an accumulation of ineffective intermediates because of the low activity of other enzymes responsible for complete activation of the drug. In particular, it has been demonstrated that guanylate kinase (GMK) does not efficiently phosphorylate GCV-monophosphate (GCV-MP) to GCV-diphosphate (GCV-DP)<sup>4,5</sup>. Using pathway engineering, we combined HSVTK and mouse GMK (MGMK/HSVTK) activities in a fusion protein and were able to achieve significant reduction in the IC<sub>50</sub> value (~175-fold) for GCV in tumor cell killing<sup>6</sup>. When tested in an animal tumor model, however, the tumor growth inhibition of wild-type fusion MGMK/HSVTK was not quite as impressive as the *in vitro* studies suggested. Therefore, further steps were taken to augment its GCV-mediated cytotoxicity. By replacing wild-type HSVTK in the fusion construct with the previously characterized improved HSVTK mutants (mutant 30 and SR39), we were able to demonstrate that the mutant chimeric proteins created in that study exhibited a superior GCV-mediated toxicity and bystander killing activity at very low doses of prodrug (25- to 150-fold lower) *in vitro* and in an *in vivo* xenograft tumor model as compared to wild-type HSVTK/MGMK and their respective single gene constructs. The results reported here demonstrate that mutant chimeric proteins offer a significant advantage to the suicide gene therapy approach over that of the widely used wild-type HSVTK gene, previously characterized HSVTK mutants, or the previously created MGMK/HSVTK fusion construct (Chapter 2).

Further studies directed towards GMK and its activity towards GCV-MP may aid in better understanding the role of GMK in activating other anti-neoplastic agents

such as 6-thioguanine (6TG), which has been primarily used as a treatment for childhood and adult leukemia since the 1950s<sup>7</sup>. Intracellularly, 6-TG is activated by hypoxanthine-guanine phosphoribosyltransferase (HGPRT) to form 6-TG-monophosphate (6-TGMP), which is then further phosphorylated to 6-TG-diphosphate (6-TGDP) and 6-TG-triphosphate (6-TGTP) by GMK and nucleoside diphosphokinase, respectively<sup>8</sup>. Despite the wide application of 6-TG as an anti-leukemic agent, one major drawback is the development of drug resistance and subsequent treatment failure. Several mechanisms of resistance to 6-TG have been reported but a subset of drug resistant cells cannot be explained by those mechanisms. Because GMK is responsible for the conversion of 6-TGMP to 6-TGDP, we proposed that mutations in GMK could result in drug resistance. We reported three amino acid substitutions at serine 37 (S37) in mouse GMK displayed activity towards GMP but demonstrated a resistance phenotype towards 6-TGMP. Mutations in guanylate kinase, therefore, represent a previously undescribed mechanism for 6-TG resistance. Ultimately, a better understanding of the molecular factors that result in the loss of drug potency may lead to the development of improved dosing regimens and treatment options for patients (Chapter 3).

Another suicide enzyme that displays poor activity towards its prodrug is bacterial cytosine deaminase (bCD). Absent in mammals, bCD is being explored for use in suicide gene therapy due to its ability to convert the antifungal agent 5-fluorocytosine (5FC) to the potent antimetabolite, 5-fluorouracil (5FU)<sup>9-11</sup>. The low enzyme activity of bCD towards 5FC requires high doses of the drug and results in undesirable side effects primarily due the presence of microbes in the intestinal tract that encode CD. From earlier studies, residue D314 in wild-type bCD was shown to play a key role in substrate recognition<sup>12,13</sup>. Here we describe an expanded regio-specific random mutagenesis, targeting two key regions of the active site, and selection experiments that yielded enzyme variants with significant improvement in

5FC sensitization. From over a million bCD variants, only three bCD variants were found to have significant improvement in 5FU production. These three mutants were evaluated using enzyme kinetic analyses and then assayed in three cancer cell lines for 5FC sensitization, bystander effects and formation of 5FU metabolites. All variants displayed 18 to 19-fold shifts in substrate preference toward 5FC, a significant reduction in  $IC_{50}$  values and improved bystander effect compared to wild-type bCD. One mutant in particular, mutant 1525, consistently displayed the greatest improvement in tumor cell killing and bystander activity in three cancer cell lines examined and was selected for further evaluation in a xenograft tumor model. *In vivo* studies revealed that mutant 1525 was able to prevent tumor growth at lower doses of 5FC than is observed when tumor cells expressed wild-type bCD. Crystallographic analyses of this construct demonstrate the basis for improved activity towards 5FC. Structural studies revealed mutation at D317 allows the aspartate at 314 to swing away from the fluorinated substrate and therefore creating a neighboring cavity and reducing the local negative charge (Chapter 4).

As with the MGMK/HSVTK fusion protein, pathway engineering to combine bCD and uracil phosphoribosyltransferase (UPRT) resulted in enhanced tumor cytotoxicity *in vitro* and *in vivo*<sup>14,15</sup>. UPRT is an important enzyme involved in the pyrimidine salvage pathway, catalyzing the transfer of a ribosyl-phosphate group to uracil to form uridine-monophosphate. In the 5FC activation pathway, UPRT is also responsible for the conversion of 5FU to 5FU-monophosphate (5FUMP). Similar to CD, UPRT is absent in mammalian cells and present in fungi and bacteria. We took a further step aimed at improving prodrug-mediated toxicity by incorporating mutant 1525 into the fusion bCD/UPRT construct and analyzed the resulting mutant fusion construct, 1525/UPRT, for its *in vitro* cytotoxicity and bystander killing in rat glioma cells. Because 1525/UPRT offered only a modest increase in sensitivity toward 5FC and showed no improvement in regards to bystander killing effect, we hypothesized



that the conversion of 5FU to 5FUMP by UPRT became another rate limiting step in this drug activation pathway. To overcome this limitation, we performed region-specific random mutagenesis to generate UPRT mutants and, coupled with genetic complementation in *E. coli*, identified variants with increased activity towards 5FU. Three UPRT mutants, constructs 3662, 3802, and 4312, were identified to confer 5FU sensitivity to *E. coli*. Kinetic analyses suggested that only two mutants (3802 and 4312) displayed a modest shift in substrate preferences toward 5FU. *In vitro* analyses of fusion construct 1525/3662, 1525/3802, and 1525/4312 revealed that no improvement in tumor cytotoxicity was detected. Further investigation is needed to provide explanations to this problem. This work is discussed in detail in Chapter 5.

In summary, while HSVTK is widely used, there are two key reasons for optimizing additional suicide enzymes and novel fusion enzymes: 1) not all cancers are equally responsive to the same drug and 2) should treatment with one suicide gene fail, alternate suicide genes that the immune system has not been exposed to previously, could be used in a second round of therapy to ablate tumors. The identification of enzymes with enhanced or novel functions for suicide gene therapy of cancer is critical and has already accelerated the current effectiveness of this therapy. Such superior enzymes or fusion enzymes with exceptional prodrug converting properties will allow administration of lower and less toxic doses of prodrugs concomitant with improved tumor killing. Towards that end, we believe the mutant enzymes created in these studies will provide resources and are promising candidates for translational gene therapy studies. Ultimately, the application of such novel fusion enzymes will likely improve the clinical outcome of suicide gene therapy in cancer patients and compensate for the inefficiencies of current delivery methods.

### ***Future perspective***

Suicide gene therapy has had its ups and downs since it was first described more than 2 decades ago. Despite the vast preclinical information available that demonstrates the efficacy of suicide gene therapy to treat cancer, successes observed in preclinical studies have yet to be attained in clinical applications. Many limiting factors are responsible for this discrepancy, including insufficient gene transfer, rapid clearance of delivery vectors by hosts' immune system, and poor enzyme activity of suicide enzymes towards their prodrugs. Nevertheless, suicide gene therapy is maintaining momentum because it offers much safer and less toxic treatments than chemotherapy. However, it is reasonable to state that the field has been gradually moving towards combining suicide gene therapy with standard radiation, chemotherapy and/or surgery approaches. By combining suicide gene therapy with these treatments, reduced doses of chemotherapeutic/radiation can be administered to achieve complete tumor ablation while minimizing toxicity to normal cells.

In the future, advances in gene delivery systems particularly in the development of carrier cells, such as T or B cells, and stem (progenitor) cells to conceal viruses from the host immune system and to improve specific targeting to tumor site may be able to overcome the barriers of rapid viral clearance by hosts' immune system. Furthermore, two major benefits in using immune cell-mediated delivery lies in the enhanced tumoricidal activity and the capability to stimulate even more robust immune reaction caused by the carrier cell itself during therapy. The robust immune system stimulated by T or B cells-based therapy will be clinically beneficial in order to achieve complete tumor eradication in patients as well. Moreover, immune cells also easily travel throughout the circulatory system, a characteristic that makes them attractive for systemic delivery and in targeting metastatic tumor sites. Current research has also focused on the use of stem

(progenitor) cells due to their excellent tumor homing ability and support of viral replication. One particular subtype of stem cell with promising potential as a cell carrier is the mesenchymal progenitor cells (MPC). MPC are a subpopulation of bone marrow stromal cells that play a role in the maintenance and regeneration of connective tissues and also critical in hematopoiesis. Numerous characteristics such as simple isolation, easy *in vitro* culture under minimal growth conditions, susceptibility to *ex vivo* transduction, high metabolic activity, and ability to be delivered systemically make MPC feasible cellular vehicles. But even with carrier cell preferential targeting, only a small fraction of originally administered cells, and thus the oncolytic virus it would be carrying, actually reach targeted tumor sites. Therefore, future work to engineer carrier cells to express tumor-specific surface molecules is crucial in promoting higher levels of accumulation of infected carrier cells to tumor site. A successful surface molecule must possess unique anti-tumor characteristics to make it a capable candidate for tumor targeting. In addition, over the past two decades, these greater efforts have been supported by deeper understanding of the interplay between mammalian cells and their viral parasites. Complicated and delicate techniques to enhance the transduction efficiency, safety, and tumor-specific cytotoxicity of oncolytic viruses have been performed. And with advances this viral delivery field, highly sophisticated oncolytic viruses will continue to be generated as a means to overcome the barriers of adequate transduction and safety. With the future applications of such vectors and/or carrier cells, combined with the use of optimized enzyme/prodrug combinations with superior prodrug-mediated tumor cytotoxicity and bystander effect, it is anticipated that significant and reproducible clinical success using suicide gene therapy strategies will be realized sooner rather than later. The future of suicide gene therapy is bright and promising.

## References

1. Black, M. E., Newcomb, T. G., Wilson, H. M. & Loeb, L. A. Creation of drug-specific herpes simplex virus type 1 thymidine kinase mutants for gene therapy. *Proc Natl Acad Sci USA* 93, 3525-3529 (1996).
2. Black, M. E., Kokoris, M. S. & Sabo, P. Herpes simplex virus-1 thymidine kinase mutants created by semi-random sequence mutagenesis improve prodrug-mediated tumor cell killing. *Cancer Res* 61, 3022-3026 (2001).
3. Kokoris, M. S., Sabo, P. & Black, M. *In vitro* evaluation of mutant HSV-1 thymidine kinase for suicide gene therapy. *Anticancer Res* 20, 964 (2000).
4. Boehme, R. Phosphorylation of 9- $\beta$ -D-arabinofuranosylguanine monophosphate by *Drosophila melanogaster* guanylate kinase. *J Biol Chem* 258, 12346-12349 (1984).
5. Brady, W. A., Kokoris, M. S., Fitzgibbon, M. & Black, M. Cloning, characterization, and modeling of mouse and human guanylate kinases. *J Biol Chem* 271, 16734-16740 (1996).
6. Willmon, C. L., Krabbenhoft, E. & Black, M. E. A guanylate kinase//HSV-1 thymidine kinase fusion protein enhances prodrug-mediated cell killing. *Gene Ther* 13, 1309-1312 (2006).
7. Karran, P. & Attard, N. Thiopurines in current medical practice: molecular mechanisms and contributions to therapy-related cancer. *Nat Rev Cancer* 8, 24-36 (2008).
8. Sekulic, N., Shuvalova, L., Spangenberg, O., Konrad, M. & Lavie, A. Structural characterization of the closed conformation of mouse guanylate kinase. *J Biol Chem* 277, 30236-30243 (2002).
9. Niculescu-Duvaz, I. & Springer, C. J. Gene-directed enzyme prodrug therapy: a review of enzyme/prodrug combinations. *Expert Opin Investig Drugs* 6, 685-703 (1997).
10. Huber, B. E., Austin, E. A., Richards, C. A., Davis, S. T. & Good, S. S. Metabolism of 5-fluorocytosine to 5-fluorouracil in human colorectal tumor cells transduced with the cytosine deaminase gene: significant antitumor effects when only a small percentage of tumor cells express cytosine deaminase. *Proc Natl Acad Sci USA* 91, 8302-8306 (1994).
11. Mullen, C. A., Kilstrup, M. & Blaese, R. M. Transfer of the bacterial gene for cytosine deaminase to mammalian cells confers lethal sensitivity to 5-fluorocytosine: a negative selection system. *Proc Natl Acad Sci USA* 89, 33-37 (1992).
12. Mahan, S. D., Ireton, G. C., Stoddard, B. L. & Black, M. E. Alanine-scanning mutagenesis reveals a cytosine deaminase mutant with altered substrate preference. *Biochemistry* 43, 8957-8964 (2004).

13. Mahan, S. D., Ireton, G. C., Knoeber, C., Stoddard, B. L. & Black, M. E. Random mutagenesis and selection of *Escherichia coli* cytosine deaminase for cancer gene therapy. *Prot Eng Des Sel* 17, 625-633 (2004).
14. Erbs, P. *et al.* *In vivo* cancer gene therapy by adenovirus-mediated transfer of a bifunctional yeast cytosine deaminase/uracil phosphoribosyltransferase fusion gene. *Cancer Res* 60, 3813-3822 (2000).
15. Tiraby, M. *et al.* Concomitant expression of *E. coli* cytosine deaminase and uracil phosphoribosyltransferase improves the cytotoxicity of 5-fluorocytosine. *FEMS Microbiology Letters* 167, 41-49 (1998).